REGULATION OF FLT3 GENE EXPRESSION IN HAEMATOPOIETIC AND LEUKAEMIC STEM CELLS

by

GIACOMO VOLPE

A thesis submitted to the

University of Birmingham

for the degree of

DOCTOR OF PHILOSOPHY

School of Immunity and Infection
College of Medicine and Dental Sciences
University of Birmingham
December 2009

ABSTRACT

The interaction between the tyrosine kinase receptor Flt3 and its ligand leads to signalling during the commitment of haematopoietic stem cells. Constitutive activation of the Flt3/FL pathway is a key factor in enhanced survival and expansion in acute myeloid leukaemia (AML). Although there is extensive knowledge regarding mutations leading to the constitutive activation of Flt3 receptor activity, the molecular mechanisms underlying the regulation of the *flt3* gene in HSCs, and how such mechanisms might be altered in leukaemia, are still poorly understood. Here, by using HSC and leukaemic cell lines, I locate several regulatory elements in the *flt3* locus by DNaseI mapping and have characterized their epigenetic environment. Analysis of the methylation and acetylation status of histones H3 and H4 around *flt3* *cis*-regulatory regions highlights a distinct combination of epigenetic modifications specific to AML cells in a region that distinguishes the $Flt3^-$ and $Flt3^+$ stages of HSC differentiation. Moreover, I show the link between the *in vivo* binding of C/EBPα and c-Myb on regulatory elements and chromatin remodelling in the differential regulation of *flt3* in leukaemic cells. Finally, I identify the histone modifiers TIP60 and CBP as potential mediators of the epigenetic regulation of *flt3* in AML cells.

A mio nonno,

bersagliere, maestro di vita e uomo d'onore

(1921-2008)

ACKNOWLEDGMENTS

There is a long list of people that I should acknowledge, to thank for the help support and friendship that I've been given during the last few years.

Before anybody else, I should definitely thank my girlfriend Natalia, for the unconditioned support and love and for tolerating my passion and dedication to research, even when I was getting grumpy and annoying. Thank you for being there for me, with all the love of my heart.

I also need to thank my parents Anna and Nino, my sisters Daniela and Marina, my brother Beppe and my sister in law Rossana. Thanks for never stopping to believe in me.

A great thanks goes to my supervisors. Steph Dumon for your heroic and never ending support, for everything you have done for me, and trust me, you have done a lot. I don't think I would be writing this thesis if it wasn't for your help. You are an amazing boss and a fantastic friend. I should definitely be grateful to Jon Frampton, for being a fantastic source of inspiration, for the fruitful conversations and the great ideas, and also for the indefinite number of beers I had the pleasure of drinking with you in the staff house. It has been great being your student; you have all my respect and admiration. A great thank you must also be given to Jon's amazing group. In particular, I'm very grateful to Dave, for the great support, for being my English back up, for the musical exchanges and the great times I've had with you in the lab, I've had lots of fun!! Emilie, for being so nice and sweet with me, for the great

discussions and for the help with my work, it has been very nice to “fight” with you all the time in the lab!! Paloma, for being the oracle of the group, and always a source of joy and knowledge. Mary, for the fantastic help with the sorting and the lovely and smooth sneezing!!! Maelle, for being very supportive and helpful with computer problems. Oscar for being a great smoking companion (even in the rain and in the freezing cold) and for the amazing football discussions. Lozan, for cheering me up all the times that my computer crashed. Tom, for lovely conversations in “brummie”.

From the IBR I should also thank Kai, for the fantastic coffee breaks, Yotis for being my “big brother” and always giving me great advices, Eliza for the great help with Endnote and the fantastic musaka, Manuela for the great cooking and reminding me how good is to be Italian, Pete for the great laughs and all the other people of the Watson’s, Bicknell and Jayaraman’s groups.

Thanks also to Walter, alias “Mr Dumon”, for being a great friend, for the computer help and for the fantastic musical experience.

Undoubtedly, a great thank you must go to the Italian community in Birmingham, in particular to Cristiano, Francesco Crea and Marco, for the memorable moments spent together and for the amazing support you have given to me during difficult moments. Also Andrea Pisi, Luca, Anna, Fabio Citi, Stefano, Giorgio Perkiozzi, Antonio, Adriana, Mino, Ludovico e Sebastiano. Thanks for making my stay here much more pleasant, I will always have great memories of all the parties at Ciccioland United and the great evenings spent together. Also I should mention my good friends Eugenio, Nathalie, Miha, Sabina, Vasilios, Angeliki, Donato and all the

people of Milano Restaurant. Thanks to everybody, I will always have great memories of you all.

DECLARATION

As officially declared to The University of Birmingham all results presented in this Thesis as novel were obtained by myself with the exception of the following work:

1. Operation of the cell sorter was carried out by Roger Bird, Division of Immunity and Infection, College of Medicine and Dental Science, University of Birmingham.
2. RNA extraction and cDNA preparation from shRNA transfected cells was performed by Dave Walton, Division of Immunity and Infection, College of Medicine and Dental Science, University of Birmingham.

TABLE OF CONTENTS

LIST OF FIGURES

CHAPTER 4

LIST OF TABLES

CHAPTER 1: INTRODUCTION

1.1 The haematopoietic system

The haematopoietic system is organized as a hierarchy of clonogenic cell types that differ in their abilities for self-renewal, proliferation and differentiation (Szilvassy, 2003). The apex of this hierarchy is represented by a population of cells, defined haematopoietic stem cells (HSCs), which are able to sustain blood cell production, generating mature cells committed along specific lineages of the blood, bone marrow (Constantinidou et al., 2006), spleen and thymus (Szilvassy, 2003; Szilvassy et al., 2003; Ho, 2005). HSCs gradually lose self-renewal potential as they start to differentiate towards their immediate progeny, the multipotent progenitor (MPP). These MPP cells lack in vivo self-renewal ability but have the capacity for multilineage differentiation (Adolfsson et al., 2001), giving rise to the common myeloid progenitors (CMP) and common lymphoid progenitors (CLP). CLPs populate the lymphoid compartment, which consists of B and T lymphocytes and natural killer (NKs) cells. CMPs can develop along the six major haematopoietic lineages of the myeloid compartment, that is, megakaryocytes/platelets, erythrocytes, monocytes/macrophages, basophils/mast cells, eosinophils and neutrophil /granulocytes. Dendritic cells (DC) can arise from both the CMP and CLP in response to specific stimuli (Iwasaki et al., 2005) (Figure 1.1).

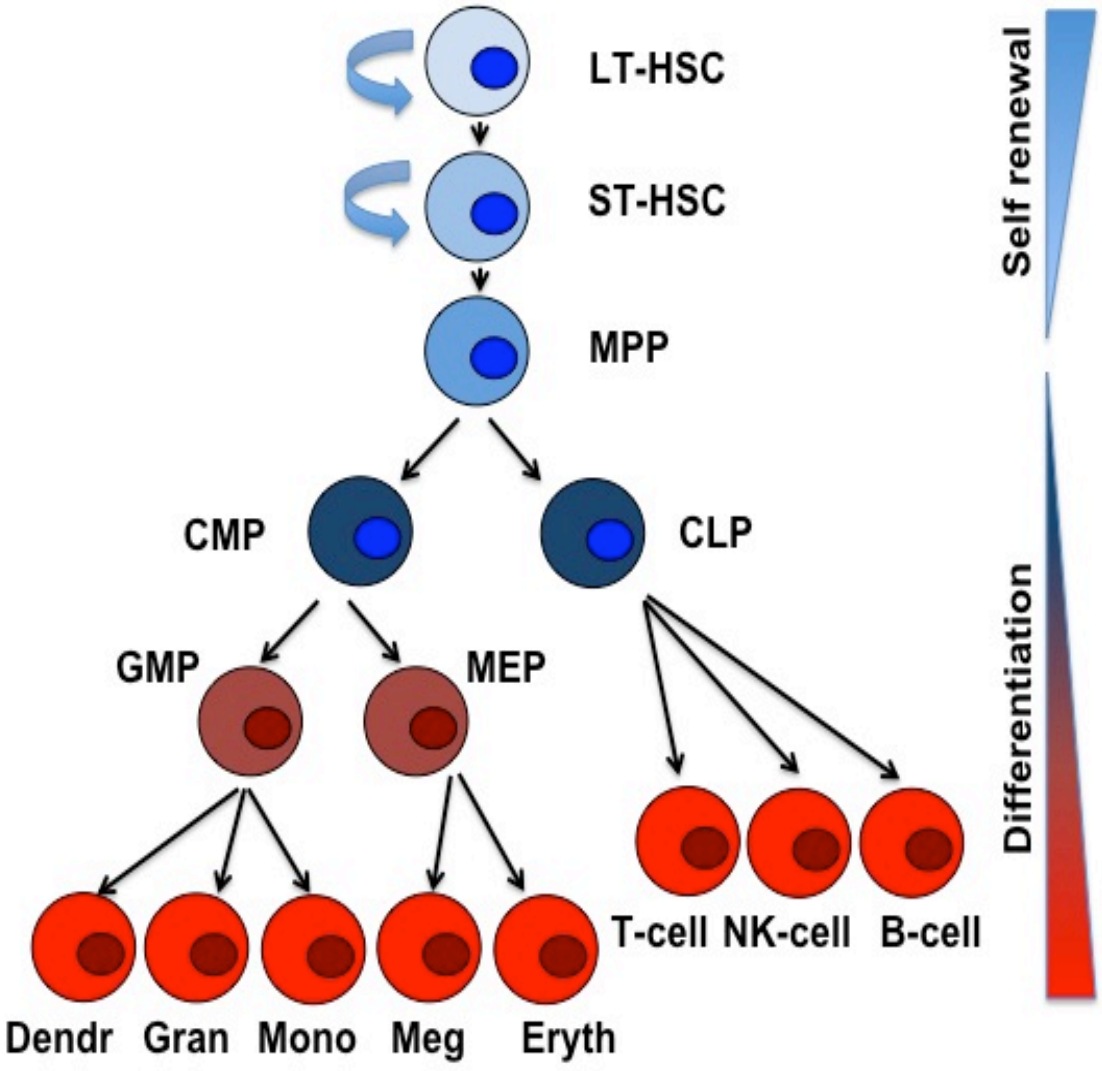

Figure 1.1 Schematic representation of the haematopoietic hierarchy. This figure represents the generation of mature myeloid and lymphoid haematopoietic cells from long-term haematopoietic stem cells (LT-HSC). ST-HSC: short term haematopoietic stem cells; MPP: multipotent progenitors; CMP: common myeloid progenitors: CLP: common lymphoid progenitors; GMP: granulocyte/macrophage progenitors; MEP: megakaryocyte/erythrocyte progenitors; Dendr: dendritic cells; Gran: granulocytes; Mono: monocytes; Meg: megakaryocytes; Eryth: erythrocytes; NK: natural killer cells.

Each of the myeloid and lymphoid cell types has got a specific function. Megakaryocytes are the cells responsible for the generation of platelets, which are essential for normal blood clotting. Erythrocytes are the most abundant blood cell, their principal task consisting of the delivery of oxygen to the body tissues and removal of carbon dioxide. Monocytes, macrophages and granulocytes (neutrophils, eosinophils and basophils) are phagocytic cells, which together with NK cells take part in both innate immunity and cell-mediated immunity. Finally, the lymphoid cells, that is, B-cells and T-cells, are the cornerstone of the adaptive immune system.

Terminally differentiated blood cells have a range of lifespans, which in humans varies from 1 day (neutrophils) to 120 days (erythrocytes), so that the maintenance of their number requires lifelong production of cells, from a very small number of stem cells. Under physiological conditions, homeostasis of the haematopoietic system must be maintained, while in response to haematological stress, stem cells must undergo a burst of activity in order to replenish any blood lineage affected. Once the physiological conditions are restored, the stem cells must return to their normal steady state.

1.2 Ontogeny of the haematopoietic system

The complex process of haematopoietic development occurs in different sites during vertebrate embryogenesis according to the different demands of the developing organism (Bellantuono, 2004). The first site of primitive haematopoiesis is the yolk sac (YS) (Auerbach et al., 1996), which at day 7.5 *post coitum* (dpc) is generating

mainly embryonic counterpart of megakaryocytes, macrophages and erythrocytes and non-haematopoitic cell lineages. Embryonic megakaryocytes exhibit a lower degree of ploidy and an accelerated production of platelets compared to their adult counterparts. Embryonic macrophages synthesise a different set of enzymes compared to those in the adult, while erythrocytes in the embryo are nucleated and express embryonic isoforms of haemoglobin (βH1 and ε). Collectively, these cells ensure protection from infection and bleeding, tissue remodelling, removal of dead cells and efficient oxygen supply to the developing embryo.

For several years, the YS was believed to be the only source of *de novo* stem cell formation, with the HSCs originating from the YS by differentiation of the mesoderm (Moore and Metcalf, 1970). It was initially proposed that HSCs originated in the YS and migrated via the blood to colonise the foetal liver. This idea was supported by the *in vitro* presence among the YS progenitors of spleen colony forming unit (CFU-S), cells that are equivalent to multipotent myeloid progenitors (Moore and Metcalf, 1970). In earlier studies involving the generation of chicken-quail chimeras (Dieterlen-Lievre, 1975), it was observed that YS cells failed to support definitive erythropoiesis and haematopoietic precursors found throughout life were derived from an intra-embryonic source. This source was localized to the dorsal level, which consists of the aorta and the developing urogenital system, in the Para-Aortic Splanchnopleura/Aorta-Gonado-Mesonephros (PAS/AGM) region. In the early 1990s the presence of progenitors at day 10 dpc capable of long-term reconstitution was discovered in the AGM region (Muller et al., 1994; Medvinsky and Dzierzak, 1996). Subsequently, Godin and colleagues isolated YS and PAS progenitors at

day 8.5 dpc that were capable of giving rise to multiple myeloid lineages and B-cells, introducing the idea that multipotent progenitors may arise simultaneously in the PAS and the YS (Godin et al., 1995); whether either or both of these tissues provide the HSCs that will colonise the foetal liver and the bone marrow, is still unclear although few years later it has been showed that only PAS progenitor cells are able to generate lymphoid cells (Cumano et al., 1996). The adult haematopoietic system begins to form at day 10 dpc in mice in the foetal liver (FL), which will become the main organ where HSCs undergo expansion and maturation. A large pool of multipotent progenitors expands in the FL, these cells being phenotypically characterised as $AA4.1^{+}Lin^{low}$ or $AA4.1^{+}Lin^{low}Sca\text{-}1^{+}$, and representing 0.05% of cells at day 14 dpc. Immediately after birth, the bone marrow is populated by haematopoietic cells from the FL, and becomes the predominant site for adult haematopoiesis (Mikkola and Orkin, 2006).

1.3 The haematopoietic stem cell

Since the existence of HSCs was proven by Till and McCulloch in 1961 (Till and McCulloch, 1961), these cells have become the best characterised stem cell type. HSCs not only have the ability to differentiate into mature blood cells, but also have the essential capacity to reproduce themselves, a process known as self-renewal (Siminovitch et al., 1963). Through self-renewal, one or both daughter cells retain the exact developmental potential of the parental stem cell and thereby ensure the maintenance of a lifelong pool of stem cells. “Asymmetric” division results in the generation of two distinct daughter cells, one identical to the “parent cell” and the other being slightly more committed and with an increased tendency to differentiate.

“Symmetrical” division, on the other hand, results in the production of two daughter cells that are either identical to the parental one or are both committed (Pina and Enver, 2007). The balance between symmetric and asymmetric division is required both to support a fast and robust response to haematological stress and to maintain homeostasis (Wanger, 2002).

Self-renewal requires careful regulation; hence, sustained commitment of stem cells without replacement would lead to depletion of the stem cell pool while excessive self-renewal could lead to leukaemia (Dick, 2003). Moreover, self-renewal is influenced and regulated by the so-called stem cell niche, which profoundly affects the decision of stem cells to enter symmetrical or asymmetric division (Spradling et al., 2001; Li and Xie, 2005).

Under normal conditions the majority of HSCs and many progenitors are quiescent in G0 phase of the cell cycle (Cheshier et al., 1999). During haematological stress, such as bleeding or infection, the quiescent HSCs enter the cell cycle, undergoing a symmetrical division in order to generate more committed daughter cells in response to the substantial demand for one specific lineage (Horvitz and Herskowitz, 1992; Mayani et al., 1993). When the stress ceases and the demand for blood cells returns to normal, the stem cell pool will be replenished by self-renewal. Under normal physiological conditions, HSCs undergo asymmetric division in order to maintain blood homeostasis (Morrison and Kimble, 2006). If the number of HSCs in the bone marrow stem cell pool exceeds the number required, they can enter into an apoptotic program (Domen, 2001) (Figure 1.2).

1.4 Phenotypic characterization of HSCs

The stem cell compartment of the bone marrow includes a heterogeneous population of cells that can be divided into three subpopulations based on their ability to reconstitute the haematopoietic system of lethally irradiated mice. The most immature fraction of the HSC compartment is the long-term stem cell population (LT-HSC), which has the greatest capacity for self-renewal and the ability of repopulate the haematopoietic system of irradiated mice for more than six months and to subsequently be serially transplanted into secondary recipients (Morrison and Weissman, 1994). LT-HSCs generate their immediate progeny, short-term stem cells (ST-HSC), which are capable of multilineage commitment but have reduced self-renewal potential, are only able to repopulate irradiated mice for 6-8 weeks and lack the ability to be serially transplanted (Adolfsson et al, 2001; Christensen and Weissman, 2001). The third subpopulation of the bone marrow stem cell compartment consists of MPP cells; these have no reconstitution potential and give rise to lineage-restricted oligopotent progenitors, the common lymphoid progenitors (CLPs) and the common myeloid progenitors (CMPs) (Kondo et al., 1997).

Even though HSCs are present at a very low level in the bone marrow, it is possible to isolate them in nearly pure form based on their immunophenotypical characteristics. HSCs consist of a population characterized by the lack of expression of lineage markers of granulocytes (Gr-1), macrophages (Mac-1), erythrocytes (Ter119), B-cells (B220), T-cells (CD5) and natural killer cells (CD8a). These lineage negative (Lin^-) cells are further characterized by their expression of the stem cell antigen Sca-1 (Ly6A/E) and of the tyrosine kinase receptor c-Kit

(CD117) (Ikuta and Weissman, 1992). The HSC population described as c-Kit^{+} Sca-1^{+} Lin^{-} (KSL) contains LT-HSCs, ST-HSCs and the MPPs described above, which can be discriminated based on the expression of CD34 (Osawa et al., 1996) and the tyrosine kinase receptor, Flt3 (Adolfsson et al., 2001). Hence, LT-HSCs, ST-HSCs and the MPPs are respectively in the CD34^{-}Flt3^{-}, CD34^{+}Flt3^{-} and CD34^{+}Flt3^{+} subfractions of the KSL population (Figure 1.3).

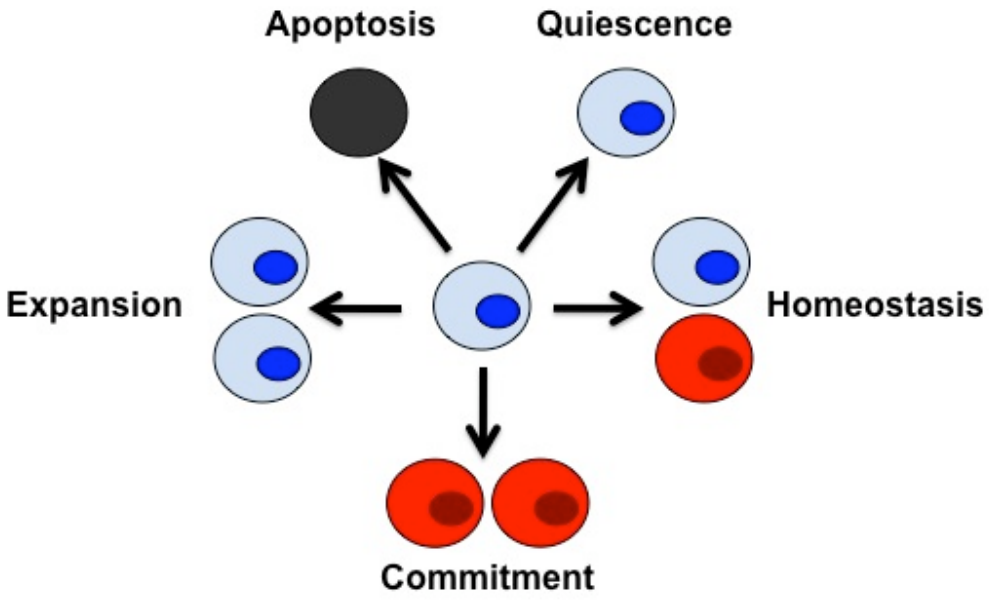

Figure 1.2 Haematopoietic stem cell fate choices. This figure represents the haematopoietic stem cell fate choices in the bone marrow. The processes of expansion, commitment and homeostasists results in generation of two identical HSCs, two committed cells and the generation of identical HSC and one committed cell, respectively. HSCs and quiescent cells are represented in light blue, committed cells in read and cells entering the apoptotic program in black.

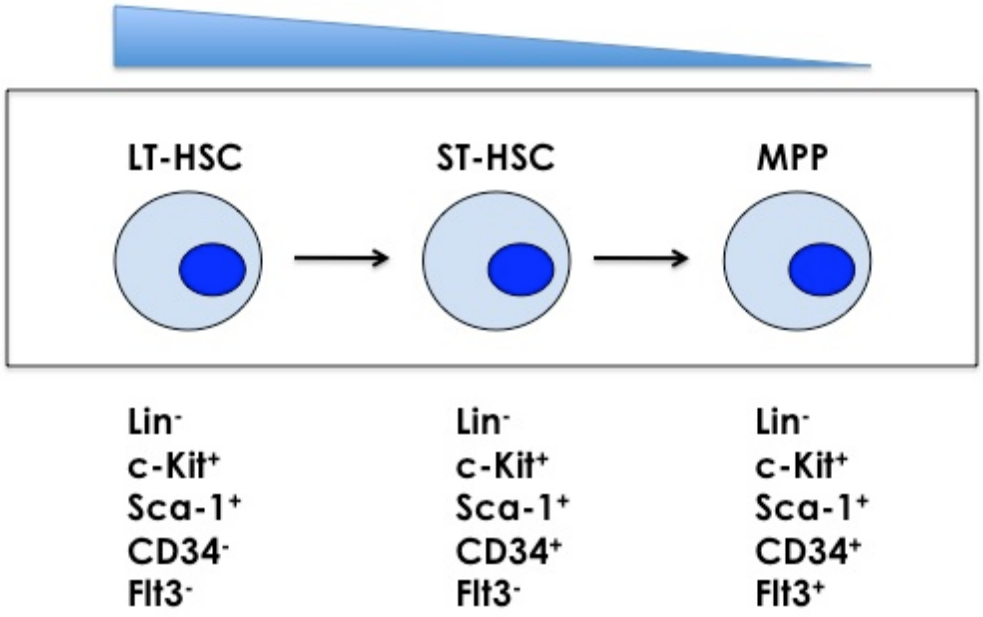

Figure 1.3 Phenotypic characterisation of haematopoietic stem cells. This figure represents the phenotype of HSCs with the KSL compartment and the subdivision in LT-HSC, ST-HSC and MPP based on the expression of surface antigens CD34 and Flt3.

1.5 Aberrant haematopoiesis: Leukaemia

Leukaemia is defined as a cancer of the myeloid or lymphoid blood cells, characterized by the rapid proliferation of abnormal cells that disturb the homeostasis of normal haematopoiesis (Sawyers et al., 1991). Leukaemia includes a large spectrum of diseases and is clinically and pathologically divided into acute and chronic forms:

- Acute leukaemia: Defined by the rapid progression and accumulation of malignant cells in the bone marrow. Immediate treatment is required in order

to prevent malignant cells from entering the bloodstream and colonizing other organs. Acute forms of leukaemia are the most common in children.

- Chronic leukaemia: Usually characterised by the deregulation of relatively mature cells of a particular lineage. This disease normally arises after a long latency, and it is often monitored for some time before treatment to ensure maximum effectiveness. This is a disease that occurs predominantly in elderly people, but can theoretically occur in any age group.

Leukaemias are classified into lymphoid or myeloid types according to the nature of the abnormal cells found in the blood:

- Acute myelogenous leukaemia (AML)
- Acute lymphocytic leukaemia (ALL)
- Chronic myelogenous leukaemia (CML)
- Chronic lymphocytic leukaemia (CLL)

AML develops by the clonal expansion of primitive myeloid progenitor cells, termed myelobasts, as a result of genetic alterations affecting growth or maturation and differentiation. Immature leukaemic cells, which have the ability to divide and proliferate but lack normal differentiation capacity, accumulate in the bone marrow leading to a severe impairment of normal haematopoiesis (Sawyers, Denny et al., 1991). The accumulation of malignant cells affects the normal structure of the bone marrow and a consequent decrease in the production of red blood cells (anaemia),

platelets (bleeding disorders) and white blood cells (increased susceptibility to infections). The general symptoms observed are fatigue, shortness of breath, bleeding and easy bruising, and elevated risk of infections (Lowenberg, Downing et al., 1999).

According to the French-American-British (FAB) classification, AML is divided into 8 subtypes, M0 to M7, based on the type of cell from which the leukaemia developed and its degree of maturity:

- **M0:** undifferentiated AML
- **M1:** myeloblastic without maturation
- **M2:** myeloblastic with maturation
- **M3:** promyelocytic
- **M4:** myelomonocytic
- **M5:** monoblastic or monocytic
- **M6:** erythrocytic
- **M7:** megakaryocytic

AML is the most common acute leukaemia that affects adults, but is rare in childhood, with approximately 1000 new cases per year in the UK. The incidence of AML increases with age, the median age at diagnosis being 63 years. AML is a potentially curable disease, the primary treatment for which consists of chemotherapy. Treatment is divided into two phases: *induction* (to achieve a complete remission by reducing the amount of leukaemic cells to an undetectable

level*)* and *postremission* or *consolidation* therapy (to eliminate any undetectable disease and achieve a cure). Despite aggressive chemotherapy only one quarter of patients enjoy “life long disease-free” survival. For a patient with relapsed AML, the only potentially curative therapy is a stem cell transplant, which could either be *allogeneic* (using stem cells from a compatible donor) or *autologous* (using the patient’s own stem cells).

1.6 Leukaemic stem cells

The aberrant haematopoietic processes that lead to the accumulation of leukaemic blasts in the bone marrow are initiated by rare cells termed leukaemic stem cells (LSC). The existence of LSCs, originally referred to as “leukaemia initiating cells”, was proposed over 40 years ago (Bruce and Van Der Gaag, 1963), although their identification and characterization has taken place largely in the last decade, initiated by the seminal work of Dick and colleagues, who purified the immature ($CD34^+CD38^-$) and committed cell populations ($CD34^+CD38^+$) of leukaemic blasts from AML patients and transplantated them into immunocompromised non-obese diabetic-severe combined immunodeficiency (NOD-SCID) mice (Bonnet and Dick, 1997). It was observed that only the immature fraction of leukaemic blasts could propagate the leukaemia and it became apparent that the leukaemogenic process was entirely dependent on a small subfraction of cells, with the properties of stem cells, including surface phenotypic characteristics (Lapidot et al., 1994; Bonnet and Dick, 1997). However, these findings are still the subject of debate and there now appears to be a greater heterogeneity in the surface antigen phenotype of LSCs.

The revised view of the LSC phenotype arose from the observation of the negative effect the CD38 antibody has on the engraftment ability of the AML repopulating cells in NOD/SCID mice (Taussig et al., 2008). Hence, it was shown that CD38-coated committed sorted cells from AML patients are cleared by the residual innate immune system of the NOD/SCID hosts (Taussig et al., 2008; Taussig et al., 2010). Consistent with these observations, it was reported that $CD34^{+}CD38^{+}$ leukaemia blasts efficiently engrafted when transplanted into NOD/SCID mice treated with anti-natural killer cell antibody (Hogan et al., 2002; Taussig et al., 2010).

At present, there is an on-going debate about the origin of LSCs. Since normal HSCs and LSCs share the ability to self-renew and proliferate, it has been hypothesized that LSCs derive from HSCs. However, LSCs could also derive from more differentiated, or even mature cells, which have reacquired stem cell-like self-renewal potential (Figure 1.4) (Bonnet, 2005b). Whether one or both ideas are correct, LSCs have either sustained or reacquired self-renewal capacity as a result of accumulated mutations or epigenetic changes that affect haematopoietic differentiation (Bonnet, 2005a; Bonnet, 2005b). Additionally, as a consequence of constitutive or deregulated activation of signal transduction pathways, LSC have gained proliferative or survival advantage, generally through activating mutations in RAS family members and in the receptor tyrosine kinases c-Kit and Flt3 (Passegue et al., 2003; Gilliland et al., 2004).

Figure 1.5 summarizes those properties of LSCs that dictate the nature of leukaemia. The prevention of differentiation is generally caused by fusion proteins, such as BCR-ABL and other AML-associated fusion proteins that activate aberrant

signalling pathways, which in turn interfere with the normal program of haematopoietic development. An important feature of LSCs and a crucial event in their leukemogenic transformation is the increased survival that these cells have gained through the prevention of apoptosis. Thus, the predisposition towards leukemogenesis could derive from activating mutations in the Bcl-2 family genes, which act as programmed cell death antagonists in response to apoptotic signals, or silencing mutations in Bax family members, which function to promote apoptosis. Furthermore, LSCs must possess an increased or constitutive self-renewal ability in order to perpetuate the disease, and this can be brought about through the activation of c-Myc or cyclin D1, Wnt, Notch and Shh signalling pathways, or via the upregulation of Hox genes (Figure 1.5) (Passegue et al., 2003).

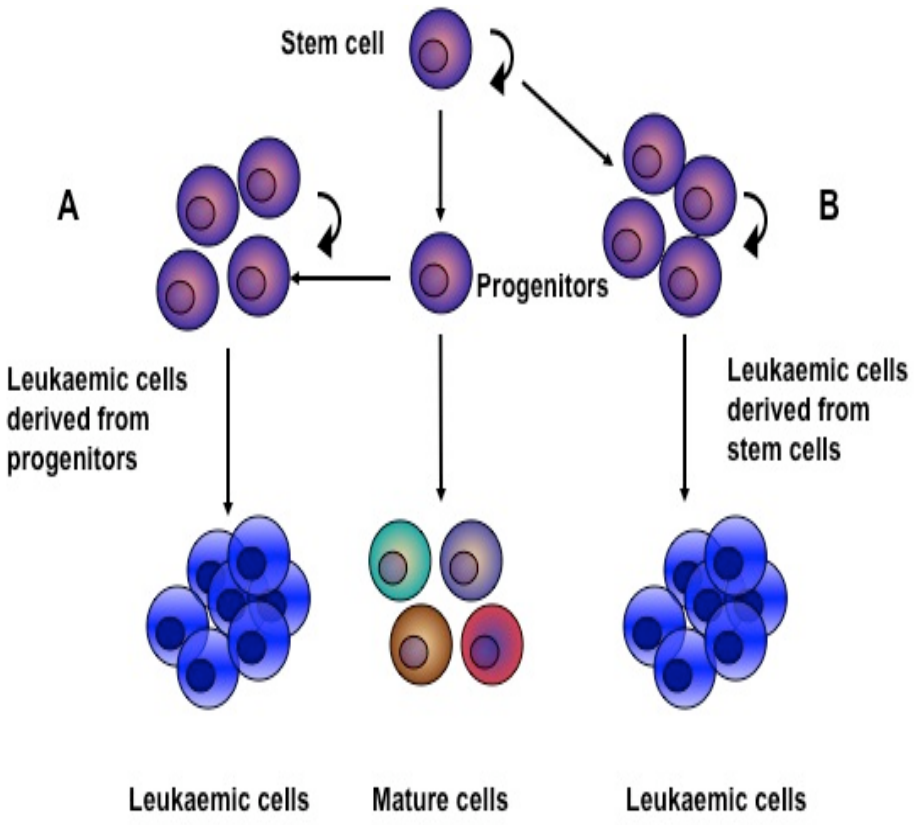

Figure 1.4 Origin of leukaemic stem cells (adapted from "Normal and leukaemic stem cells"; Bonnet D. 2005). This figure illustrates how the leukaemic transformation process can happen in different cells. Panel A shows the transformation event occurring committed progenitor cells. Panel B indicates the origin of leukaemic cells from HSCs.

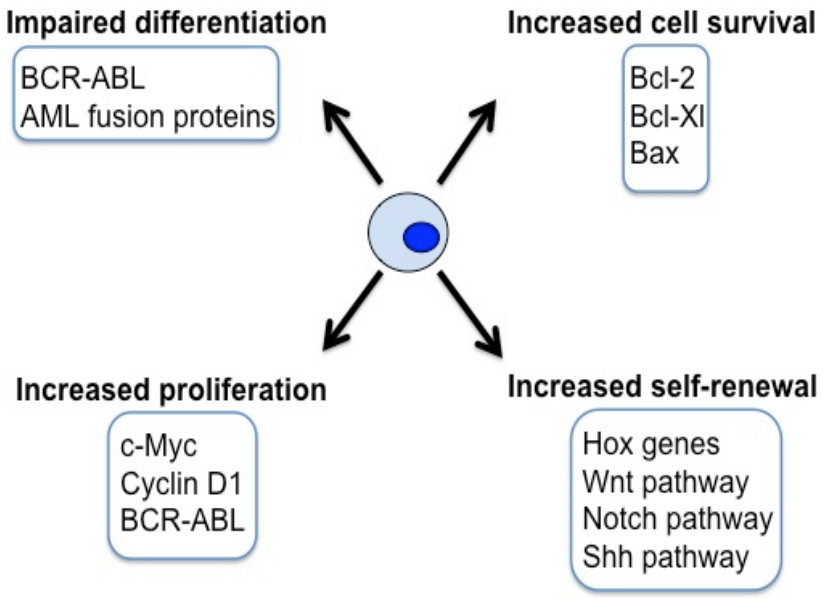

Figure 1.5 Leukaemic stem cell signalling pathways (adapted from "Normal and leukaemic haematopoiesis: Are leukaemias a stem cell disorder or a reacquisition of stem cell characteristics"; Passegue et al.; 2003). This figure depicts the deregulated signalling pathways that lead to leukaemia, showing the general mechanisms involved in the transformation process, such as impaired differentiation, increased cell survival, increased proliferation and increased self-renewal.

1.7 Transcriptional regulation of haematopoiesis

Regulation of the haematopoietic hierarchy from the stem cell through to the fully mature blood cells requires precise control of gene expression. The importance of transcription factors in influencing cell fate relies on their ability to recognize specific DNA elements and recruit co-activators or co-repressors to the promoter and enhancer regions of the target genes. Furthermore, transcription is a complex enzymatically driven process in which transcription factors may recruit of be recruited by specific proteins that mediate chromatin changes, therefore leading to either gene activation or silencing (Kouzarides, 2003). Diverse transcription factors are critical regulators of haematopoietic development and through specific combinatorial interactions establish the lineage- and stage-specific patterns of gene expression, ultimately defining cellular identity.

1.7.1 Transcription factors involved in haematopoiesis

Critical transcriptional regulators of haematopoiesis have been initially identified through the investigation of genes whose aberrant activation was causal for leukaemia (Orkin, 1995). Indeed, many chromosomal aberrations or altered transcriptional programs targeting those genes result in the various haematological malignancies described above (Orkin, 1995; Zhang, 2008; Lionberger and Stirewalt, 2009). One of the aims of this thesis is to investigate the transcriptional regulation of the *flt3* gene in HSCs. Doing so will identify transcription factors that are known to exert their function in the bone marrow stem cell compartment where flt3 expression has been shown to be critical. In this section I describe the main

transcription factors associated with normal haematopoietic development that may be potential regulators of flt3 expression.

1.7.1.1 *SCL*

The transcription factor *SCL*, also known as *TAL-1* (T-cell acute leukaemia-1), was initially discovered through its involvement at the site of chromosomal rearrangement in T-ALL (Begley and Green, 1999). Mice lacking the expression of *SCL* die between E8.5 and E10.5 due to the inability to form blood cells in the YS, resulting in severe anaemia (Shivdasani et al., 1995). Moreover, ES cells in which both alleles have been inactivated (homozygous knock out, *SCL-/-*) do not contribute to any definitive lymphoid or myeloid lineage cells in chimeras generated by the introduction into wt blastocysts. Conditional gene deletion revealed an absolute requirement for *SCL* in the genesis of both primitive and definitive haematopoiesis, but its sustained expression appears to be dispensable for the maintenance of the HSC pool in the adult bone marrow (Porcher et al., 1996; Mikkola et al, 2003).

1.7.1.2 *LMO2*

Described as a partner of *SCL*, *LMO2* has been found to be expressed at high levels in leukaemic blasts and is a common target of chromosomal rearrangement in ALL (Rabbitts, 1998). Mice deficient in *LMO2* die around E10.5 due to the abrogation of the formation of the erythroid cells in the YS. As for loss of *SCL* function, *LMO2-/-* cells do not contribute to lymphoid and myeloid lineages in ES cells chimeras (Warren et al., 1994).

1.7.1.3 *Runx1*

Runx1 (Runt-related transcription factor 1, also known as *AML1* (Acute Myelogenous Leukaemia factor 1), has been shown to be a critical regulator of definitive haematopoietic development during embryogenesis (Okuda et al., 1996). It has been described to be strictly required for early haematopoiesis in the embryo, but like *SCL* is dispensable in the adult bone marrow. The targeted disruption of the *Runx1* gene results in embryonic death at E12.5-13.5, with no signs of definitive haematopoiesis (Okuda et al., 1996). Conditional knock out experiments revealed the importance of *Runx1* for megakaryocytic commitment, resulting in a decreased number of platelets, and B- and T-cell maturation (Ichikawa et al., 2004; Growney et al; 2005). Additionally, *Runx1* is one of the most frequently mutated genes, and a very common target of translocation in human acute leukaemia (Erickson et al., 1992).

1.7.1.4 *CBFβ*

Initially identified as a gene involved in chromosomal rearrangement in AML (Miyoshi et al., 1991), *CBFβ* is the dimerisation partner of *Runx1* (Downing, 2001)oc. Similar to the phenotype of *Runx1* knock out models, mice deficient for the expression of *CBFβ* die *in utero* at E12.5-E13.5 due to the complete absence of haematopoiesis in the foetal liver, while YS erythropoiesis is unaffected (Wang et al; 1990; Niki et al., 1997). Miller and coworkers showed that controlled restoration of its expression re-established foetal liver haematopoiesis, although with a smaller number of primitive precursor cells (Miller et al., 2002).

1.7.1.5 *GATA2*

Knock out mice for the zinc-finger transcription factor *GATA2* die *in utero* between E10 and E11 due to severe anaemia and exhibit a drastic reduction in the number of haematopoietic progenitors (Tsai et al., 1994). Erythroid progenitors are largely absent, and the number of macrophage progenitors is reduced. The analysis of AGM region also revealed a reduced number of HSCs (Ling and Dzierak, 2002). In addition, Rodrigues and colleagues described that mice haploinsufficient for *GATA2* have a low number of HSCs in the bone marrow and a reduced level of granulocyte-monocyte progenitors (Rodrigues et al., 2005).

1.7.1.6 *c-Myb*

This is a key regulator of haematopoiesis. *c-myb* null mice are embryonic lethal at E15 due to severe anaemia, although embryonic erythropoiesis in the YS is not affected, as indicated by the presence of primitive nucleated erythrocytes (Mucenski et al., 1991). Definitive haematopoiesis in the foetal liver is drastically impaired, with the only mature haematopoietic cells present being megakaryocytes and macrophages (Mucenski et al., 1991). Analysis of *c-myb-/-* embryos at E13 revealed the presence of progenitor-like cells, although these cells were not able to differentiate into fully mature cells, indicating that *c-myb* is not essential for the generation of adult HSCs but is necessary for their expansion and differentiation (Sumner et al., 2000).

1.7.1.7 *PU.1*

This is a member of the ETS family transcription factor and has been described as being essential in the specification of haematopoietic lineages. It is highly expressed in myelomonocytic cells and in B-cells, with lower expression in HSCs and CMPs (Klemsz et al., 1990; Akashi et al., 2000). The importance of *PU.1* was revealed by the generation of knock out mice, which exhibited late embryonic or early neonatal death due to lack of B-cells and myelomonocytic development (Scott et al., 1994; McKercher et al., 1996).

1.7.1.8 *Ikaros*

This is a zinc-finger transcription factor that has been shown to be necessary for lymphoid specification (Georgopoulos et al., 1994). To date, ten different isoforms of *Ikaros* have been identified, all of which share the dimerisation domain that is necessary for the interaction with other proteins, although not all the splicing variants have the zinc-finger domain that is necessary for the DNA binding (Sun et al., 1996). Among the several mutant alleles generated, mice engineered for the deletion of the zinc-finger domain showed the most severe phenotypes, underlining the importance of *Ikaros* during lymphoid commitment. The disruption of *Ikaros* results in the lack of both primitive and adult B- and T-cells (Winandy et al., 1999) and a decrease in LT-HSC repopulation capacity (Nichogiannopoulou et al., 1999).

1.7.1.9 *HoxA9*

Is a member of the homeobox gene family and has been extensively investigated because of its importance in both haematopoiesis and leukaemia (Argiropoulos and

Humphries, 2007; Hu et al., 2009; Novotny et al., 2009). The targeted disruption of the *HoxA9* gene resulted in a severe phenotype, involving the impairment of several haematopoietic lineages (Lawrence et al., 1997). Furthermore, repopulation assays revealed that *HoxA9-/-* HSCs failed to reconstitute the bone marrow compartment, indicating its relevance in early HSC function. In contrast, its overexpression strongly supports *in vivo* reconstitution, suggesting an important role in HSC self-renewal (Thorsteinsdottir et al., 2002; Lawrence et al., 2005)

1.7.1.10 *Meis1*

This is a partner of *HoxA9* with which it forms dimeric (HoxA9-Meis1) or trimeric (HoxA9-Meis1-Pbx1) complexes (Shen et al., 1997; Shen et al., 1999), and is frequently up regulated in cases of AML and ALL (Wang et al., 2006). *Meis1* null mice die at E14.5 due to severe haemorrhaging caused by the lack of megakaryocytes in the foetal liver. Additionally, the total number of colony forming cells is dramatically reduced. *Meis1-/-* cells fail to repopulate adult haematopoietic tissues, underlining the importance of this transcription factor in the self-renewal and proliferation of HSCs (Hisa et al., 2004).

1.8 Chromatin structure and epigenetic regulation of haematopoiesis

DNA is tightly packaged inside the nucleus of the cell as an intricate assembly of nucleic acid and small nuclear proteins, known as the nucleosome, which acts as the basic building block of chromatin. Chromatin can show different levels of

packaging, from the transcriptionally active “beads on a string” structure, in which the DNA is wrapped around the nucleosome, to a condensed higher order fibre associated with gene silencing (Kornberg, 1974). The nucleosome consists of an octamer of histone proteins incorporating two copies of each of the histone core proteins H2A, H2B, H3 and H4, assembled as two H2A/H2B dimers and a H3/H4 tetramer (Kornberg and Thomas, 1974; Luger et al., 1997) (Figure 1.6). Nucleosomes are joined together by a 60bp “linker DNA” fragment and sealed off at the entry and exit sites of the DNA by the histone protein H1, which functions to stabilize the structure of the chromatin.

Both histone H3 and H4 have long flexible amino-terminal tails that protrude from the nucleosomal core; these tails are potentially subjected to a vast range of covalent modifications. This “information” in the form of specific chemical groups exposed at the surface of the nucleosome can be “read” by specific effector proteins, leading to consequences either in terms of the structure or the function of the chromatin. The main modifications are methylation, acetylation, phosphorylation, glycosylation, sumoylation and ubiquitination (Margueron et al., 2005; Nightingale et al., 2006).

Normally the tight packaging of chromatin around silenced genes hinders almost all biochemical processes involving DNA. Accumulating evidence suggests that genes that are about to be transcribed undergo a stepwise process of chromatin alteration, in which specifically recruited enzymes either modify the accessibility to chromatin or mark the histone proteins with covalent modifications. In the former case, nucleosomes that normally block the accessibility of DNA binding proteins are

literally pushed away so that the naked DNA can become accessible to transcription factors. The covalent modifications instead constitute a sort of "code" displayed on the histones that can then be read by other effector proteins, usually in the form of multienzymatic complexes, to modulate the pattern of gene expression (Turner et al., 1992; Strahl and Allis, 2000).

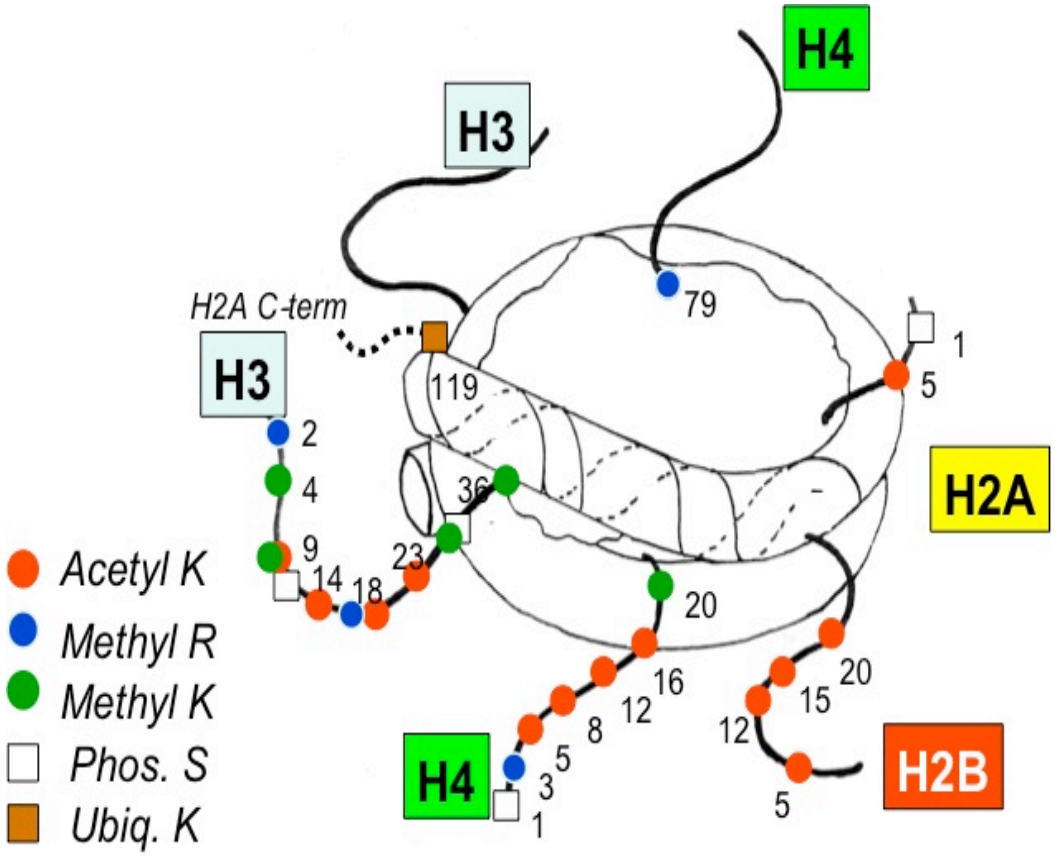

Figure 1.6 Schematic representation of chromatin structure and post-translational modifications. (from "Reading signals on the nuclkeosome with a new nomenclature for modified histones"; Turner BM. 2005). This figure provides a schematic representation of chromatin structure and shows the post-translational modifications occurring on the N-terminus of histone tails. The modifications shown in figure are lysine acetylation (Acetyl K, indicated by red dots), lysine and arginine methylation (Methyl R and Methyl K, indicated with blue and green dots, respectively), serine phospholation (Phos S, white square) and lysine ubiquitination (Ubiq K, orange square).

1.8.1 DNA methylation

Since its discovery in the early 1980s, DNA methylation has been the most investigated and is the best understood epigenetic modification. Catalysed by S-adenosyl methionine-dependent DNA methyltransferase, this modification consists of the deposition of a methyl group on the carbon 5 of the cytosine ring, predominantly at CpG dinucleotides. It has been demonstrated that DNA methylation, which is associated with gene silencing, is fundamental for development, being involved in many processes such as imprinting, X-chromosome inactivation and tumorigenesis (Bird and Wolffe, 1999). Approximately 70-80% of CpGs are methylated in mammals, and the remaining unmethylated ones are generally located at gene promoters, in so-called CpG islands that are rich in CG content. Normally, methylated DNA is not accessible for the binding of transcription factors but can interact with other proteins called methyl-CpG-binding domain proteins (MDBs) that recruit other chromatin modifying enzymes (such as the histone deacetylases), and thus confer to the chromatin a compact, more repressed conformation (Herman and Baylin, 2003). The importance of this modification in developmental gene regulation is apparent from the demonstration that the disruption of genes coding for methyltransferases result in embryonic lethality. Furthermore, recent studies performed by Chen and coworkers have established a correlation between loss of DNA methylation and genomic instability (Chen et al.; 1998). During the cell cycle, methylation activity must be controlled and maintained in order to avoid the generation of unmethylated DNA daughter strands. The loss of

methylation is a common feature during tumourigenesis, since one of its functions is to silence many tumour suppressor genes (Di Croce et al., 2002).

1.8.2 Histone modifications

The last decade has seen growing interest in histone modifications and the link that these modifications have with the “activated” or “repressed” state of chromatin. Particular modifications, such as lysine and arginine methylation or lysine acetylation, have attracted particular attention since several studies have established that actively transcribed genes are associated with increased abundance of these marks. The information associated with the methylation status varies based on the residue involved. Hence, di- and tri-methylation of histone 3 lysine 4 (H3K4me2 and H3K4me3) and mono-methylation of histone 3 lysines 36 and 79 (H3K36me and H3K79me) are generally enriched at the promoter of actively transcribed genes. In contrast, the di- and tri-methylation of histone 3 lysines 9 and 27 (H3K9me2, H3K9me3 and H3K27me3) and the mono-methylation of histone 4 lysine 20 (H4K20me) are normally observed on genes that are transcriptionally silent (Margueron et al., 2005; Turner, 2005). Recent publications have pointed to a dual role for the H3K9me2 modification, since it can also be associated with actively transcribed genes when present in combination with acetylation marks. Acetylation status as well is a strong indicator of gene activity as demonstrated for the lysine 9 of histone 3 (H3K9ac) and lysine 8 of histone 4 (H4K8ac) (Turner et al., 1992). Acetylated histones alter the interaction between DNA and the nucleosomes, conferring to the chromatin a more “open” configuration, thus increasing transcription factor accessibility (Turner, 2003). This covalent modification has

functional outcomes via two mechanisms: i) it leads to charge neutralization of the positively charged lysine and direct changes in the chromatin structure and ii) leads to the recruitment of proteins containing specialized acetyl-histone domains termed “bromodomain protein”. Bromodomain proteins and other chromatin remodelling proteins are specifically recruited to chromatin sites either prior to or as a consequence of transcription factors binding to DNA (Deuring et al., 2000; Lachner et al., 2001).

These chromatin remodelling complexes play important roles in all the DNA-dependent processes as they can translocate nucleosomes along the DNA repositioning or evicting them from the DNA in order to promote transcription (Becker PB, 2002). On the other hand, these complexes can also repress transcription by inducing nucleosomes spatial changes and chromatin assembly (Clapier and Cairns, 2009). In the past few years many complexes have been characterised, among which ACF, Chd1, Mi-2 and NURF, and have been involved in detecting altered nucleosome positions and enabling the binding of the transcription factors to their cognate binding sites (Denslow and Wade, 2007). Moreover these dynamic changes in the chromatin structure have been shown to occur at specific gene cis-regulatory regions, as a consequence of transcriptional activation. Therefore, the binding of a transcription factor to the promoter of a given gene would result in the recruitment of a specific complex containing histone modifying enzymes and/or chromatin-remodelling proteins, which are responsible for the deposition of active histone marks and the repositioning of nucleosomes (Clapiers and Cairns, 2009). Furthermore, Lefevre and colleagues have shown that the recruitment of

chromatin remodelers at promoters and enhancer regions, is associated with DNAseI hypersensitive site formation (Lefevre et al, 1999). DNAseI hypersensitive site mapping will be discussed in more details in section 2.4 and 4.3.

The biochemical processes that lead to the marks mentioned above are reversible through the action of opposing classes of specific enzymes, that is, histone methyltransferases (HMTs) and histone acetyltransferases (HAT), are countered respectively by histone lysine demethylases (HKDMs) and histone deactetylases (HDACs).

1.8.3 Mixed Lineage Leukaemia (MLL) family methyltransferases

MLL family members are H3K4-specific methylases that, through ensuring the appropriate transcription of Hox genes, are strictly required during embryogenesis and haematopoiesis. *MLL* is the mammalian homologue of *Drosophila melanogaster* Trithorax, a group of methyltransterases that positively regulate gene expression (Gu et al., 1992; Tkachuk et al., 1992). Most MLL proteins display the typical HMT signature sequence, that is, the C-terminal SET (Su(var) 3-9 Enhancer-of-zeste, Trithorax) domain.

The 430kDa MLL multi-domain protein is cleaved by Taspase1 into a large 320kDa N-terminal fragment (MLL^N) and a small 180kDa C-terminal fragment (MLL^C). After cleavage the two fragments move into the nucleus where they form a non-covalently associated heterodimeric complex. MLL^C contains the SET domain responsible for the methylase activity and a binding domain for the acetyltransferase CREB-binding protein (CBP). MLL^N on the other hand is composed of three “AT hook” motifs and

a CxxC zinc-finger domain homologous to the DNA methyltransferase DNMT1. Functional studies have suggested the involvement of these domains in the formation of MLL complexes (Nakamura et al., 2002; Hsieh et al., 2003; Slany, 2005).

Several studies have reported the association of MLL with other proteins, including WDR5, which is essential in maintaining the stability of MLL complexes, CREB-binding protein and MOF, which both activate gene expression via their acetyltransferase activity, and the tumour suppressor protein Menin. The latter has been shown to be essential in maintaining Hox gene expression, in particular that of HoxA9, for which it was demonstrated that in the absence of Menin its regulation by MLL was completely abrogated (Slany, 2005).

A number of research groups have focused their attention on the role of *MLL* in haematopoiesis since it was reported that the targeted disruption of *MLL* results in embryonic lethality with severe deficiency in both yolk sac and foetal liver haematopoietic progenitors (Yu et al., 1995; Ernst et al, 2004).

1.8.4 Polycomb group (PcG) proteins

The Polycomb group constitutes another family of chromatin remodelling proteins that plays a pivotal role in silencing Hox gene expression during development, including a crucial role in the regulation of HSC self-renewal, proliferation and commitment (Lund and van Lohuizen, 2004). Several recent publications have described how the Trithorax group (TrxG) and the PcG proteins act antagonistically as a binary epigenetic switch in regulating cell fate in haematopoiesis and other

biological processes. The TrxG proteins are involved in the maintenance of active gene expression, while PcG proteins exert their function by repressing gene expression. PcG proteins form multiprotein complexes, referred to as Polycomb Group Repressive Complexes 1 and 2 (PRC1 and PRC2). PRC1 is composed of several polypeptides: Polyhomeotic (PH), Posterior sex combs (PSC) and Polycomb HPC1 and HPC2. PRC2 is instead constituted by Extra sex combs (ESC), EED, a suppressor of Zeste domain SUZ12 and the EZH2 enhancer of Zeste. It has been demonstrated that the EZH2 component of PRC2 methylates lysines 9 and 27 of histone 3, marks usually associated with inactive chromatin. PRC1 appears instead to be involved in stabilizing the state of gene repression by recognizing the H3K27me3 mark deposited by the PRC2 complex (van der Vlag and Otte, 1999; O'Carroll et al., 2001; Cao et al., 2002; Kuzmichev, et al., 2004).

1.9 Haematopoietic deregulation in leukaemia

Many haematopoietic malignancies develop from perturbation of the molecular processes governing lineage specification and proliferation programs. The hallmark properties of leukaemia, that is, differentiation block, hyperproliferation and inhibition of apoptosis, can result from a disruption of the transcriptional machinery (Orkin, 1995). Many transcription factors have been linked to leukaemia and, as already discussed above, were often identified initially through their association with specific types of diseases.

1.9.1 *Runx1*

The disruption of *Runx1* is a very common aberration in leukaemia. Chromosomal translocations at the *Runx1* locus have been extensively investigated since the RUNX1/ETO fusion gene is found in 40% of AML-M2 cases and the TEL/RUNX1 fusion is associated with 20% of ALL (Harada et al., 2003; Harada et al., 2004). In addition, many point mutations have been identified in the *Runx1* gene, most of which alter the DNA binding capacity or transactivation activity of the protein (Osato, 2004). Recent studies have reported the association of point mutations that in 5-10% of AML-M0 cases result in the formation of truncated proteins with severe functional defects (Osato et al., 1999; Preudhomme et al., 2000).

1.9.2 C/EBPα

The CCATT/enhancer binding protein alpha is a leucine-zipper transcription factor that plays a pivotal role in granulocyte development but also has an activity as a tumour suppressor in the haematopoietic system (Yamanaka et al., 1997; Yamanaka et al., 1997). Aberrant activity of *C/EBPα,* which can develop either as a result of the action of fusion proteins (such as AML1/ETO) or from direct mutation at the *C/EBPα* locus, causes abnormal granulocytic outgrowth in 10-15% of AML-M1 and M2 cases (Snaddon et al., 2003).

1.9.3 *PU.1*

Reflecting its important role as a master regulator of haematopoiesis, the disruption of *PU.1* function often leads to leukaemia, in particular AML. Experimentally, the graded reduction of *PU.1* levels in mice results in myeloid leukaemia resembling

AML (Vangala et al., 2003; Dakic et al., 2007; Kastner and Chan, 2008). Furthermore, the oncogenic proteins RUNX1/ETO, Flt3/ITD and PML-RARα have been shown to suppress *PU.1* expression in acute leukaemia, indicating a possible tumour suppressor role for *PU.1* in myeloid cells (Dakic A, 2007 Vangala et al. 2003).

1.9.4 *HoxA9*

Dysregulation of *HoxA9* has been documented to be a dominant mechanism of leukaemic transformation in many cases of AML, and is often associated with poor prognosis. The experimental enforced expression of *HoxA9* leads to long-latency leukaemia, while the combined co-expression of HoxA9 and its partner protein Meis1 results in the rapid onset of AML, indicating that *HoxA9* plays a central role in initiating leukaemogenesis by conferring growth advantage, but is itself not able to support the progression of leukaemia (Wang et al., 2006). Moreover, Hox family members are associated with chromosomal translocations that result in the formation of the fusion gene NUP98/Hox (Mayotte et al., 2002) and are a direct target of *MLL* fusion genes. Additionally, *HoxA9* is strictly required for MLL/ENL-induced leukaemogenesis (Zeisig et al., 2004).

1.9.5 *Meis1*

Meis1 is frequently up regulated in AML and ALL. Furthermore, overexpression of *Meis1* synergizes with *HoxA9* and Hox fusion genes (eg NUP98/HoxA9) in enhancing leukaemogenesis in murine cell models (Mayotte et al., 2002). *Meis1* and *HoxA9* form either dimeric (Meis1-HoxA9) or trimeric (Meis1/HoxA9/Pbx1)

complexes, and it has been shown that Meis1 alone is not able to induce leukaemia. *HoxA9* on the other hand is eventually able to induce leukaemia alone, but only after a long latency period. Co-expression of both *Meis1* and *HoxA9* results in the rapid onset of AML, underlining the cooperative role of *Meis1* in accelerating *HoxA9*-induced leukaemia (Wang et al., 2006).

1.9.6 *c-myb*

The involvement of *c-myb* in leukaemia has been unclear in spite of its original identification as the transduced oncoprotein in the AMV and E26 avian acute leukaemia viruses (Frampton et al., 1996). Increased *c-myb* expression is associated with several cases of myeloid and lymphoid leukaemia, although no evidence of mutation in the c-Myb coding sequence has been provided. Recently, *c-myb* has been shown to be essential for leukaemogenesis in a BCR/ABL-induced chronic leukaemia model, in which a decreased level of *c-myb* reduced the clonogenicity of p210 BCR/ABL-transformed progenitors (Lidonnici et al., 2008). Furthermore, recent studies have identified a chromosomal translocation between the *c-myb* and T-cell receptor β genes and c-myb gene duplication in a heterogeneous subset of ALLs (Clappier et al., 2007). To date, whether *c-myb* is directly involved in leukaemia or not is yet to be determined.

1.10 Chromatin modifying enzymes

1.10.1 MLL

Chromosomal translocations involving the MLL gene are frequent in infant and adult AML (Ayton and Cleary, 2001). Many MLL fusion partners have been described,

although only a few of them appear to be of clinical relevance in AML. The most investigated MLL rearrangements are MLL-AF4 (t(4;11) (q21;q23)), MLL-AF9 (t(9;11) (p22;q23)), and MLL-ENL (t(11;19) (p12;q23)). The presence of these translocations is often associated with a particularly poor outcome (Schichman et al., 1994; Lochner et al., 1996). Most of the MLL fusion proteins are associated with an altered transcriptional programme in which transcription of the two genes HoxA9 and Meis1 is known to be causal for AML. The mechanism of this transcriptional derepression is still unclear, though many fusion proteins recruit activating transcription factors or histone acetyltransferase activity to target promoter. This idea is supported by the involvement of the MLL partner ENL as an RNA polymerase II elongation factor (Shilatifard et al., 1996). Moreover, recent studies have described a phenomenon of epigenetic compensation in which the decreased H3K4 methyltransferase activity is balanced by the acquisition of H3K79 methyltransferase activity, resulting therefore in a sustained and unique transcriptional programme (Krivtsov and Armstrong, 2007).

1.10.2 MYST Family of acetyltransferases

MYST proteins are part of a large family of histone acetyltransferase that serve as a co-activator for several haematopoietic transcription factors. Several family members are well known for their involvement in cellular transformation (Iwasaki et al., 2005). The monocytic leukaemia zinc-finger protein MOZ in particular is involved in many chromosomal translocations generating the fusion proteins MOZ-CBP, MOZ-p300, and MOZ-TIF2, which occur in 6% of AML-M4 and AML-M5 (Yang and Seto, 2007; Yang and Ullah, 2007). MOZ fusions involving the replacement of

the MOZ C-terminal region with CBP or p300, hence incorporating the acetyltransferase activity of the co-activator, result in an unusual hyperacetylated status of the chromatin and consequent aberrant patterns of gene expression (Kitabayashi et al., 1998). Another family member, the Tat-interactive protein TIP60 has been associated with different types of cancer, although is involvement in leukaemia is still unclear. It has never been associated to any chromosomal translocation in leukaemias, however, altered TIP60 expression could comprise the transcriptional activity of C/EBPα, which normally functions as a tumor suppressor in many myeloid leukaemias (Bararia et al., 2008).

1.11 Flt3 as a paradigm for normal and abnormal gene regulation in HSC and leukaemia

1.11.1 The Flt3 receptor

FMS-like tyrosine kinase 3 (Flt3), also known as foetal liver kinase-2 (Flk-2), stem cell kinase-1 (Stk-1) and CD135, is a membrane-bound receptor tyrosine kinase (RTK) expressed in immature haematopoietic cells (Rosnet et al., 1991; Rosnet et al., 1991). Together with its ligand FL, Flt3 plays an important role in the normal development of stem cells and the immune system (Drexler, 1996; Rosnet et al., 1996a; Rosnet et al., 1996b). Flt3 is a member of the Type III RTK subfamily that includes the macrophage colony-stimulating factor receptor (c-Fms), stem cell factor (SCF) receptor (c-Kit) and the platelet-derived growth factor receptors α and β (PDGFRα/β). Each of these cytokines and their receptors take part in the process of differentiation and proliferation of haematopoietic cells (Mathews and Vale, 1991).

The human flt3 gene located on chromosome 13 (13q12) is over 100kbp long and is composed of 24 exons encoding a 993 amino acid protein (Carow et al., 1995). Flt3 protein can be present as an unglycosylated form of 140KDa or a 160KDa membrane-bound protein that is glycosylated at the N-linked glycosylation site in the extracellular domain (Lyman et al, 1993; Carow et al, 1996). Flt3 consists of five immunoglobulin-like extracellular domains, a transmembrane region, a cytoplasmic juxtamembrane (JM) domain, and two cytoplasmic kinase domains linked by a kinase-insert domain (Agnes et al., 1994) (Figure 1.7). Flt3 binds its ligand FL inducing dimerization, autophosphorylation and the consequent phosphorylation of substrates involved in the initiation of signal transduction pathways that regulate the ability of stem cells to potentiate downstream multilineage expansion.

1.11.2 Flt3 ligand (FL)

The FL gene encodes a Type I transmembrane protein belonging to the family of cytokines that includes SCF and macrophage colony-stimulating factor (M-CSF) (Lyman et al., 1993; Hannum et al., 1994; Lyman et al., 1994). The structure of FL consists of an amino-terminal signalling peptide, an extracellular domain that is responsible for the ligand activity, a spacer and a tether region that anchor the protein to the cell, a transmembrane domain and a cytoplasmic domain (Savvides et al., 2000). FL mRNA is expressed in most haematopoietic and non-haematopoietic tissues, although the FL protein, either in soluble or membrane-bound form, is detectable only in T lymphocytes and stromal fibroblasts in the bone marrow (Lyman et al. 1993; Hannum et al. 1994).

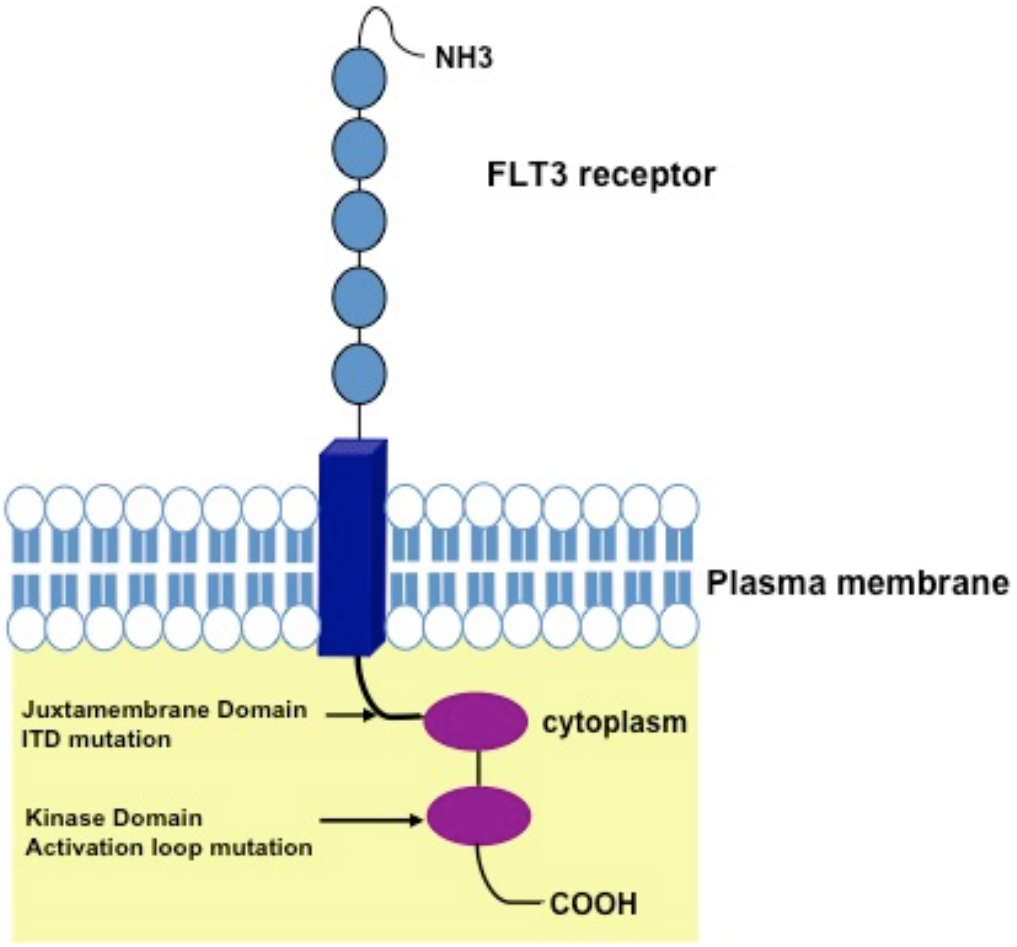

Figure 1.7 Schematic representation of Flt3 receptor structure (from "FMS-like tyrosine kinase 3 in normal haematopoiesis and acute myeloid leukaemia" Parcells et al, 2006). This figure depicts the structure of the membrane-bound flt3 receptor. The extracellular N-terminal Immunoglobulin-like domains, the transmembrane domain, the juxtamembrane domain and the C-terminal kinase domains are indicated.

FL is not able to promote the proliferation of myeloid and lymphoid progenitors efficiently by itself, but experimental evidence indicates that FL is able to induce proliferation in the stem cell compartment in synergy with haematopoietic growth factors and cytokines, such as interleukin-3 (IL-3), granulocyte colony-stimulating factor (G-CSF), colony-stimulating factor-1 (CSF-1) and granulocyte macrophage colony-stimulating factor (GM-CSF) (Lyman, 1995; Ray et al., 1996; Ebihara et al.,

1997)Strict regulation of the export of FL to the cell surface in essential to avoid hyperstimulation of primitive haematopoietic cells, which would otherwise initiate a leukaemic process (Wodnar-Filipowicz, 2003).

1.11.3 Flt3 signalling

Binding of FL to Flt3 initiates a downstream signalling cascade involving phosphorylation and activation of multiple cytoplasmic effector molecules on pathways connected with apoptosis, proliferation and differentiation (Lyman et al., 1993; Hannum et al., 1994; Lyman et al., 1994). Prior to the cloning of FL, studies on Flt3 signalling pathways were performed using a chimeric receptor consisting of the extracellular domain of the human c-Fms and transmembrane and cytoplasmic domains of Flt3 (Dosil et al., 1993). Activation of the chimeric Fms-Flt3 protein in murine NIH3T3 fibroblast and in immature lymphoid BaF3 cells by stimulation with M-CSF resulted in a proliferative response independent of the presence of other cytokines or growth factors. The response to stimulation involved the interaction with phospholipase Cγ1, Ras GTPase-activating protein (GAP) and Src family tyrosine kinases, or proteins that function as adaptors for other downstream effectors, like PI 3'-kinase (PI3K), signal transducer and activator of transcription protein 5 (STAT5), Nck and growth factor receptor-bound protein 2 (Grb2) (Dosil et al., 1993; Rottapel et al., 1994; Zhang et al., 2000). The subsequent cloning of FL in 1993 by Lyman and colleagues enabled confirmation of the observations obtained with the chimeric receptor. Hence, binding of FL to Flt3 leads to triggering of the RAS and PI3K pathways and sustained cell proliferation and inhibition of apoptosis. The activity of PI3K is modulated by Flt3 through interaction with SH2-containing

proteins (SHCs), the proto-oncogene CBL and Grb2-binding protein (Gab2). Furthermore, Flt3-induced PI3K activation blocks apoptosis by phosphorylation of the Bcl-2 family protein Bad. On the other hand, activation of Ras stimulates Raf, MAPK/Erk and STAT5 pathways, which result in the transcription of genes involved in cell proliferation (Zhang et al. 2000; Stirewalt et al 2003; Parcells et al, 2006) (Figure 1.8).

1.11.4 Flt3 and haematopoiesis

The murine *flt3* cDNA was first isolated from foetal liver cells (Matthews et al., 1991) and subsequently the human homologue was cloned in 1994 (Rosnet et al., 1996a; (Rosnet et al.; 1996b). As discussed above, the expression of the *flt3* gene in the bone marrow is restricted to the multipotent progenitor population of the HSC compartment, phenotypically characterized as $Lin^{-}Sca^{-}1^{+}Kit^{+}Flt3^{+}$ (Figure 1.9). Flt3 is highly expressed in early progenitor cells with lymphoid and myeloid potential and to a lesser extent in a subset of B-cells and in myeloid dendritic precursor cells (Adolfsson et al., 2001; Adolfsson et al., 2005). Mackarehtschian and colleagues generated mice genetically engineered to lack the expression of functional Flt3 in 1995; these developed as healthy adults with normal mature haematopoietic populations and normal peripheral blood counts but with specific deficiencies in primitive B lymphoid progenitors (Mackarehtschian et al., 1995). Furthermore, bone marrow transplantation assays revealed a reduced ability of stem cells lacking Flt3 to contribute to both B cells and myeloid cells, demonstrating an important role for Flt3 in the development of multipotent stem cells and B-cells (Mackarehtschian et al., 1995; McKenna et al., 2000). Similarly, targeted disruption of FL resulted in a

significantly reduced number of B-cell progenitors, dendritic cells and NK cells in the bone marrow and lymphoid organs, the phenotype of these mice being partially reverted by the administration of FL (McKenna et al., 2000). Moreover, transgenic mice engineered to over express FL developed leukaemia after a long latency, highlighting the importance of Flt3 and its ligand in normal haematopoietic development (Hawley et al., 1998). It was also demonstrated that the activation of Flt3 by FL enhances *in vitro* and *in vivo* expansion of CD34+ progenitor cells, although the responses induced were dependent on the cell type and on synergy with other growth factors (Ray et al., 1996; Rusten et al., 1996; Veiby et al., 1996). Hence, stimulation of Flt3 alone was able to induce commitment of early heamatopoietic progenitors cells along the monocytic lineage, but resulted in a more robust response in combination with IL-3 and SCF, strongly enhancing the growth of both early precursors and granulocyte and monocyte progenitor cells, although no significant effect was observed on megakaryocytes and erythroid cells. In addition, FL seems to play a key role during lymphoid differentiation, since it promotes B-cell commitment and stromal cell-independent expansion of pro-B cells when applied together with IL-7. In addition, FL induces the growth of immature thymic progenitor cells in combination with IL-3, IL-6, IL-7 and the expansion, but not the differentiation, of NK cells in combination with IL-15 (Rusten et al. 1996). Maraskovsky and colleagues reported that mice treated *in vivo* with FL in combination with IL-4 showed a drastic development of dendritic cells in the bone marrow, spleen, thymus and peripheral blood (Maraskovsky et al., 2000). All of these studies have underlined the important, but not unique, role of Flt3 and its

ligand in normal haematopoiesis and immune system development (Maraskovsky et al., 1996; Namikawa et al., 1999; Stirewalt and Radich, 2003).

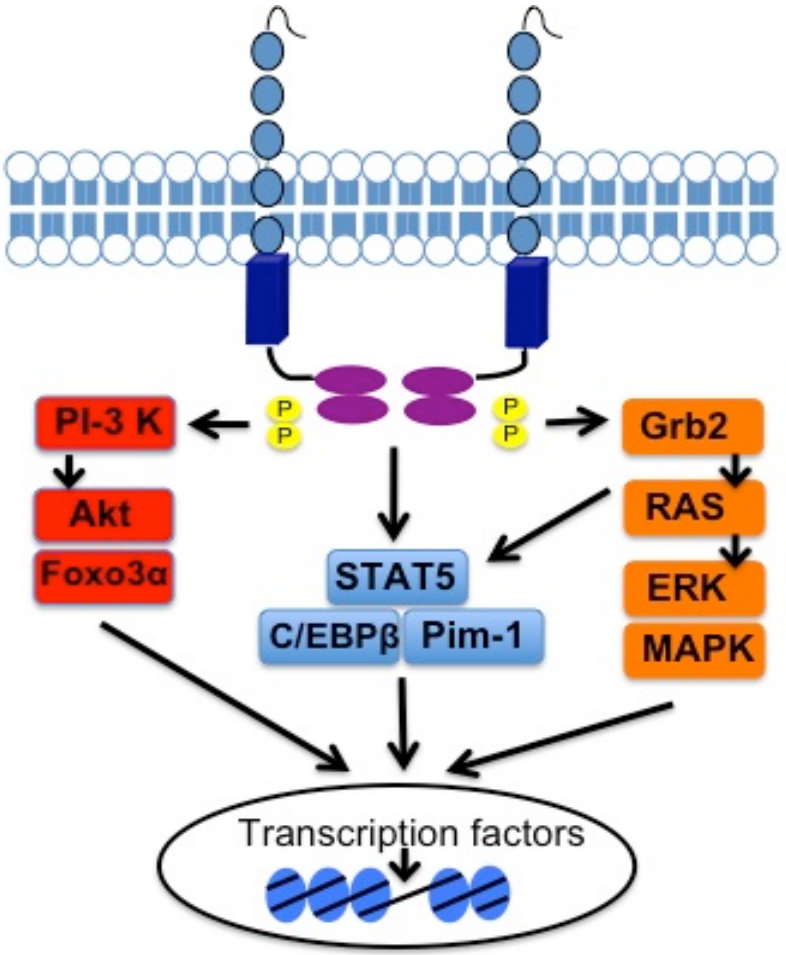

Figure 1.8 Signal transduction pathways downstream Flt3 receptor activation (adapted from "FMS-like tyrosine kinase 3 in normal haematopoiesis and acute myeloid leukaemia" Parcells et al, 2006). This figure shows the downstream signalling following Flt3 receptor activation. PI-3K: phosphatidylinositol 3-kinase; STAT5: signal transducer and activator of transcription 5; C/EBPβ: CCAAT enhancer binding protein β; Grb2: growth factor receptor-bound 2; ERK: extracellular-signal regulated kinase; MAPK: mitogen-activated protein kinase.

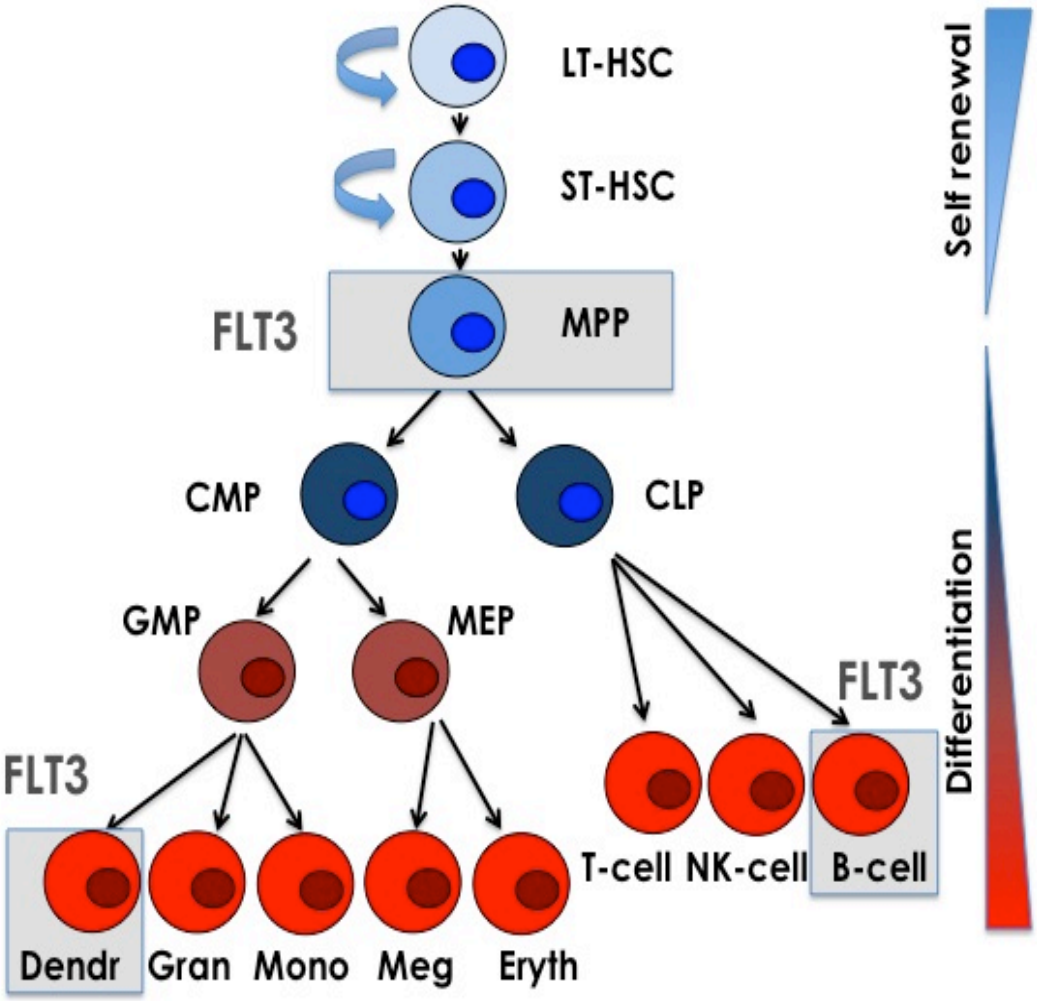

Figure 1.9 Flt3 expression in the haematopoietic hierarchy. This figure indicates the expression of the Flt3 receptor in multipotent progenitor (MPP) cells, in pre-pro B-cells and dendritic cells. LT-HSC: long term haematopoietic stem cells; ST-HSC: short term haematopoietic stem cells; CMP: common myeloid progenitors: CLP: common lymphoid progenitors; GMP: granulocyte/macrophage progenitors; MEP: megakaryocyte/erythrocyte progenitors; Dendr: dendritic cells; Gran: granulocytes; Mono: monocytes; Meg: megakaryocytes; Eryth: erythrocytes; NK: natural killer cells.

1.11.5 Flt3 and leukaemia

A high percentage of haematopoietic malignancies, including 70% to 100% of AML of all subtypes, B-precursor cell ALL, and a fraction of lymphoid blast crisis, are characterized by high level expression of the *flt3* gene (reviewed by Gilliland and Griffin, 2002). Quantitative reverse transcription-polymerase chain reaction (RT-PCR) data revealed a remarkably high expression of *flt3* mRNA in 33 of 33 B-lineage ALL and 11 of 12 AML cases compared to the normal bone marrow (Carow et al., 1996). In addition, *flt3* expression on leukaemic blasts was reported in 18 of 22 AMLs and 3 of 5 ALL cases by Rosnet and colleagues. Since self-renewal potential and growth factor-independent proliferation are important features of leukaemogenesis, the involvement of *flt3* in proliferation in the stem cell compartment underlines its importance in signalling and its oncogenic potential. Moreover, Flt3 is the most commonly mutated protein in AML, either through an internal tandem duplication (ITD) (see below) or single point mutation (eg in the kinase domain). In a clinical study performed by Nakao and colleagues, analysis of *flt3* mRNA revealed the presence of elongated fragments of the JM domain encoded by exon 14 and 15 in 17% to 26% of AML cases (Nakao et al., 1996). In all the patients with this mutation, analysis of the genomic DNA sequence showed an in-frame tandem duplicated sequence in the JM domain and occasionally the insertion of additional nucleotides. The disruption of the JM domain, which negatively modulates kinase activity, results in the auto-activation of the receptor, although the molecular mechanisms supporting this process are yet to be fully clarified. Functional studies involving the Flt3-ITD demonstrated the constitutive activation of PI3K, Ras/MAPK and STAT5 downstream signalling pathways, implying an oncogenic

function through prevention of apoptosis and differentiation. Of the eight different single point mutations defined, the most recurrent results in the substitution of tyrosine for aspartic acid at position 835 in the kinase domain; this mutation (termed Flt3-D835) is observed in 5% to 10% of cases (Kottaridis et al., 2001; Moreno et al., 2003; Scheijen et al., 2004). Whether mutated or not, flt3 gene expression is up regulated in almost all the cases of AML.

1.11.6 Flt3 gene regulation

The mechanisms leading to up-regulation of flt3 gene transcription in the most mature component of the HSC compartment compared to persistent expression of the gene in leukaemias are largely undefined. Recently, some evidence has emerged regarding how *flt3* gene expression is regulated in AML cells. This work has been performed using a cultured progenitor cell model in which Meis1 and HoxA9 transcription factor expression cooperates to induce myeloid progenitor expansion (Wanget al., 2006). Cells transformed by Meis1/HoxA9 (but not HoxA9 alone) constitutively express *flt3* (Wang et al., 2005; Hess et al., 2006; Wang et al., 2006). Chromatin immunoprecipitation analysis revealed that HoxA9 was recruited to the proximal promoter and enhancer regions on the *flt3* locus in progenitors expressing either HoxA9 alone or co-expressing Meis1 and HoxA9, whereas Meis1 was recruited to the promoter and enhancer regions only in progenitors immortalized by Meis1/HoxA9 co-expression.

Regulation of the *flt3* gene has also been investigated in B cell development. Holmes and colleagues observed that in *Pax5* null mice the sustained expression of *flt3* was combined to the block of B-cell differentiation, suggesting that one possible

function of Pax5 was to repress *flt3*. In order to confirm this hypothesis, Pax5-/- pro-B cells were transfected with a retroviral vector expressing the inducible Pax5 ER, and it was showed that the induction of Pax5 resulted in the repression of *flt3*. This was also confirmed to be a direct effect, as Pax5 was shown to in vivo interact with the flt3 promoter (Nutt et al., 1999; Holmes et al., 2006). Furthermore, work carried out in our laboratory (Garcia et al, 2009), has suggested that *flt3* gene expression may be directly regulated by c-myb. Hence, conditional deletion of the *c-myb* gene was found to result in a rapid down regulation of *flt3* mRNA levels in the KSL compartment of HSCs. The mechanism by which *c-myb* acts is yet to be fully clarified.

1.12 Aims of the project

The main objective of this thesis was to examine and understand the regulation of the *flt3* gene in normal and leukaemic haematopoietic stem cells. Here are listed some of the main questions/approaches, described in this thesis:

- To phenotype HPC7 and FMH9 cells in terms of their morphology, gene expression, cell surface antigens and differentiation capacity, and validate them as cellular models for the study of haematopoietic and leukaemic stem cells.
- To identify any cis-regulatory regions in the flt3 locus using DNAseI hypersensitive site (HSS) analysis, employing both a Southern blot analysis and a quantitative PCR approach in both cell lines and primary sorted cells.
- To identify in vivo transcription factor binding in the vicinity of specific HSSs in the flt3 locus, performing chromatin immunoprecipitation (ChIP) assays with antibodies against specific transcription factors.
- To identify by ChIP analysis epigenetic marks associated with transcriptional regulation of the flt3 gene, using antibodies that recognize particular histone modifications associated with either activation or repression of transcription.

CHAPTER 2: MATERIALS AND METHODS

2.1 Cell Culture

The HSC-like line (HPC7) was kindly provided by Dr Leif Carlsson (Umea, Sweden). These cells were cultured at a density of 0.8-1.2*10^6/ml in Stem Pro medium (Invitrogen) supplemented with serum replacement (Gibco), 50 U/ml penicillin and 50 μg/ml streptomycin (Gibco), 12 μM L-glutamine (Invitrogen) and 100 ng/ml of murine SCF (Peprotech) at 37°C in a 5% CO_2 atmosphere.

The LSC-like line (FMH9), derived from purified bone marrow progenitors co-transformed with a retrovirus co-expressing the homeodomain transcription factors HoxA9 and Meis1, was kindly provided by Dr Robert Slany (Erlangen, Germany). These cells were grown at a density of 10^6/ml in RPMI (Sigma) supplemented with 10% Fetal Bovine Serum (FBS, Autogen Bioclear), 50 U/ml penicillin and 50 μg/ml streptomycin (Gibco), 12 μM L-glutamine (Invitrogen), 5 ng/ml IL-3, 5 ng/ml IL-6 and 5 ng/ml GM-CSF (Peprotech) at 37°C in 5% CO_2.

2.2 Cell analysis

2.2.1 Surface marker expression analysis and cell sorting

HPC7 and FMH9 cells were harvested, washed with phosphate buffered saline (PBS) and resuspended in 200 μl of RPMI supplemented with 10% FBS in a 96 V-bottom well plate; centrifugation steps were carried out at 1100 rpm for 2 min at 4°C.

Non-specific binding was prevented by incubation with 5 μg/ml purified anti-mouse CD16/CD32 Fc-block antibody (FcγRII/III) (eBioscience) for 10 min on ice (except for staining for FcγRII/III analysis). Primary antibodies conjugated to specific fluorochromes were used at a concentration of 10 μg/ml for 30 min on ice, followed by washing in PBS at 1000 rpm for 2 min at 4°C. The primary antibodies used and the respective isotype controls are specified in Table 1. Stained cells were resuspended in PBS/ 5% FBS and analysed on a FACSCalibur flow cytometer using CellQuest software (Becton Dickinson). Live cells were selected by gating on forward scatter (FSC) / side scatter (SSC).

For the sorting of primary cells bone marrow from five mice was flushed from tibias and femurs using 10 ml RPMI medium (Sigma) supplemented with 10% FBS in a 10 ml syringe with a 23-gauge needle. The bone marrow was subsequently filtered using a 70 μM cell strainer followed by centrifugation and washed in PBS. The next step involved red cell lysis by resuspending the cells for 5 min at room temperature in ACK solution (0.15 M ammonium chloride, 1 mM potassium bicarbonate, pH 7.3 disodium EDTA). Cells were then centrifugated, resuspended in 300 μl of RPMI supplemented with 10% FBS and stained as described above. Cell sorting was performed using a MoFlo high-speed cell sorter (Cytomation) and the cells collected into sterile tubes containing RPMI / 10% FBS and washed. The antibodies used for the isolation of KSL and CMP cell are listed in Table 2 and Table 3, respectively.

2.2.2 Analysis of cell differentiation

For the differentiation assay, $5x10^6$ HPC7 cells, initially cultured as described above, were transferred to Stem Pro medium supplemented with a lower amount of SCF (20 ng/ml) and 200 ng/ml of recombinant human thrombopoietin (rhTPO) for 48 hours. Subsequently, the cells were cultured for 96 hours in the same conditions but in the presence of 200 ng/ml rhTPO alone to allow the cells to differentiate. The next step consisted of the purification of mature megakaryocytes by isolation in a 0-3% BSA gradient (4 ml 3% BSA / PBS followed by 4 ml 1.5% BSA / PBS and 4 ml of cell suspension in PBS layered successively in a 15 ml tube); cells sedimenting to the lower layer represent the mature fraction of megakaryocytes.

In order to test the response of HPC7 to IL-3 stimulus, $5x10^6$ cells were similarly cultured in Stem Pro medium supplemented with 5 ng/ml IL-3 for 96 hours at 37°C in 5% CO_2. Subsequently, undifferentiated or differentiated cells were washed in PBS, loaded into cytospin funnels on microscope slides and centrifuged for 5 min at 400 rpm. The slides were then treated using the Diff-Quick protocol, which entails sequential staining by dipping the slides 5 times for 1 sec each in (i) 2 μg/ml Fast Green Methanol, (ii) 1.22 mg/ml Eosin G in phosphate buffer (pH 6.6) and (iii) 1.1 mg/ml Thiazine Dye in phosphate buffer (pH6.6). Excess liquid was drained on paper after each solution. The slides were air-dried and covered by mounting medium and a cover slip.

2.2.3 Analysis of Cell DNA content

The analysis of the DNA content was achieved using Propidium Iodide (PI) staining. For this purpose, 10^6 of both HPC7 and TPO-induced HPC7 cells were washed in PBS, resuspended in PBS supplemented with 1% NP-40, and PI added to a concentration of 0.5 μg/ml. The cells were immediately analysed on a FACSCalibur flow cytometer using Cell Quest software (Becton-Dickinson). Events were acquired on a logarithmic scale and dead cells were excluded by FSC / SSC gating.

2.3 RNA analysis

2.3.1 RNA extraction

Total RNA was isolated using Qiagen RNeasy mini kit. Cells were harvested by centrifugation for 5 min at 1100 rpm and then disrupted by addition of RLT buffer, followed by a vigorous shake. One volume of 70% ethanol was added and the whole solution transferred into the appropriate RNeasy spin column in a 2 ml collection tube, and spun at 10000 rpm for 15 sec. RW1 buffer was then added to the spin column, followed by washes with RPE buffer. After each addition the tubes were centrifuge and the flow-through discarded. Columns were eluted with RNase-free water and spun at 13000 rpm for 2 min. Removal of contaminating genomic DNA was achieved by treatment with RNase-free DNase I (Qiagen).

2.3.2 cDNA synthesis

5 μg of RNA was added to each reaction containing 5 mM dNTPs (Invitrogen) and 5 μg/μl of oligoDT primers (Invitrogen) and incubated for 5 min at 65°C then placed on

ice for 2 min to cool down. Subsequently, 10 nM DTT (Invitrogen), 1 U/ml RNaseOut inhibitor (invitrogen), 5X first strand buffer (Invitrogen) and 2 U/ml of SuperscriptIII reverse transcriptase (Invitrogen) were added to a final volume of 50 μl. Reverse transcription was then carried out for 1 hour at 50°C, followed by a 15 min heat inactivation at 75°C.

2.3.3 Semi-quantitative RT-PCR

All oligonucleotide primers were designed using Primer Express software and obtained from MWG Biotech. PCR reactions were performed in 50 μl of Ready Mix PCR Master Mix (Abgene) containing 200 mM of the gene-specific primers. Each PCR program involved 40 cycles, each of which consisted of steps of 95°C for 30 sec, X°C for 30 sec (annealing temperature varies based on the primers used) and 72°C for 30 sec; an extra denaturation step was applied at the start of the program for 5 min at 95°C. β-Actin was used as the normalisation control. For each PCR reaction, time points were taken at intervals of 3 cycles to assess the linear phase of amplification. PCR products were analysed by electrophoresis on 2% agarose gels. The primer sequences and respective annealing temperatures are listed in Table 4.

2.4 DNAaseI Hypersensitive Site (HSS) analysis

2.4.1 Southern blot

To perform HSS mapping, $2x10^6$ cells per point were harvested, washed twice with cold PBS and then resuspended in 1 ml of Digestion Buffer per point (15 mM Tris-HCl pH 7.5, 15 mM NaCl, 60 mM KCl, 5 mM $MgCl_2$, 200 mM Glucose, 0.5 mM EGTA, 0.1% NP40). Cells were vortexed and then aliquoted in 15 ml tubes.

DNaseI (Roche) was diluted to 5 units per μl in DNaseI diluent (25 mM Tris-HCl pH 7.5, 50% glycerol) and then added at increasing concentrations to each sample every 15 sec, as follows:

0 unit	5 unit	10 unit	20 unit	40 unit	60 unit
0 μl	1 μl	2 μl	4 μl	8 μl	12 μl

Samples were incubated for 10 min at 37°C in a water bath, and then the DNaseI reaction was stopped by adding 330 μl of Stop Reaction Buffer (100 mM EDTA, 4% SDS). Subsequently, 10 μl of RNaseA at a concentration of 10 mg/ml was added. After 1 hour of incubation at 37°C, 100 μg of proteinase K (15 mg/ml, Roche) was added, and the samples maintained in the water bath at 37°C overnight. Phenol / chloroform extraction was performed, followed by EtOH precipitation and resuspension of the pellet in an appropriate volume of water. The DNA concentration of each sample was determined by quantifying the optical density at 260nm on the Nanodrop (Nanodrop Technologies). The ratio between absorbance at 260nm and 280nm was also measured as a measure of DNA purity. Subsequently, 10μg of DNA from each sample was digested with restriction endonucleases StuI (for the 5' region) and BamHI (to investigate the intronic region) in a solution supplemented with 2 mM spermidine, 2.5 mM $MgCl_2$, 100X BSA and water up to 50μl. The reaction was carried out overnight at 37°C and then the samples were run on a 0.8% agarose gel in 1X TAE buffer at 50 mV overnight. The

agarose gel was washed in 1l of Denaturing Solution (600 ml dH20, 300 ml 5M NaCl, 100 ml 5M NaOH) for 1 hour and then further washed with Neutralising Solution (400 ml dH2O, 300 ml 5M NaCl, 121.14g Trizma) for one extra hour. The gel was then rinsed in 10X SSC buffer for 10min and transferred overnight to a nylon membrane using a transfer apparatus which consisted of the gel, on which the nylon membrane was placed, followed by 3 layers of Whatman paper and a box of paper towels to allow sufficient capillary transfer. The day after, the transfer apparatus was dismantled and the nylon membrane was first quickly rinsed in 6X SSC and then placed to dry in the oven at 80°C for 2 hours. To proceed to the hybridisation step, the nylon membrane was incubated for 2 hours at 60°C in pre-warmed Church Buffer. The probe was prepared and radiolabelled with [32P] dCTP using the Stratagene Prime-It II kit and incubated overnight on the membrane. Subsequently, the membrane was washed with 2X SSC / 0.1%SDS and then 0.1X SSC / 0.1%SDS, exposed to film or scanned on a phosphoimager. Probe sequences are provided in Table 5.

2.4.2 Real Time PCR

Real Time PCR was performed with Sybr Green (ABgene) with specific oligonucleotide primers designed using Primer Express software and obtained from MWG Biotech. These primers were designed to generate products between 110 and 220 bp and tested for the formation of primer dimers. The primer efficiency was tested by serial dilution of both DNA and primer concentration. 40ng of DNA was amplified in 96 well plates in a total volume of 20 μl, using Absolute QPCR SYBR Green Mix (ABgene) and 200 mM of each primer pair. Following an initial 15 min of

denaturation and activation step at 95°C, PCR cycles were performed at 95°C for 20 sec, 56-64°C for 20 sec and 72°C for 20 sec, and repeated 40 times. The MxPro software of the Stratagene Real Time PCR machine calculated the amplification efficiency and the Ct-value of each sample. The primer sequences are listed in Table 6.

2.5 Cross-linked chromatin immunoprecipitation

X-ChIP experiments were performed following a modified version of the Abcam protocol (www.abcam.com/technical), the buffers compositions being the same unless specified. $2x10^7$ cells were incubated in culture medium with 1% formaldehyde for 10 min at room temperature on a shaker. Chromatin crosslinking was stopped by addition of glycine pH 7.5 at a final concentration of 0.125 M. The cells were washed twice with cold PBS and resuspended in 1.5 ml of lysis buffer (50 mM HEPES-KOH pH 7.5, 140 mM NaCl, 1 mM EDTA pH8, 1% Triton X-100, 0.1% sodium deoxycholate, 0.1% SDS, 5 mM sodium butyrate and protease inhibitors). The chromatin was sheared by 12 pulses of 2 min sonication using the VibraCell sonicator (Sonics & Material inc) with amplitude of 25 to obtain DNA fragments of 300-600 bp in length. After sonication, the chromatin preparation was centrifuged for 1 min at room temperature at 13000 rpm. At this stage the supernatant was collected and stored at -70°C. To test the DNA concentration and the efficiency of the sonication step, a 50 µl aliquot was precleared for one hour in dilution buffer with 15 µl of Protein G Agarose and 15 µl of Protein A Agarose beads (Upstate Ltd) at 4°C on a rotating wheel. The chromatin was then subjected to reverse crosslinking and DNA extracted as described in the Abcam protocol. The amount of DNA was

estimated by optical densitometry and the sonication efficiency was analysed on a 1.5% agarose gel. Typically, 20-25 µg of sonicated DNA and 8 µg of antibody were used for each immunoprecipitation.

Specific antibodies or the relative IgG control (mouse, goat or rabbit) were incubated in dilution buffer (1% Triton X-100, 2 mM EDTA pH 8, 150 mM NaCl, 20 mM Tris-HCl pH 8, 5 mM sodium butyrate and protease inhibitors) with 15 µl each of protein A and G agarose/salmon sperm, for 3 hours at 4°C on a rotating wheel. Meanwhile, the shared chromatin, diluted 10X in dilution buffer, was first precleared with 15 µl each of protein A and G agarose/salmon sperm DNA for 1 hour at 4°C on a rotating wheel. After spinning 1 min at 3500 rpm, the precleared chromatin was incubated with 8 µg of normal IgG for 2 hours at 4°C on a rotating wheel and then incubated for another hour with protein A and G agarose/salmon sperm DNA. Next, the precleared chromatin was added to the antibody-protein A/G agarose preconjugates and incubated overnight at 4°C on a rotating wheel. The next day, the immunoprecipitates were washed sequentially using wash buffers (basic buffer: 0.1% SDS, 1% Triton X-100, 2 mM EDTA pH8, 20 mM Tris-HCl pH 8) containing increasing amounts of NaCl (500 mM, 600 mM and 750 mM). Elution was performed for 1 hour at 65°C in 200 µl of Q2 elution buffer (20 mM Tris-HCl pH 8, 5 mM EDTA pH8, 150 mM NaCl, 1% SDS, 5 mM sodium butyrate, 1 µg/ml RNAseA) and reverse cross-linking was achieved by addition of 1 µl of proteinase K (15 mg/ml) followed by incubation at 65°C for 2 hours. The immunoprecipitated DNA was extracted once with phenol-chloroform-isoamyl alcohol and ethanol precipitated

before analysis by quantitative PCR. Table 7 and 8 provide details of antibodies used for epigenetic and transcription factor analysis.

2.6 Downregulation by ShRNA and overexpression studies

The genetic manipulation of c-Myb and C/EBPα expression levels was achieved by transfecting $10x10^6$ cells from each cell line with pSiren-ShMyb (home made) and pGFP-V-RS-ShC/EBPα (Origene) respectively, or their corresponding non effective scrambled vectors. The plasmids used for the overexpression studies were pcDNA3-Myb and pCMV6-C/EBPα, which were compared to the empty control vectors.

2.6.1 Cell transfections

Transfections of ShRNA and expression vectors were performed using AMAXA Nucleofector kit (Lonza Technologies). For this purpose 4 µg of each plasmid were resuspended in electroporator cuvettes in 100 µl of AMAXA L solution, together with 1 µg of a GFP-expressing vector in order to assess the efficiency of the transfection by FACS analysis. 10^7 cells were washed twice with PBS, resuspended in the DNA solution and transfected with the AMAXA electroporator (program X-001). Immediately after transfection, cells were placed in warm RPMI medium (without serum or antibiotics) and incubated for 1 hour at 37°C 5% CO_2. Cells were then resuspended in their specific medium (Stem Pro medium for HPC7 and RPMI for FMH9) supplemented with serum and antibiotics, and incubated overnight at 37°C 5% CO_2.

2.6.3 Transfection efficiency and analysis

The efficiency of transfection was evaluated by measurement of the proportion of GFP-expressing cells 24 hours after electroporation. Cells were harvested, washed once with PBS and resuspended in 300 µl of medium. Dead cells were excluded by gating. Dot plots for the analysis of GFP expression are represented in Figure 2.1. Total RNA from GFP sorted cells was extracted and corresponding cDNA was analysed by Q-PCR to assess the expression levels of c-Myb, C/EBPα and flt3. GAPDH was used as housekeeping control. The primer sequences used for this analysis are listed in table 9.

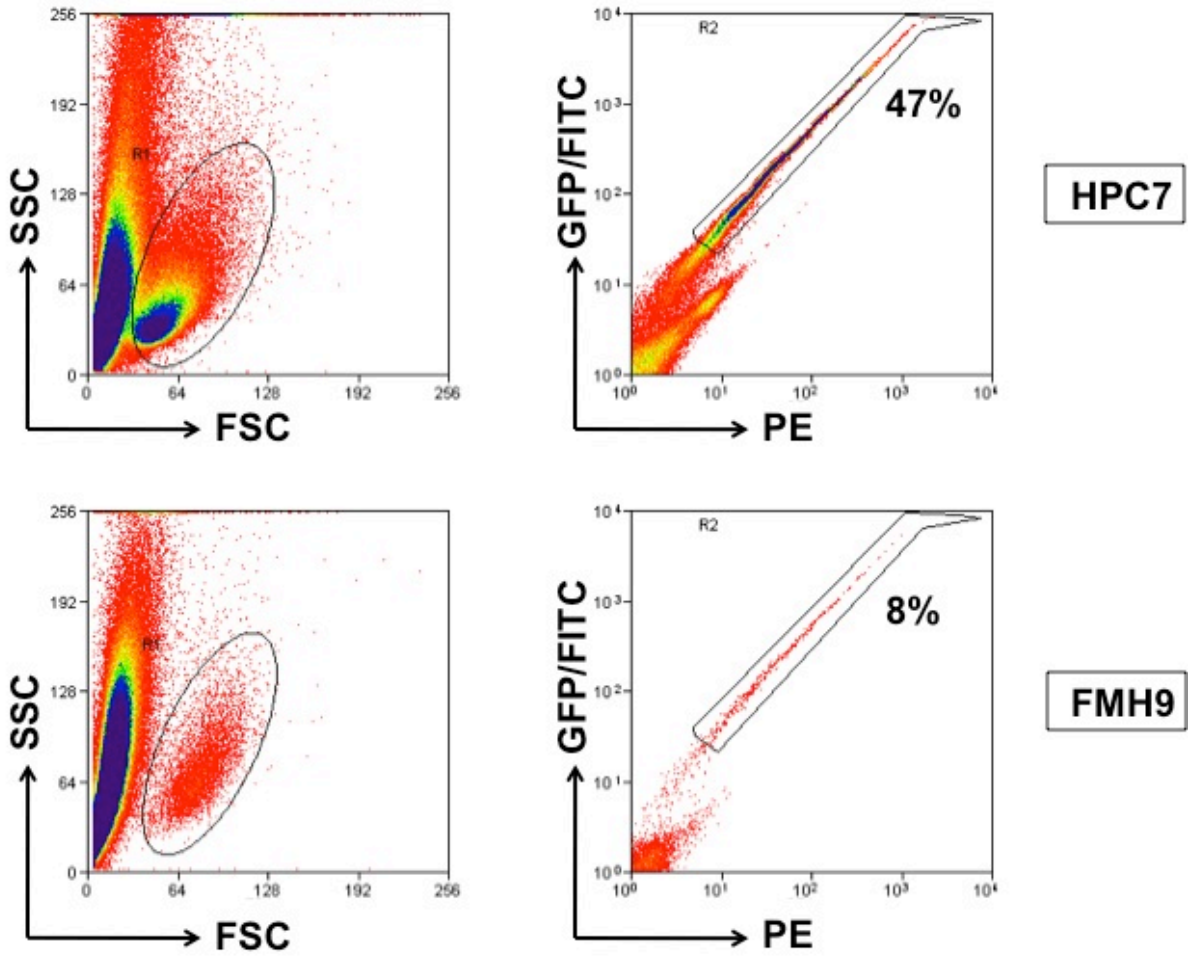

Figure 2.1 Analysis of Flow Cytometry in ShRNA transfected cells and GFP sorting. Two-dimensional dot plot representing live cells gated on forward scatter (FSC) versus side scatter (SSC) in both HPC-7 (top panel) and FMH9 (bottom panel). The dot plots on the right represent the percentage of GFP positive cells after transfection. The fluorescence from GFP positive cells was detected in the FITC channel.

Table 1: Monoclonal antibodies used for flow cytometric analysis of surface antigens

Specificity	Conjugate	Isotype	Supplier
CD117 (c-kit)	FITC	Rat IgG2b	eBioscience
CD34	APC	Rat IgG2b	BD Pharmigen
Sca1	APC	Rat IgG2a	eBioscience
Gr-1	FITC	Rat IgG2a	eBioscience
CD11b (Mac-1)	FITC	Rat IgG2b	eBioscience
CD135 (Flt3)	PE	Rat IgG2b	eBioscience
CD16/32(Fc γRII/III)		Rat IgG2b	eBioscience

Table 2: Monoclonal antibodies used for KSL cell sorting

Specificity	Conjugate	Supplier
CD5	FITC	eBioscience
CD8a	FITC	eBioscience
CD11b (Mac-1)	FITC	eBioscience
Gr-1	FITC	eBioscience
B220	FITC	eBioscience
Ter119	FITC	eBioscience
CD117 (c-Kit)	Cy5	eBioscience
Sca-1	APC	eBioscience
CD135 (Flt3)	PE	eBioscience
CD16/32(Fc γRII/III)		eBioscience

Table 3: Monoclonal antibodies used for CMP sorting

Specificity	Conjugate	Supplier
CD5	FITC	eBioscience
CD8a	FITC	eBioscience
CD11b (Mac-1)	FITC	eBioscience
Gr-1	FITC	eBioscience
B220	FITC	eBioscience
Ter119	FITC	eBioscience
CD117 (c-Kit)	Cy5	eBioscience
Sca-1	APC	eBioscience
CD34	Biotin (*)	eBioscience
CD16/32(Fc γRII/III)	PE	eBioscience

(*) Required a Streptavidin APC-Cy7 conjugated secondary antibody

Table 4: RT-PCR primer sequences

β-Actin	5'-ctttgcagctccttcgttgc-3' 5'-tctgacccattcccaccatca-3'	**GATA3**	5'-cacgatccagcacagaag-3' 5'-atagtcaggggtctgttaat-3'
Ets1	5'-cagtcatccttcaacagcc-3' 5'-ctcttgaaaggtctcagcag-3'	**c-Myb**	5'-ctcccacaccattcaaac-3' 5'-caaaatcaggctcttctctc-3'
Ets2	5'-gctcaacaccgtcaatgtc-3' 5'-ttttttcctcttcccccac-3'	**c-kit**	5'-gctcataaatggcatgctcc-3' 5'-aagttgcgtcgggtctatgt-3'
PU.1	5'-tggaagggttttccctcacc-3' 5'-tgctgtccttcatgtcgccg-3'	**Flt3**	5'-aagttcagttacacccgcc-3' 5'-acatcgcttcttctgcctc-3'
Fli1	5'-agccagatccttatcagatcc-3' 5'-cagtaaagtgagagctggaac-3'	**Meis1**	5'-gggttcctcggtcaatgacg-3' 5'-cgaatctgtttggcgaacacc-3'
Elf2	5'-agccacgaaccaatgaaaaag-3' 5'-gctctggagcagttcagaggag-3'	**HoxA9**	5'-ctccgaaaacaatgccgaga-3' 5'-tgcctttcggtgaggttga-3'
Elk4	5'-aacagattgatccctccacgtc-3' 5'-cagtctccctcaatcctggcta-3'	**HoxB4**	5'-cttggatgcgcaaagttca-3' 5'-acttcatgcgccgattct-3'
Tel1	5'-taactctcaccctctcccttc-3' 5'-ccccagtaagagtgatgagcag-3'	**CBP**	5'-aggcaggaggcatgacca-3' 5'-tcccactgatgtttgcaactg-3'
GATA1	5'-cccttgtgaggccagaga-3' 5'-acctgatggagcttgaaatag-3'	**MLL1**	5'-ggccaagcactgtcggaatt-3' 5'-gcggatttcagcttgacct-3'
GATA2	5'-tgggctctaccacaagatga-3' 5'-gtgacttctcttgcatgcac-3'	**p300**	5'-tcatgaacggttccattgga-3' 5'-ctgaatttggagaccaaggcc-3'

Table 5: Primer sequences for probes used for Southern Blot approach

StuI	5'-gaggagctaagagcaatggtgg-3'	5'-aactttatggtcaaacctcccct-3'	676bp
BamHI	5'-ctcaccacacttggcaaaatcac-3'	5'-agacctcagaaatgcatgctagg-3'	550bp

Table 6: Real time PCR primer sequences

-3503	5'-cccctgtttgtgtggttctgg-3' 5'-tttttcttccattctgtggattacc-3'	**-2584**	5'-caaaacaagtattcaacaccatgcc-3' 5'-cacttactgcttcttggctcagg-3'
-2496	5'-acttactgcttcttggctcaggtt-3' 5'-ccctgtaataacgactctgaggg-3'	**-2404**	5'-atgggagtttgtaacttcggg-3' 5'-tctccaactagctcataacccaa-3'
-2261	5'-cctgtaataacgactctgagggtaat-3' 5'-taagagattctatcggagctggg-3'	**-1641**	5'-tcttaggcgttggtgtcttctctt-3' 5'-tctgagaactgtcctgggatg-3'
-1344	5'-gagcaccacatgctcggaga-3' 5'-aggtagctgtgtgggaattgc-3'	**-1059**	5'-tcactgtggtgtgcaggaatg -3' 5'-ccatgtcatttccacagtgg-3'
-953	5'-gcccatgtcattttccacagt-3' 5'-tgtgcttgtatgctctcaggg-3'	**-778**	5'-gacacgagagatggagcgata-3' 5'-cctgtgctttcaatattcagctt-3'
-426	5'-tcagtccacaatgcacatctacc-3' 5'-aagaggtctgtgtgtcacca-3'	**-258**	5'-acggagtccaggcaacttccc-3' 5'-cacgtgggatcggctgcag-3'
-152	5'-cagactgcgccagttca-3' 5'-aatctgtggtcagtgacgcg-3'	**-72**	5'-accagtccgagggaatctgtgg-3' 5'-ccggcggcctggctacc-3'
+447	5'-aaactaatgggaaaactgcg -3' 5'-agtggctagttactttggaaatact-3'	**+599**	5'-cccctctccatacttttcttatt-3' 5'-agaagcatagctgtgattgaaa-3'
+693	5'-gcatagctgtgattgaaaatactaac-3' 5'-gaagacaaggggttgga-3'	**+6970**	5'-tttggtttaacgtactgcatagct-3' 5'-gaggtgccttgtttttgtcg-3'
+7263	5'-gagacagggtctctcgtgagc-3' 5'-caagtcacggacggttgttaa-3'	**+7559**	5'attgcataagatcctaaaagaggaac-3' 5'-ggagccaagaatccgctatag -3'
+7614	5'-tattatgttgattgggagccaaga-3' 5'-aggtacacactaaattctgtcttcaaa-3'	**+7768**	5'-ggatcttgtcatttttttctctcaaat-3' 5'-aggcttcccagtgctacttattc -3'
+7799	5'-tggctttgcactgaagtttct-3' 5'-cagaaagggagacagagtctga-3'		

Table 7: Antibodies used for epigenetic studies

Specificity	Isotype	Supplier
H3K4me3	Rabbit IgG	Laura O'Neill
H3K9ac	Rabbit IgG	Laura O'Neill
H3K9me2	Rabbit IgG	Laura O'Neill
H4K8ac	Rabbit IgG	Laura O'Neill
H3K79me3	Rabbit IgG	Laura O'Neill

Table 8: Antibodies used for transcription factor ChIP

Specificity	Isotype	Supplier
HoxA9	Goat IgG	Santa Cruz
Meis1	Goat IgG	Santa Cruz
Pbx1	Rabbit IgG	Santa Cruz
Pbx2	Rabbit IgG	Santa Cruz
c-Myb	Rabbit IgG	Santa Cruz
PU.1	Rabbit IgG	Santa Cruz
GATA-1	Rabbit IgG	Santa Cruz
GATA-2	Rabbit IgG	Santa Cruz
Sox2	Rabbit IgG	Upstate Ltd
C/EBPα	Rabbit IgG	Santa Cruz
RUNX1	Goat IgG	Santa Cruz
MLL1	Mouse IgG	Upstate Ltd

Table 9: Primers used for genetic manipulation studies

GAPDH	5'-aactttggcattgtggaagg-3'	5'-acacattgggggtaggaaca-3'
c-Myb	5'-ggagaggtggcacaaccatttg-3'	5'-tggctggctttggaaggctg-3'
C/EBPα	5'-tggacaagaacagcaacgac-3'	5'-tcactgaactccagcac-3'
flt3	5'-cgcgaatgcaccaagctgt-3'	5'-ggtcctgtttgtggagtaggt-3'

CHAPTER 3: CHARACTERIZATION OF THE MODEL CELL SYSTEMS USED IN THIS STUDY

3.1 Introduction

The study of haematopoietic stem cells begun in the 60s when Till and McCulloch reported that the injection of bone marrow cells into irradiated hosts resulted in the formation of spleen colonies (Till and McCulloch, 1961), and was followed by the discovery by Metcalf and Bradley that bone marrow cells were able to give rise to heterogeneous colonies in semi-solid medium (Bradley and Metcalf, 1966). However, the existence of long-lived stem cells in the bone marrow was deduced only 20 years after in subsequent experiments involving clonal tracking of serial transplantation, performed independently by Dick (Dick et al, 1985) and Leminschka (Lemischka et al, 1986). Since then, many efforts have converged in the generation of experimental models that suitably mimic haematopoiesis, in order to define the molecular mechanism governing the self-renewal process and to understand and describe how the determination of different cell lineages takes place (Ceredig et al., 2009).

The last two decades have seen a marked improvement in the ability to isolate and purify HSCs and a growing interest in the clinical application that these cells have, leading to the establishment of several culture systems for the in vitro expansion of

HSCs, although these systems have had only modest success due to the lack of knowledge about the processes governing HSC self-renewal (Domen and Weissman, 1999). As an alternative, several research groups have established immortalized multipotent stem cell lines. In 1980 Greenberger and coworkers reported that the infection of cultured bone marrow cells with spleen focus-forming virus resulted in the generation of an IL3-dependent multipotential haematopoietic cell line, named B6SUtA. Colony-forming and differentiation assays demonstrated the capacity of B6SUtA cells to differentiate along the neutrophil-granulocyte, basophil-mast cell and erythroid lineages following specific stimulus (Greenberger et al., 1983; Greenberger et al., 1983). The commonly used haematopoietic cell line, FDCP-mix, was established in liquid culture from bone marrow. The growth of these cells requires constant supply of IL-3, as demonstrated by their rapid death after the removal of the cytokine. Moreover, FDCP-mix cultured in a low concentration of IL-3 respond to stimulation with GM-CSF and Epo by differentiating into myeloid and erythroid cells, respectively (Spooncer et al., 1984; Spooncer and Dexter, 1984). Tsai and colleagues established an SCF-dependent HSC-like line, EML, by infection of bone marrow cells with a retroviral vector harbouring a dominant-negative retinoic acid receptor. The EML cell line exhibits the ability to generate B-cell progenitors and erythroblasts in response to IL-7 and Epo, respectively (Tsai et al., 1994; Tsai et al., 1994). In spite of their ability to give rise to multilineage differentiation, these cell lines have only a modest repopulation potential in transplantation assays (Pinto do et al., 1998; Pinto do et al., 2002). One cell line, termed HSCN1, which was established by Varnum-Finney et al through retroviral-mediated insertion of the

Notch1 intracellular domain into primitive mouse bone marrow cells, was reported to give rise to functional cells in vivo when cultured in the presence SCF, IL-6, FL and IL-11, although the mechanism leading to the immortalization was unclear (Varnum-Finney et al., 2000).

As with research of HSCs, the study of acute myeloid leukaemia has been impeded by the lack of suitable cellular models. This is partly due to the large diversity of AML subtypes, but also when considering the use of murine cellular models it is not entirely clear how closely mouse AML-like phenotypes parallel the corresponding human disease subtypes (Yin et al., 2006). Since the emergence of the concept of "leukaemia initiating cell" (see Section 1.6), several murine AML-like cell lines have been generated, and they have proved useful in the study of how the modulation of transcriptional programmes or the aberration of signalling pathways can ultimately lead to leukaemia. For example, the WEHI-3 myelomonocytic leukeaemia cell line, originally generated in BALB/c mice by Ralph and colleagues in 1977, has been used to test the cytotoxicity and growth inhibitory effects of macrophage activators on monocytic leukaemia (Ralph et al., 1977; Ralph and Nakoinz, 1977). Similarly, the commonly used myeloblastic leukaemia cell line, M1, was established by Ichikawa in 1969 from a leukaemia spontaneously arising in the SL mouse strain. M1 cells have been used to study growth arrest and apoptosis of mature cells following IL-6 treatment and can be induced to commit towards mature macrophages in the presence of GM-CSF (Ichikawa, 1969; Kawashima et al., 2001).

All the cell lines described above possessed several features of HSC-like (first part) and AML-like cells (last part). However none of these cells lines could have been of

interest for my work, since the choice of the cell models was dictated by the expression of flt3. This chapter is focussed on the characterization, in terms of surface antigen expression, morphology, differentiation capacity and gene expression, of the cell system used to study the regulation of flt3 gene expression in HSC-like and AML-like cells. Ultimately this chapter is also providing a detailed description of the strategy adopted for sorting the primary cells used to confirm some of the data obtained in cell lines.

3.2 HPC7: A model for murine HSCs

The HPC7 line was generated from haematopoietic stem cells obtained by differentiation of ES cells that had been transduced with a retrovirus expressing the LIM-homeodomain protein Lhx2. ES cells infected with the murine stem cell virus (MSCV) retroviral vector containing the mouse LX2 cDNA were expanded in culture in the presence of leukaemia inhibitory factor (LIF); cells from individual colonies being grown in media supplemented with Epo, SCF and IL-3. In the absence of these cytokines the cells died within a few days, whereas growth in media supplemented with Epo and IL-3 resulted in a few rounds of division followed by differentiation towards erythrocytes and macrophage-like cells, respectively. In contrast, growth in the presence of SCF was sufficient to allow expansion for more than seven months, all of the cells maintaining a primitive blast-like morphology (Pinto do et al., 1998; Pinto do et al., 2002). In order to assess the extent to which HPC7 cells display the characteristics of HSCs, I analysed their surface antigen expression, differentiation capacity and HSC-related transcription factor expression.

3.2.1 Surface antigen expression

HPC7 cells grown in presence of SCF were tested by immunofluorescence staining and flow cytometry using antibodies against the mature blood lineage markers Gr-1 and Mac-1, and the stem cell related antigens Sca-1, c-Kit, CD34 and Flt3. This analysis revealed the expression of CD34, c-Kit and Sca-1, but the cells were negative for both Mac-1 and Gr-1, consistent with an immature stem cell-like phenotype. Flt3 expression was barely detectable on the majority of cells, although a small subpopulation (1.5%) exhibited Flt3 staining, possibly reflecting a degree of spontaneous differentiation (Figure 3.1).

3.2.2 Differentiation capacity

HPC7 cells exhibit indefinite self-renewal capacity in culture in the presence of SCF. Morphological analysis following Giemsa staining indicated that the cells cultured in SCF remained undifferentiated and blast-like (Figure 3.2A). The ability of HPC7 to differentiate towards myelomonocytic or megakaryocytic lineages was tested by culturing them in the presence of IL-3 and TPO, respectively. Cells were cultured for 48 hours in the presence of SCF (10 ng/ml) plus rhTPO (200 ng/ml) or IL-3 (5 ng/ml), and subsequently were deprived of SCF and cultured for 96 hours in rhTPO or IL-3. TPO-induced cells were subjected to BSA fractionation in order to concentrate mature megakaryocytes (as described in Materials and Methods). Phenotypic and morphological analysis showed that HPC7 cells were able to differentiate into mature myelomonocytic cells in response to IL-3 or into mature megakaryocytes in response to TPO (Figure 3.2A). Moreover, analysis of the DNA

content of the undifferentiated versus mature megakaryocytes revealed a level of ploidy of 64n, consistent with a fully mature megakaryocytic phenotype (Figure 3.2B).

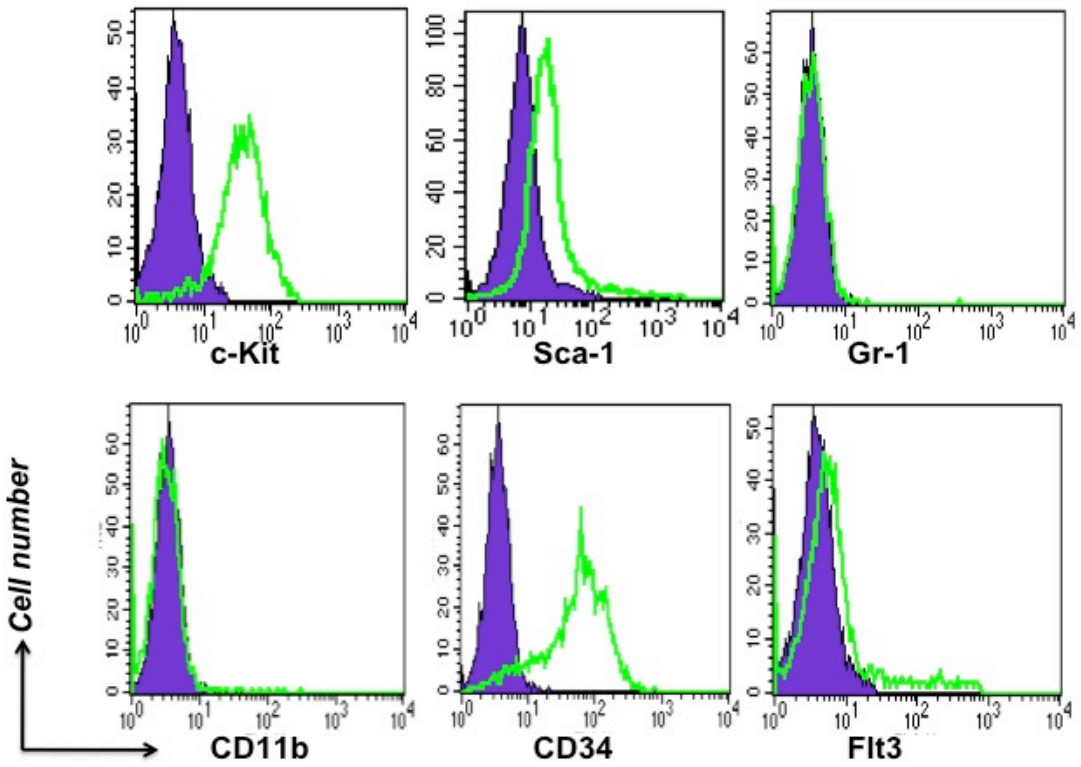

Figure 3.1 Phenotypic characterization of HPC7. The surface antigen phenotype of the HSC-like HPC7 cell line was assessed by immunofluorescence / flow cytometry using a set of labelled antibodies against stem-cell related antigens (c-Kit, Sca-1, CD34 and Flt3) and lineage specific markers (Gr-1, CD11b) together with isotype matched controls (indicated in each plot by the filled histogram). The green histogram represents the staining of each single antibody, as indicated below each plot; the positivity for each staining is determined by the shift of mean fluorescence compared to the control staining with the corresponding isotype control. This figure is representative of three indipendent experiments.

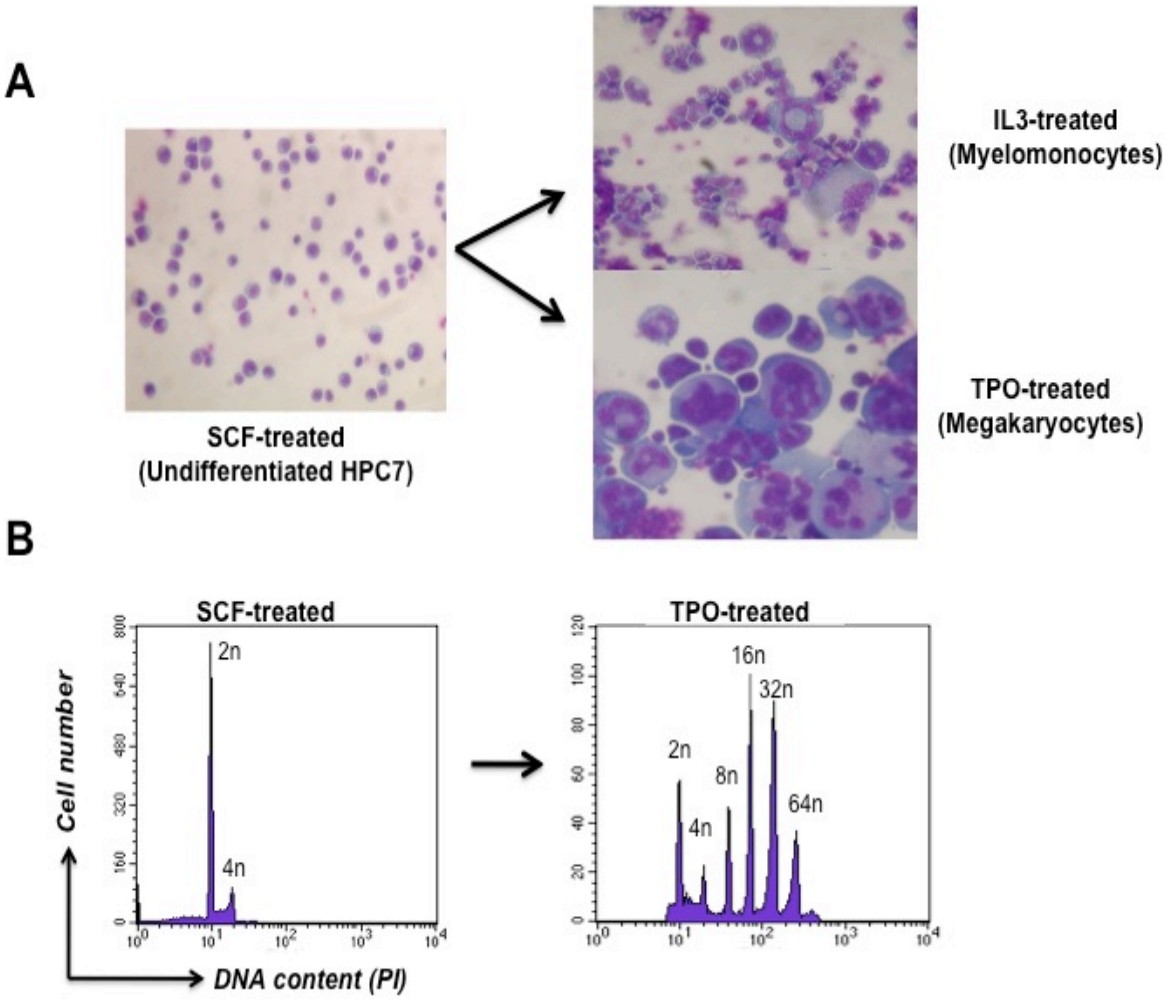

Figure 3.2 Morphological analysis of differentiation. (A) The HPC7 differentiation assay was performed for 96 hours by culturing the cells in the presence of IL-3 or TPO. Subsequently, cytospins and Diffquick stainings were performed on both HPC7 cells and their differentiated derivatives. The results demonstrate that HPC7 cells can be maintained undifferentiated in culture or can be induced to differentiate into megakaryocytes and mixed myelomonocytes. (B) The level of ploidy of TPO-treated cells was assessed by quantification of the DNA content in the cell using propidium iodide staining in combination with flow cytometric analysis. This figure represents the typical result obtained in three independent experiments.

3.2.3 RNA expression

In addition to the morphological analysis of HPC7 and the differentiated derivatives, I assessed the pattern of expression of a selected group of HSC- and lineage-associated genes by semi-quantitative RT-PCR. As expected for an HSC-like phenotype, undifferentiated HPC7 expressed high levels of *PU.1*, *Elf-2*, *GATA-1* and GATA-2, but low levels of Ets-1 and Ets-2 (Swiers et al.; 2006). Differentiation in the presence of TPO led to changes in this pattern of expression, in that the levels of *Ets-1, Ets-2, PU.1* and *GATA-2* RNAs decreased while the expression of *Fli-1* and *GATA-1* increased (Figure 3.3).

Taken together, these data support the idea that the HPC7 cell line represents a good model of haematopoietic stem cells.

3.3 FMH9: A model of Flt3^{+} AML

The FMH9 cell line was generated by infection of purified Sca+/Lin- bone marrow progenitors with retroviruses encoding the homeodomain transcription factors Meis-1 and HoxA9 (Kroon et al., 1998; Wang et al., 2006; Hess et al.; 2006). For this purpose, HoxA9 and Meis1 cDNAs where cloned downstream of the LTR (long terminal repeat) region in the MSCVneo and MSCVpuro vectors, respectively. Bone marrow cells infected with the two viruses, either alone or in combination, were grown in the presence of neomycin (HoxA9MSCVneo) and puromycin (Meis1aMSCVpuro) in order to test the drug-resistant proliferative capacity. The immortalized cells obtained were then transplanted into syngeneic recipients (Wang et al.; 2006)

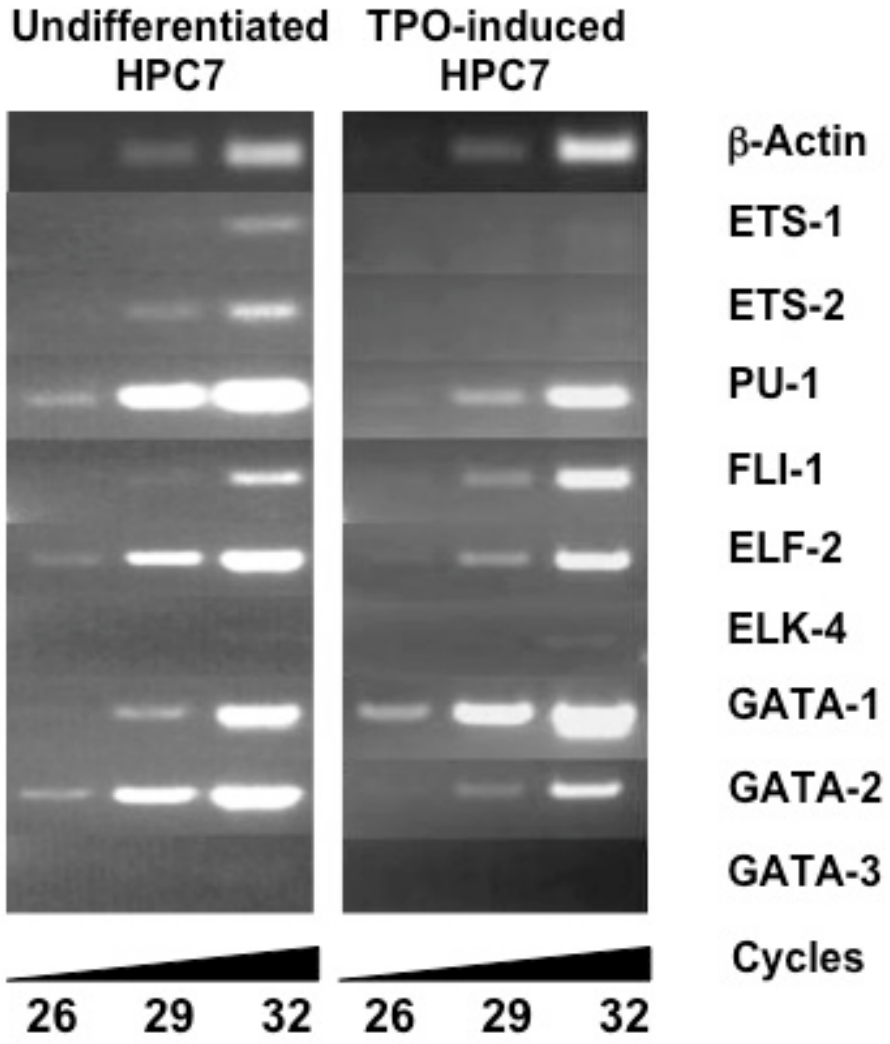

Figure 3.3 RNA expression. The gene expression of undifferentiated versus TPO-treated HPC7 cells was investigated by semi-quantitative RT-PCR. The genes analysed are indicated and primers sequences are provided in Material and Methods (Table 4). Each PCR reaction shown is represented by three samples starting at cycle 26, with three cycles intervals. The analysis of PCR products on ethidium-bromide-stained agarose gels revealed a distinct pattern of *Ets* and *GATA* factor RNA expression, distinguishing HPC7 stem cells from their differentiated derivatives. cDNA was normalized against *β-Actin*. This figure is representative of three indipendent experiments.

Only one out of nine recipients transplanted with HoxA9 immortalized progenitors developed leukaemia after a long latency (220 days) (Wang et al.; 2005). In contrast, all of the recipients of HoxA9/Meis1 immortalized cells developed leukaemia within 50 days. The cells transformed by HoxA9 and Meis1 possessed the characteristics of leukaemic blasts, that is, a high proliferative potential and blocked differentiation. Interestingly, the HoxA9/Meis1 transformed cells (FMH9) exhibited expression of Flt3, making them a potentially suitable model to investigate the deregulation of *flt3* gene expression in the context of AML. To further characterise FMH9 cells and compare them to the HSC-like HPC7 cells, I performed a similar analysis of surface antigens, differentiation capacity and transcription factors expression.

3.3.1 Surface antigen expression

FMH9 cells were stained for lineage-specific markers and stem cell-related antigens, and analysed by flow cytometry. This analysis showed positive staining for c-Kit and Sca-1, but an absence of the expression of CD34. The cells also showed high levels of expression of the lineage markers Gr-1 and Mac-1, indicative of a differentiation status roughly equivalent to a myelomonocytic progenitor. Most interestingly, the FMH9 cells were positive for Flt3, in accordance with their AML-like phenotype (Figure 3.4).

3.3.2 Differentiation capacity

Like HPC7 cells, FMH9 cells exhibit the ability to self-renew indefinitely in culture, remaining undifferentiated after multiple passages. Unlike HPC7 cells, it was

impossible to demonstrate any further maturation capacity of FMH9 cells in response to cytokines (Figure 3.5A), confirming a differentiation block at a myelomonocytic-like stage.

3.3.3 RNA expression

RT-PCR analysis was performed in order to determine the pattern of expression of specific transcriptional regulators. Compared to HPC7 cells, FMH9 exhibited similar expression of *Ets-1, Ets-2 and Fli-1*, but a lower level of *PU.1* and *Elf-2* RNAs and a complete lack of expression of the *GATA* factors (Figure 3.5B).

Taken together, these data suggest that FMH9 cells are more mature compared to HPC7, being blocked at the stage of a myelomonocytic progenitor.

3.4. Sorted Primary HSCs

As described in the Introduction (Section 1.11.4), flt3 gene expression is linked to the stage of maturation of HSCs within the KSL compartment. In order to validate findings in primary cells and to be able to compare *flt3* regulation in long- and short-term repopulating cells and MPPs, a standard sorting strategy was adopted in order to purify the $Flt3^-$ and the $Flt3^+$ fraction of the HSC KSL compartment. For each experiment, bone marrow cells were extracted from 5 mice and then stained using a cocktail of antibodies against lineage committed markers (Lin: B220, Ter119, CD5, CD8a, Gr-1 and Mac-1), combined with antibodies against the stem cell related antigens c-Kit, Sca-1 and Flt3. Cells negative for the lineage markers (Lin^-) were gated, followed by the selection of cells double-positive for Sca-1 and c-Kit (i.e. KSL cells).

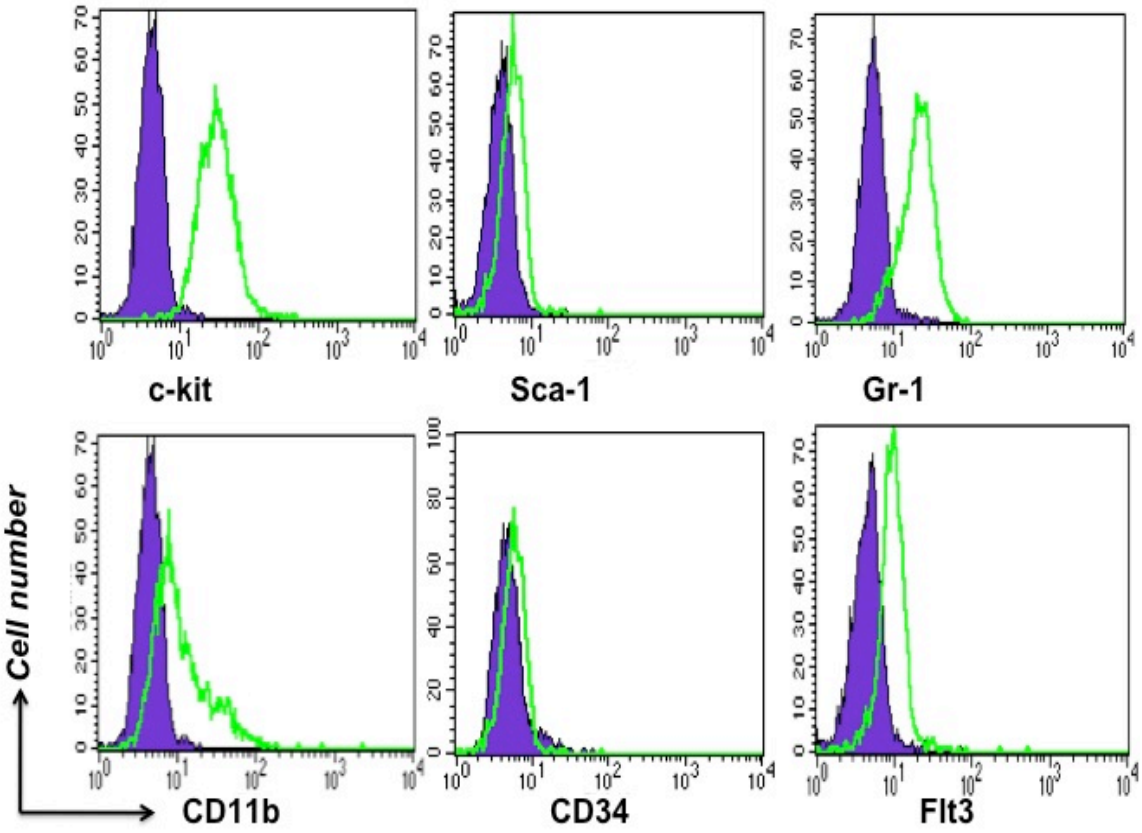

Figure 3.4 Phenotypic characterization of FMH9. FMH9 cells were stained with labelled antibodies against stem cell-related antigens (c-Kit, Sca-1, CD34 and Flt3) and lineage specific markers (Gr-1, CD11b), and analysed by flow cytometry. The filled histogram in each plot represent the matching isotype control while the line histogram indicates the staining obtained with each of the antibodies used. FMH9 cells express specific myelomonocytic markers Gr-1 and Mac-1, and show positive staining for c-Kit, Sca-1and Flt3 but not CD34. The positivity for each staining is determined by the shift of mean fluorescence compared to the control staining with the corresponding isotype control. This figure is representative of four indipendent experiments.

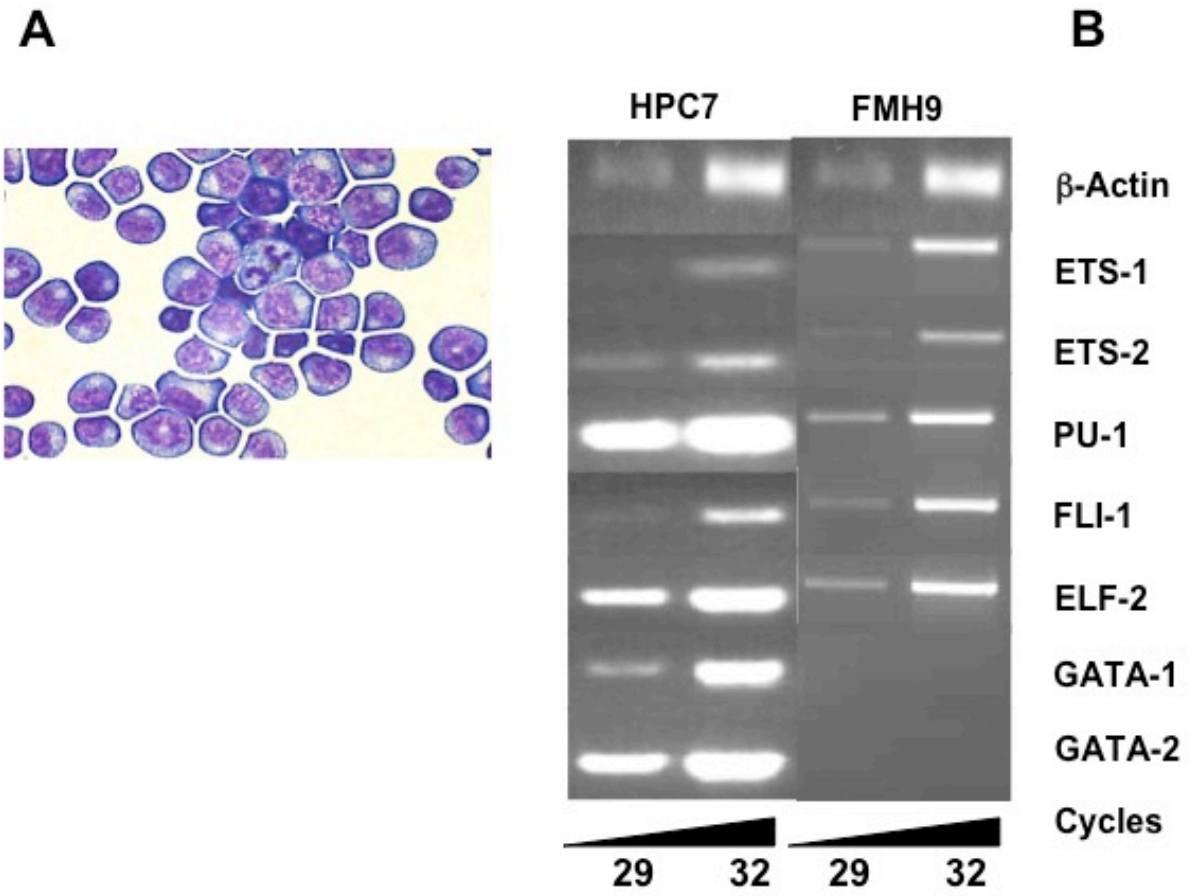

Figure 3.5 FMH9 differentiation and RNA expression analysis. (A) Diffquick staining of a cytospin prepared from FMH9 cells was carried out in order to verify the cell morphology. These cells were grown in RPMI supplemented with 10% of FBS, 5 ng/ml IL-3, 5 ng/ml IL-6, 5 ng/ml GM-CSF and 50ng/ml of SCF (described in Material and Methods, section 2.1). (B) A comparison of gene expression in undifferentiated HPC7 and FMH9 cells performed by semi-quantitative RT-PCR. The genes analysed are indicated and primers sequences are described in Materials and Methods (Table 4). The analysis of PCR products at cycles 29 and 32 was performed on ethidium-bromide-stained agarose gels. cDNA was normalized against *β-Actin* as a control. This figure represents the typical result obtained in three independent experiments.

Total KSL cells were then further fractioned, based on the expression of the Flt3 antigen; KSL Flt3$^+$ cells, which represent the MPP population, and KSL Flt3$^-$, which consist of LT- and ST-HSCs (Pohlmann et al.; 2001) (Figure 3.6). The number of purified cells obtained after sorting were roughly 2000 for KSL Flt3$^-$ and 3500 to 4500 for KSL Flt3$^+$.

3.5. Sorted primary committed progenitors

I adopted a second sorting strategy to obtain a population of cells with a higher degree of maturation relative to KSL cells, allowing comparison of the regulation of flt3 expression in cells that do not express flt3 yet (KSL Flt3$^-$), cells expressing flt3 (KSL Flt3$^+$) and cells that have lost its expression (committed progenitors). As for KSL isolation, bone marrow cells were stained using the Lin cocktail of antibodies combined with antibodies against the stem cell-related antigens c-Kit and Sca-1. In addition, antibodies against CD34 and CD16/32 were included. After the selection of Lin$^-$ cells, cells positive for c-Kit and negative for Sca-1 expression were gated and divided into three populations on the basis of their expression of CD34 and CD16/32: (i) CD34- CD16/32- (MEPs); (ii) CD34+ CD16/32+ (GMPs); and (iii) CD34- CD16/32+ (CMPs) (Akashi et al.; 2001) (Figure 3.7). The number of cells obtained was roughly 3000, 3500 and 2000 for MEPs, GMPs and CMPs, respectively.

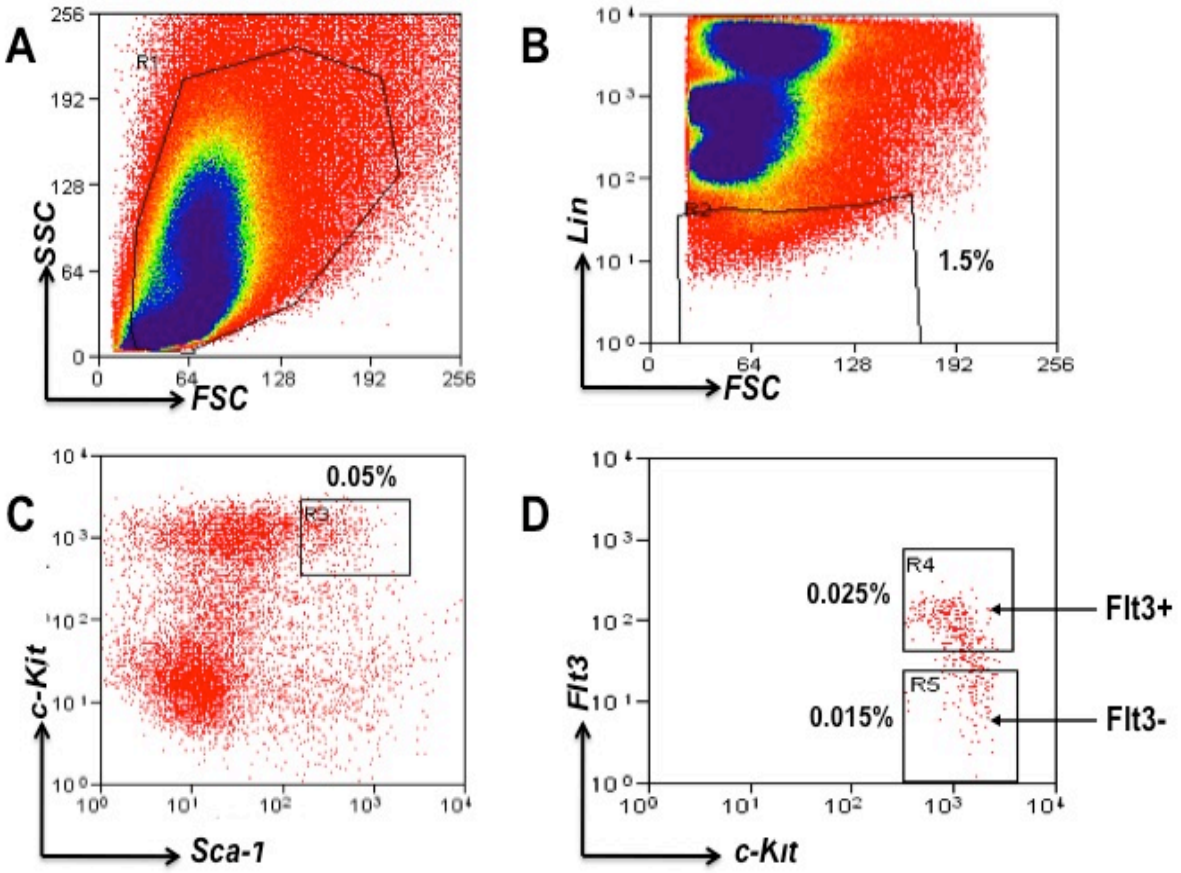

Figure 3.6 KSL sorting strategy. Total bone marrow cells were flushed from the tibias and femurs of five wild type mice. Following red cell lysis, the cell preparation was filtered to avoid cell clotting and fluorescently labelled with a cockatil of antibodies against lineage-committed markers (B220, CD5, CD8a, CD11b, GR-1 and Ter119) and stem cell-specific antigens Sca-1, c-Kit and Flt3. (A) Two-dimensional dot plot representing live cells (R1 region) gated on forward scatter (FSC) versus side scatter (SSC). (B) The two-dimensional dot plot represents the lineage negative fraction (R2 region) of the total bone marrow. (C) A two-dimensional plot representing the expression of stem cell-related antigens Sca-1 and c-Kit on the total lineage negative cells gated in panel B. Cells gated in region R3 represent the total KSL fraction of the bone marrow. (D) KSL cells were further analysed for the expression of Flt3. The Flt3+ cells in R4 region correspond to the multipotent progenitors (MPP) and Flt3- in R5 region group together both long-term (LT-HSC) and short-term stem cells (ST-HSC). This figure represents the typical result obtained in five independent experiments.

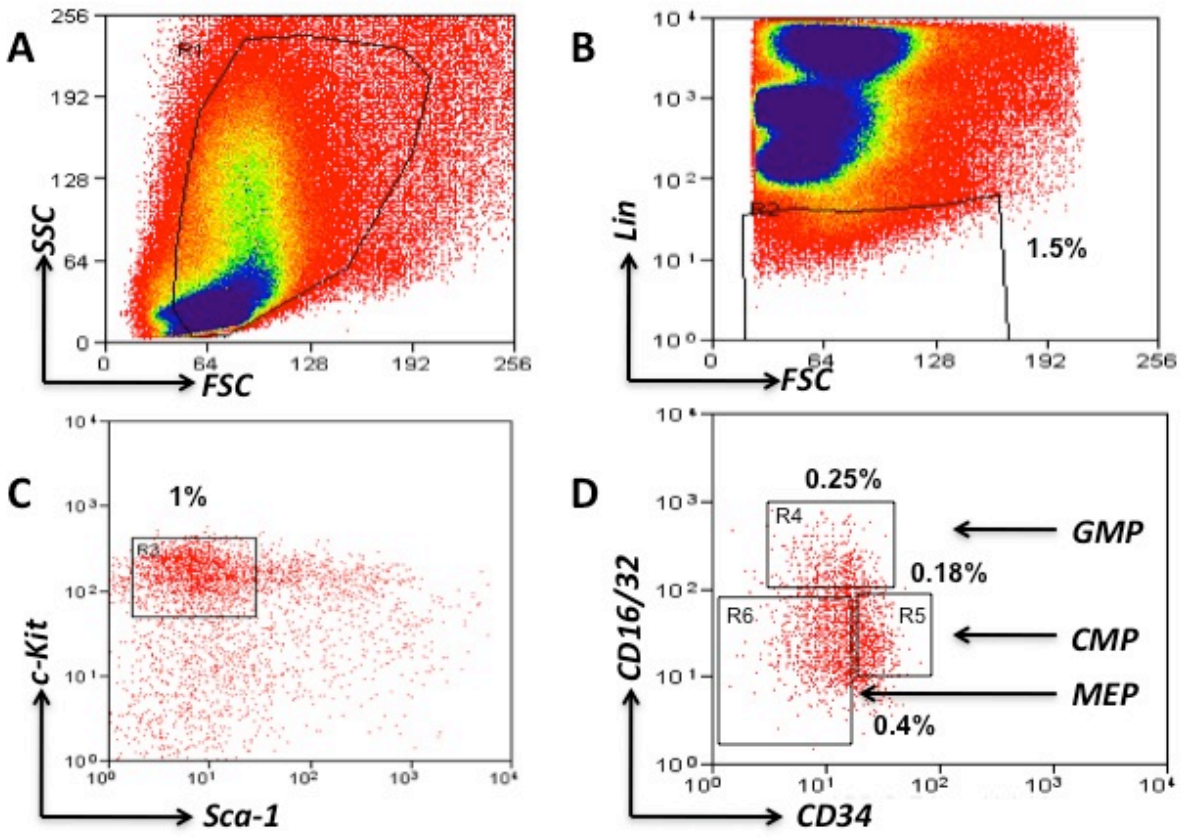

Figure 3.7. CMP/GMP/MEP sorting strategy. Total bone marrow cells were extracted from tibias and femurs of wild type mice and red cells were selectively lysed. The cell preparation was filtered to avoid cell clotting and fluorescently labelled with a cockatil of antibodies against lineage-committed markers (B220, CD5, CD8a, CD11b, GR-1 and Ter119) and stem cell-specific antigens Sca-1, c-Kit, CD34 and CD16/32. (A) Two-dimensional dot plot representing live cells (R1 region) gated on forward scatter (FSC) versus side scatter (SSC). (B) The two-dimensional dot plot respresents the lineage negative fraction (R2) of the total bone marrow. (C) Panel C shows the two-dimensional plot representing a cell population, of the total lineage negative cells gated in panel B, that shows positive staining for c-Kit and negative for Sca1. (D) Cells gated in the R3 region were further fractioned on the basis of the expression of CD34 and CD16/32. The indicated regions correspond to the Granulocyte-Macrophage Progenitors (R4), Megakaryocyte / Erythrocyte Progenitors (R5) and Common Myeloid Progenitors (R6). This figure represents the typical result obtained in three independent experiments.

3.6. Discussion

The principal objective of this chapter is to show that the cell systems used in this thesis are an appropriate representation of HSCs and AML cells and therefore suitable for the investigation of the regulation of the flt3 gene presented in the next chapter. The choice of the cell systems was dictated by the need for cell lines that both possess the typical characteristics of HSCs and AML and express *flt3*.

For this study I made use of an HSC-like line, HPC7, and an AML-like line, FMH9. In order to characterize these two cell lines, I analysed surface antigen expression, cell morphology, differentiation capacity and gene expression. I confirmed that the HPC7 cells, derived from ES cells transduced with the LIM-homedomain transcription factor Lhx2, possess characteristic stem cell-like features. Hence HPC7 exhibit self-renewal potential, a c-Kit$^+$ Sca-1$^+$ Lin$^-$ phenotype with low Flt3 expression, and multilineage differentiation potential in response to appropriate stimuli, although they showed very little or no reconstitution capacity when transplanted into irradiated recipients (Pinto do, et al., 1998). On the other hand, the FMH9 cells, generated from purified bone marrow progenitors co-transduced with HoxA9 and Meis1, revealed a more mature phenotype, being positive for Mac1 and Gr1, and apparently blocked at the stage of myelomonocytic differentiation. In addition, I showed that FMH9 cells have high expression of the stem cell marker Flt3, which normally would not be expressed at this stage of lineage differentiation (Adolfsson et al., 2001). In section 3.3, I show that FMH9 cells possess the principal characteristics of AML cells, that is, high proliferative potential and blocked differentiation. Most importantly, as shown by Wang and colleagues (Wang et al.,

2005), FMH9 cells possess the ability to establish a leukaemia when transplanted into irradiated mice. These use of these cell lines also represents a limitation of the work, first because they have a different origin; the HPC7 being derived from ES cells and the FMH9 cells from adult bone marrow, and also because they are transformed cells.

In conclusion, despite of the limitation mentioned above, HPC7 and FMH9 cells represent good models for the comparative study of HSC and AML, in regard to understanding the transcriptional and epigenetic regulation of the *flt3* gene.

CHAPTER 4:

TRANSCRIPTIONAL REGULATION OF THE FLT3 GENE IN HAEMATOPOIETIC AND LEUKAEMIC STEM CELLS

4.1 Introduction

In the past few years accumulating evidence has pointed to a pivotal role for Flt3 as a regulator of haematopoietic stem cells, several publications indicating an involvement of Flt3 in proliferation, differentiation and survival during the early stages of HSCs commitment, although the precise actions of the Flt3 receptor and its ligand are still unclear and subject of debate.

Despite the fact that there is substantial knowledge relating to the pattern of activation and nature of mutations in Flt3 in relation to leukaemia (described in Section 1.11.5), very little is known about the mechanism of transcriptional regulation that controls *flt3* gene expression either in leukaemic cells or in normal HSCs. A first hint as to how the normal or mutated *flt3* gene might be regulated was provided by Holmes and coworkers who demonstrated that the transcription factor Pax5 can have a negative effect on its expression (Nutt et al, 1999; Holmes el al, 2006). In this latter study, Pax5-/- pro-B-cells were transduced with a retroviral vector expressing Pax5 fused to the ligand-binding domain of the human oestrogen

receptor (Pax5ER); the activation of this vector upon the addition of β-oestradiol resulted in a significant decline in Flt3 expressed at the cell surface and a down regulation in *flt3* mRNA levels within four hours. Additionally, chromatin immunoprecipitation using an antibody against Pax5 revealed direct binding of the factor on the *flt3* promoter in a region within 200 bp upstream of the transcriptional start site. As described in Section 3.3, Wang and colleagues showed that the retroviral expression in myeloid progenitors of Meis1 in combination with HoxA9 results in a myeloid leukaemia resembling AML within eight weeks, and that this was associated with the up regulation of the Flt3 receptor (Wang et al.; 2006). Furthermore, the enforced expression of Meis1 in HoxA9-immortalized SCF-dependent progenitor cells resulted in increased flt3 expression and allowed proliferation in the presence of only Flt3 ligand (FL). ChIP performed on the transformed myeloid cells using antibodies against Meis1 (Meis1-FLAG) and HoxA9 (HoxA9-HA) revealed the recruitment of these two homeodomain transcription factors on the proximal promoter and enhancer regions, recruitment of Meis1 on the promoter region being accompanied by both H3K4 methylation and acetylation of histone 3, suggesting that Meis1 over expression may result in epigenetic modifications of histone 3 prior or associated with the activation of flt3 transcription.

From what I have described above and what is known about the normal and leukaemia-associated expression of *flt3*, it is apparent that there is a need to further elucidate the mechanisms of transcriptional and epigenetic regulation of the flt3 gene. In this chapter I will describe studies in which I have investigated the gene regulatory regions of the *flt3* gene in HSCs (represented by the model cell line

HPC7) in comparison to myeloid leukaemic cells (represented by the HoxA9/Meis1-transformed cell line FMH9) and primary sorted HSCs and committed progenitor cells.

The first step in the investigation of the mechanisms of regulation of a particular gene commonly involves the location of putative cis-regulatory elements, which can be achieved by DNAseI nuclease hypersensitivity mapping (Wu, et al; 1979). This can be followed using chromatin immunoprecipitation to demonstrate the in vivo binding of transcription factors and chromatin modifying enzymes and to define the modification status of individual histone tail residues. Finally, functional studies may be performed in order to elucidate the importance of the identified cis-regulatory regions and the various proteins that have been shown to bind to them.

4.2 Sequence conservation

One of the aims of this investigation is to locate and characterize the cis-regulatory elements that are involved in the control of *flt3* gene expression. Since these elements are likely to have been conserved among species, indentifying the peaks of sequence homology over the locus is the first step towards locating cis-regulatory elements. The murine *flt3* gene is located on chromosome 5 and consists of 24 exons spread over more than 80 kbp. A schematic representation of the promoter and the first intron is shown in Figure 4.1A. The *flt3* gene is characterized by an abundance of repeated sequences and an overall low degree of cross-species sequence conservation, as shown by the analysis performed using Genome Browser. The *flt3* locus on chromosome 5 is syntenic with multiple species,

including human, rat, dog and xenopus, as indicated by the presence of orthologous genes (*Pan3, Cdx2, Pdx1*) in the same orientation upstream and downstream of the *flt3* gene (data not shown). Figure 4.1 shows the alignment of the human, mouse, rat and dog sequences, revealing two regions of particular sequence conservation, one centred on the promoter and exon 1 and another in the first intron at approximately 7.6 kbp downstream of the transcription initiation site, with a smaller region of conservation located approximately 1.3 kbp upstream of the translation initiation codon (Figure 4.1B).

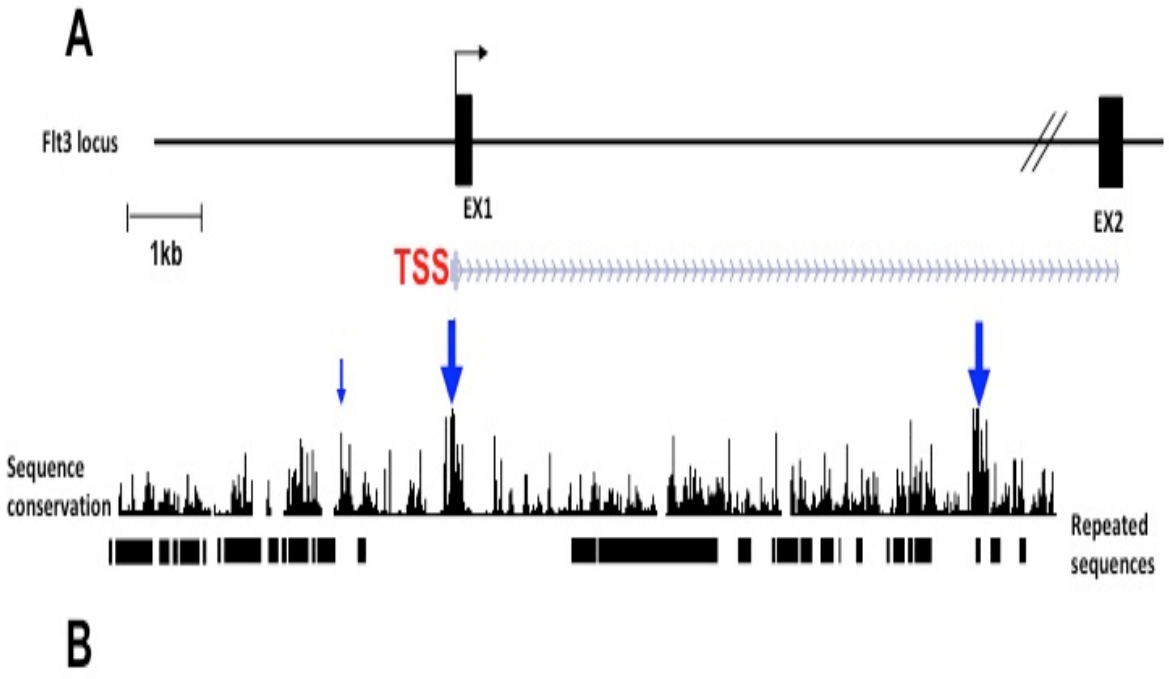

Figure 4.1 The *flt3* gene promoter region. (A) Exons 1 and 2 are represented by filled boxes with the transcription initiation site indicated by the arrow. (B) Graphical representation of a multispecies alignment taken form the NCBI database showing the homology between mouse, human, rat and dog sequences. Blue arrows indicate regions of sequence conservation. The transcriptional start site (TSS) is also indicated.

Analysis of sequence homology performed outside of mammalian species revealed (eg in vertebrates) confirmed the intronic region as the unique conserved region apart from the exons (not shown). Figure 4.1 also shows that there is a unique transcribed RNA, indicated by the grey line in the middle panel.

4.3 Identification of cis-regulatory elements by DNAseI HSS analysis

In order to further investigate the regions of sequence conservation I performed a DNAseI hypersensitive site mapping. Mapping the DNAseI HSS within nuclear chromatin is a well-established and powerful approach for identification of the regulatory elements controlling the transcription of a gene. Two approaches can be taken to map HSS: (i) Southern blot hybidization, which allows scanning of a large region of the gene body, but is suitable mainly for cell line analysis because of the large amount of DNA required; and (ii) Real time PCR, which can be applied to small number of cells, therefore making it suitable for the study of primary cells (described in Material and Methods).

4.3.1 Southern blot hybridization approach

In order to assess the importance of the two conserved regions in the regulation of the flt3 gene in HPC7 cells nuclei were treated with increasing concentrations of DNAseI and genomic DNA was then extracted as described in Materials and Methods. The DNA (5 μg) was digested with either StuI or BamHI and subsequently

blotted and hybridized respectively to probe A or probe B, fragments covering the promoter and first intron of the *flt3* gene (Figure 4.2A).

4.3.1.1 HPC7

Hybridisation of probe A to the blot of StuI-digested DNAs revealed a parental band of 8.1 kbp. This band was present in all the DNA samples, but at higher concentrations of DNAseI (60 units) it was partially cleaved into two discrete bands of 6.9 kbp and 4.1kbp, corresponding to two HSSs located at -2.4 kbp (HS2) and -0.15 kbp (HS4), and two minor bands of 2.5 kbp and 4.9 kbp, corresponding to HS1 and HS3 located at -1.4 kbp and -4kbp relative to the transcription start site (Figure 4.2). Hybridisation of probe B to the blot of BamHI-digested DNAs revealed a parental band of 18.9 kbp. In samples derived from nuclei treated with DNaseI the parental band was partially cleaved releasing a 8.9 kbp fragment corresponding to another HSS (HS5) located at +7.5 kbp (Figure 4.2). Interestingly, three of the five sites (indicated by the red arrows in panel A of Figure 4.2) are positioned over the regions of sequence conservation around the promoter (HS4) and in the first intron (HS5).

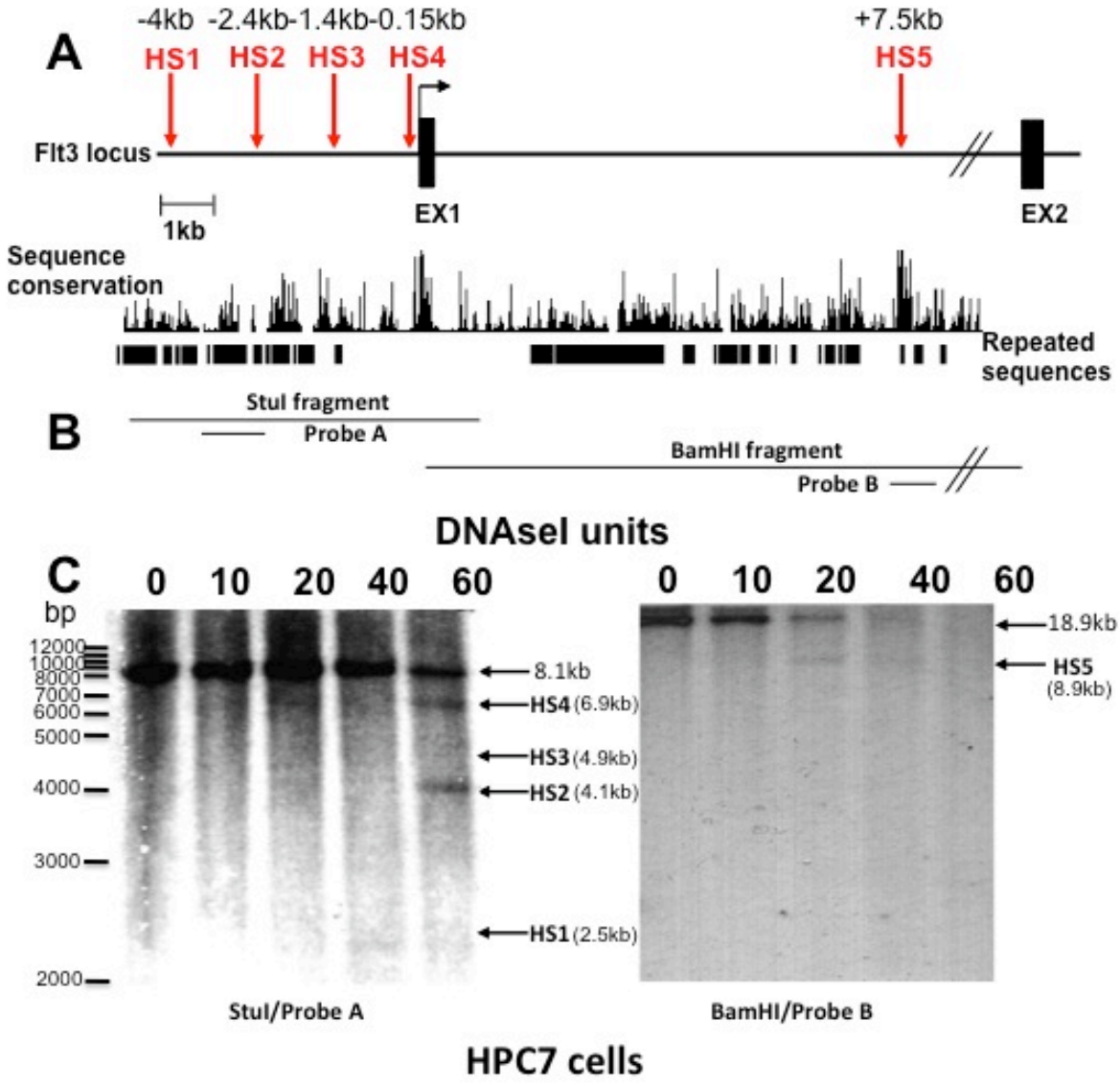

Figure 4.2 DNAseI hypersensitive site mapping in HPC7 cells. (A) Schematic representation of the *flt3* locus and regions of sequence conservation. (B) Position and length of the fragments generated by StuI and BamHI restriction digestion and the location of the probes used for Southern blot. (C) Identification of hypersensitive sites was achieved using StuI/probe A for the promoter region and BamHI/probe B for the intronic region. Probes were radiolabelled with [^{32}p] dCTP and the hybridized blot exposed to film overnight. The position of the HSSs is indicated by the arrows. This figure represents the typical result obtained in four independent experiments.

4.3.1.2 FMH9

In order to gain information about possible differences in the regulation of the *flt3* gene in HSCs compared to Flt3+ leukaemic cells, a similar hybridization analysis was performed on DNA prepared from DNAseI-treated FMH9 cell nuclei. As expected, hybridization of probe A to the blot of StuI-digested FMH9 DNAs revealed the same parental band of 8.1 kbp seen for HPC7. This band was cleaved at higher concentrations (40 units of DNAseI) giving rise to the same bands of 6.9 kbp, 4.9 kbp and 4.2 kbp (corresponding to HS2, HS3 and HS4) already seen using HPC7, and a lower band of 2.5 kbp corresponding to a HSS, indicated as HS4, located at -4 kbp upstream of the transcription start site (Figure 4.3C). Hybridization of probe B to the blot of BamHI-digested DNAs highlighted the expected parental band of 18.9 kbp. The parental band decreased in intensity in proportion to the increased amount of DNAseI units used; this band disappeared completely at high concentrations (40 units) highlighting the presence of a broad region of sensitivity, different from the HS5 seen in HPC7 (Figure 4.3C).

The Southern blot approach revealed the presence in HPC7 cell DNA of three HSS in the promoter region, two of which showed a similar degree of hypersensitivity, and one in the intronic region (Figure 4.2C). Corresponding HSS were found to be present in FMH9 but showed a different pattern of hypersensitivity, with HS4 appearing stronger compared to the HS2. HS5 in FMH9 cell DNA seemed to be replaced by a broader region of sensitivity, appearing as a smear rather than a discrete band.

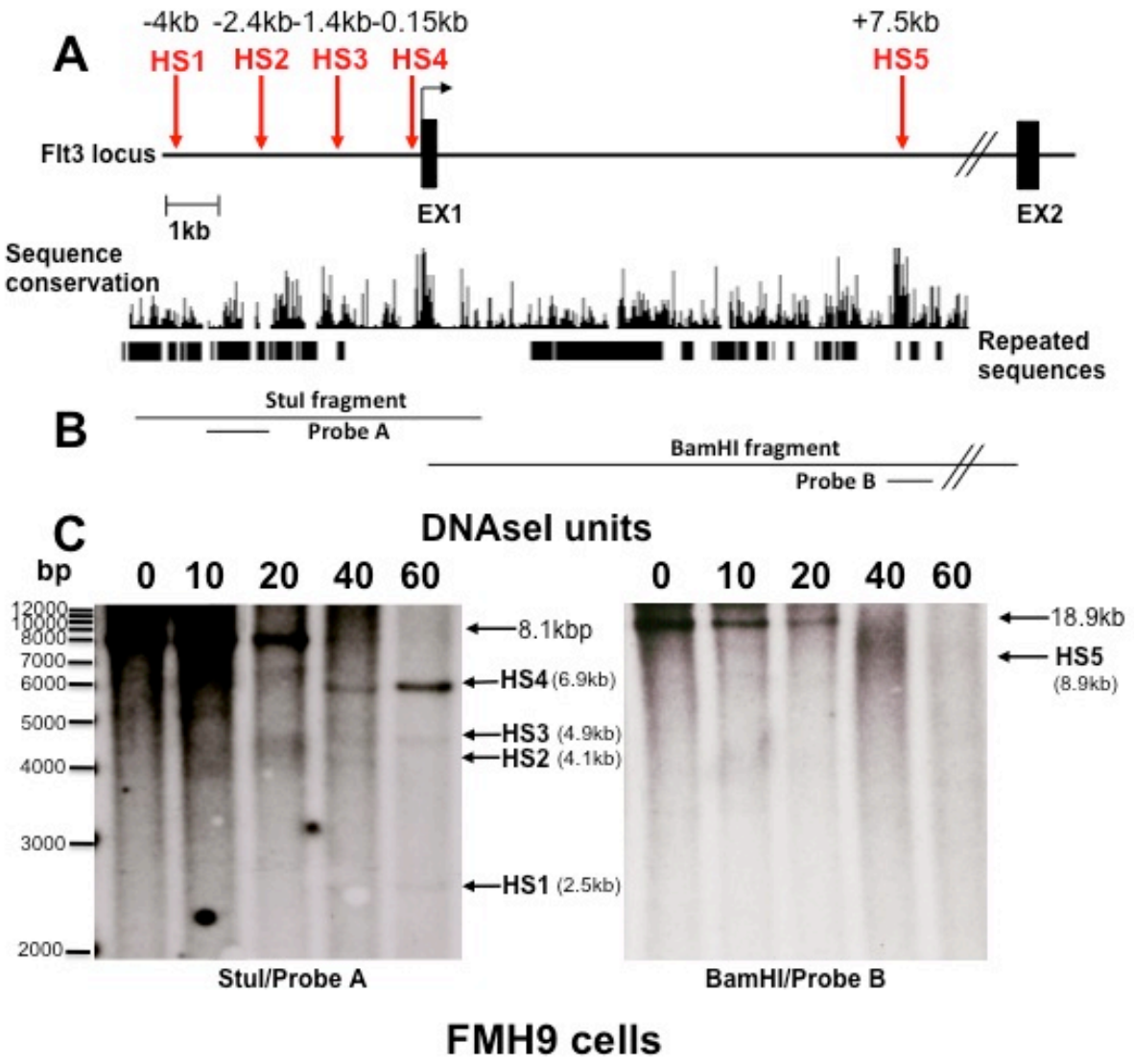

Figure 4.3 DNAseI Hypersensitive site mapping in FMH9 cells. (A) Schematic representation of the *flt3* locus and regions of sequence conservation. (B) Position and length of the fragments generated by StuI and BamHI restriction digestion and the location of the probes used for Southern blot. (C) Identification of hypersensitive sites was achieved using StuI/probe A for the promoter region and BamHI/probe B for the intronic region. Probes were radiolabelled with [^{32}p] dCTP and the hybridized blot exposed to film overnight. The position of the HSSs is indicated by the arrows. This figure represents the typical result obtained in three independent experiments.

4.3.2 Real time PCR approach

To confirm the findings obtained by Southern blot hybridization and to define more precisely the region of hypersensitivity across the promoter and first intron of the flt3 locus, the relative amount of intact DNA was determined by quantitative real time PCR, comparing DNAseI-digested versus undigested DNA samples from HPC7 and FMH9 nuclei. For this purpose specific primers spanning the regions of interest of the *flt3* locus were designed (details provided in Materials and Methods). The analysis of the HS1 was not possible because the abundance of repeats in the vicinity of this HSS precluded the design of suitable PCR primers. The data represented in Figure 4.4 depicts the ratio between DNAseI-digested versus undigested DNA, reflecting the relative amount of digestion (represented on the Y-axis) compared to the position relative to the translation start site (represented on the X-axis).

4.3.2.1 HPC7

PCR analysis of DNA prepared from DNAseI (60 units)-treated versus untreated HPC7 DNA revealed the presence of three HSS positioned at -2.4 kbp (HS2), -1.35 kbp (HS3) and -150 kbp (HS4) in the promoter region, perfectly correlating with the sites determined by Southern blot hybridization. The analysis of the intronic HSS also confirmed the presence of HS5 positioned at +7.5 kbp. Interestingly the PCR amplification across this region also revealed the existence of a second peak of DNAseI hypersensitivity located at +7.75 kbp, although this exhibited a lower degree of sensitivity (Figure 4.4, top panel).

4.3.2.2 FMH9

The analysis of the promoter and intronic regions in DNA obtained from FMH9 also confirmed the presence of the four HSS observed in HPC7. The distance from the transcription start site and the correlation of the HSS with the peaks of sequence homology are indicated in Figure 4.4 (top panel). Interestingly, the two cell lines show a similar pattern and degree of sensitivity in the promoter region, but the HS5 site in the HPC7 cells is characterized by a high degree of sensitivity compared to the other sites found in the same cell line; this observation does not reflect what is seen in the FMH9 cell line, since the different peaks show a similar degree of sensitivity (Figure 4.4, lower panel). This analysis shows that comparing the HSC and leukaemia cell lines there are both similarities and differences in the *flt3* promoter and first intron chromatin structures, suggesting common and distinct regulatory features.

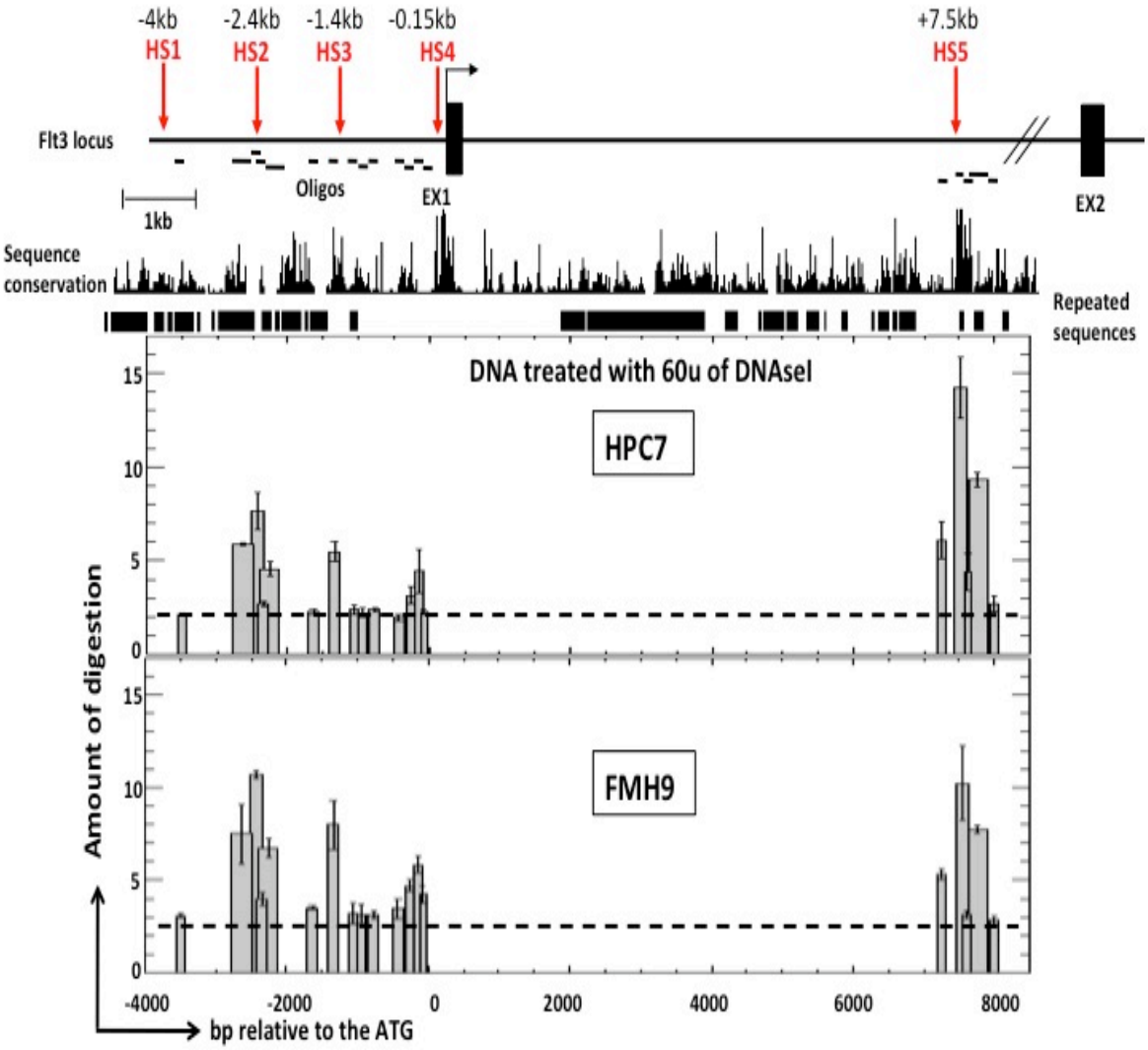

Figure 4.4. Analysis of DNAseI hypersensitivity at the *flt3* locus. Nuclei from both HPC7 and FMH9 cell lines were treated with 0 or 60 units of DNAseI and the purified DNA was used as the template for quantitative real time PCR reactions. The ratio between digested and undigested samples reflects the extent of hypersensitivity across regions covered by the PCR amplicons. The top panel shows a schematic representation of HSS mapped onto the *flt3* locus relative to the translational start site, the position of the oligos used, as well as the inter-species sequence conservation and the presence of repeated sequences. All graphics are aligned to the *flt3* locus schematic. This figure represents the typical result obtained in five independent experiments in which each PCR was performed in triplicate. The width of the bars in the plot reflects the length of the amplicons. PCR amplicons overlap as indicated.

4.3.2.3 Primary KSL

As a result of the small numbers of primary KSL cells, the amount of DNA obtainable following DNAseI digestion was only sufficient to allow an analysis restricted to the regions of the HSSs. In the case of Flt3+ KSL cells, which represent the MPPs, both HS3 and HS5 domains showed a high degree of hypersensitivity to 60 units of DNAseI when compared to the undigested DNA control. Analysis of the HS2 region revealed very little digestion, while no hypersensitivity was detected at the HS4 element (Figure 4.5, top panel). A similar analysis of Flt3- KSL cells, which represent LT- and ST-HSCS, treated with the same amount of DNAseI revealed a very pronounced sensitivity to nuclease digestion at the promoter region at HS3, equivalent to that observed in Flt3+ cells. In contrast, no hypersensitivity was observed at HS5 in the intronic region or at HS2 and HS4 in the promoter (Figure 4.5, lower panel). These findings suggest that the intronic HS5 region may be associated with the activation of *flt3* expression during the transition from ST-HSCs to MPPs.

4.3.2.4 Primary CMP

Having demonstrated that HS3 appears relevant in both Flt3- and Flt3+ KSL HSCs and that the intronic HS5 could be linked to the activation of *flt3* gene expression in MPPs, the next step was to perform DNAseI HSS analysis in a down stream cell population that has lost the expression of *flt3* following commitment. For this reason CMP, GMP and MEP committed progenitors were sorted (as described in section 3.5) and subjected to the same analysis described for KSL cells. The small number

of cells obtained also limited this approach. DNA isolated from CMP cells digested with 60 units of DNAseI exhibited no sensitivity at any of the cis-regulatory regions (Figure 4.6A). Unsurprisingly, since the expression of the *flt3* gene has been down regulated during the transition from MPP to more committed progenitors, neither GMP or MEP cell DNAs showed any signs of hypersensitivity at the selected regions (Figure 4.6B and C). No specific positive control have been used for this experiment, however the DNAseI HSS mapping in these cells was performed in parallel with the KSL cells (see section 4.3.2.3), ensuring the efficiency of this approach.

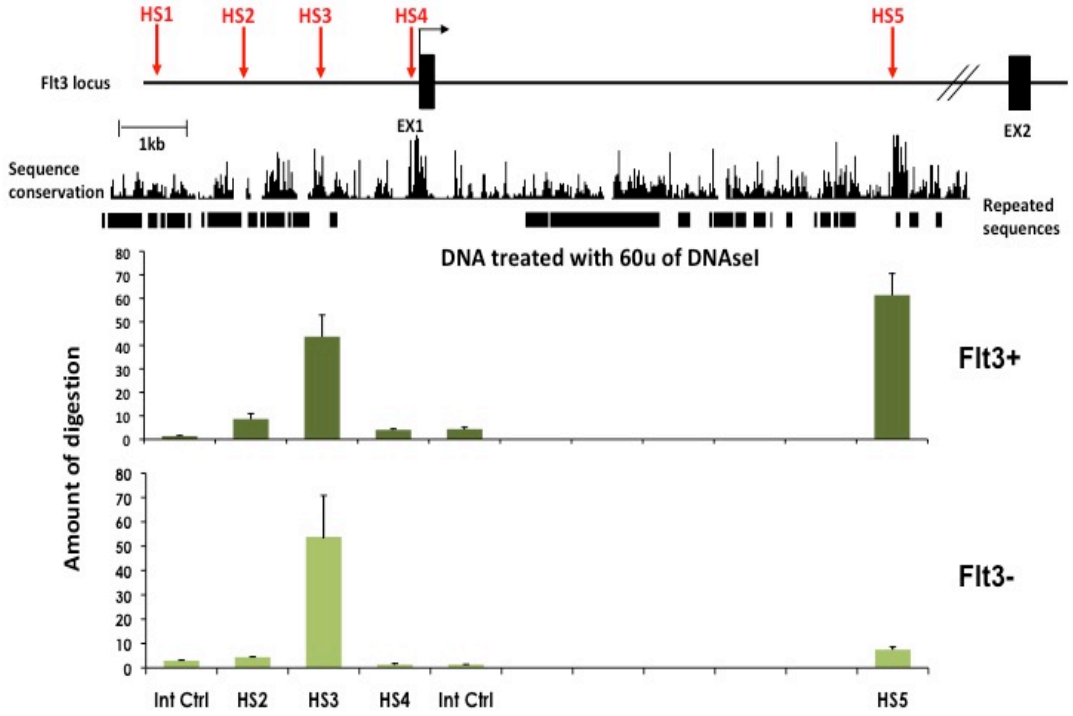

Figure 4.5 DNAseI Q-PCR HSS analysis of the *flt3* promoter and intronic region in primary Flt3+ and Flt3- KSL cells. Nuclei from sorted KSL cells were treated with 0 or 60 units of DNAseI and purified DNA was used for Q-PCR amplification using primers spanning the cis-regulatory regions of interest. The amount of DNAseI digestion at HS2-5 and two internal control regions are plotted on the Y-axis and are aligned to the schematic of the flt3 locus (top panel). Details of the PCR primers used are provided in Materials and Methods. This figure represents the typical result obtained in five independent experiments in which each PCR was performed in triplicate.

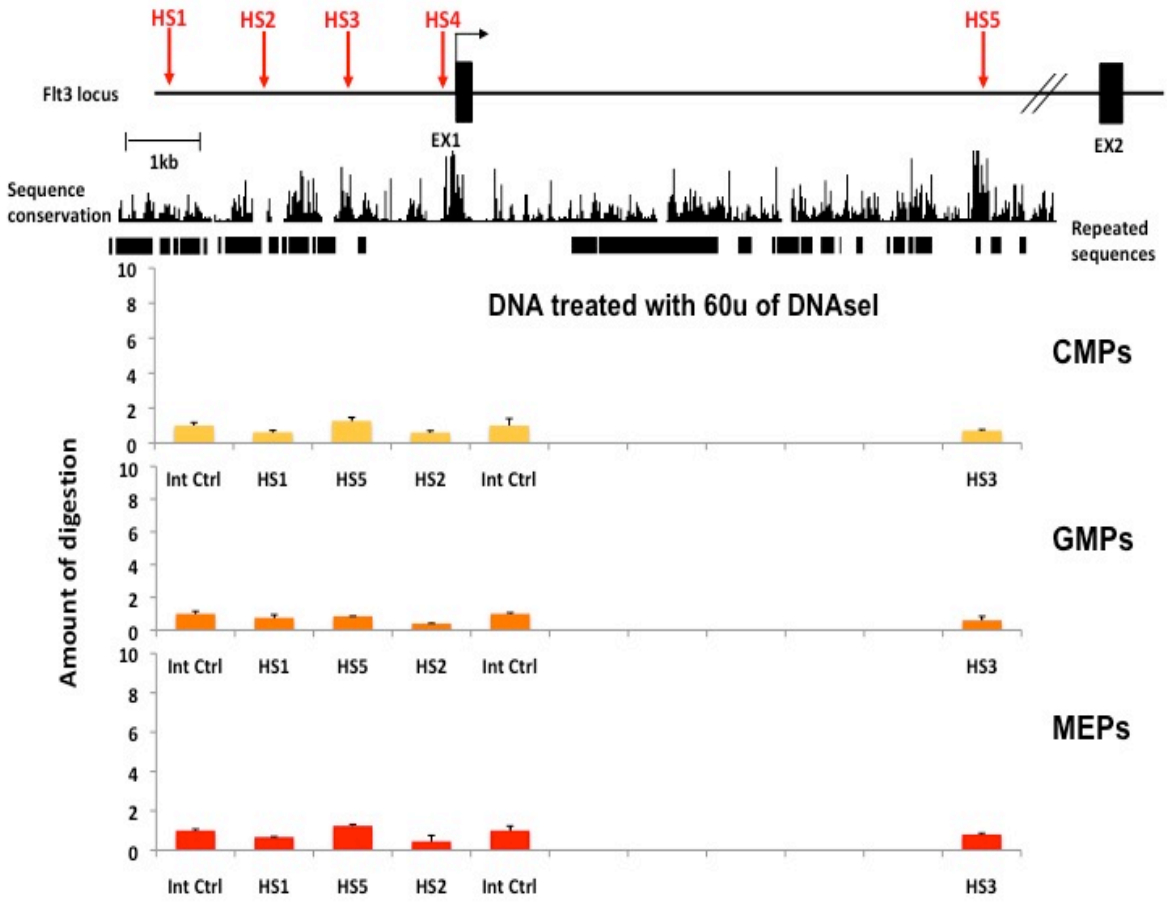

Figure 4.6 Analysis of DNAseI hypersensitivity at the *flt3* locus in sorted CMP, GMP and MEP populations. Sorted CMP, GMP and MEP cells were digested with 60 units of DNAseI and purified DNA from each cell population was used to measure hypersensitivity at the *flt3* locus relative to undigested cells. Ratios of Q-PCR amplification between digested and undigested cells shown on the Y-axis reflect the amount of digestion. Regions of interest and their relative sequence conservation are indicated in the top panel. This figure represents the typical result obtained in three independent experiments in which each PCR was performed in triplicate.

4.4 Epigenetic regulation of the *flt3* locus in normal versus leukaemia-like cells

In order to characterize the epigenetic profile on the *flt3* locus in HSC-like cells and in the Flt3+ leukaemia model cell line, I next assessed the distribution of histone marks that are associated with transcriptional activity or silencing (Turner; 2005), or that have been reported to be specifically enriched in leukaemic cells (eg H3K79me3) (Krivtsov et al.; 2008). I also wish to correlate the histone marks with the presence of the hypersensitive sites (determined in section 4.3) across the *flt3* locus. Formaldehyde cross-linkied chromatin immunoprecipitation (X-ChIP) analysis was performed using specific antibodies against acetyl groups on lysine 9 and 8 of histones 3 and 4, respectively (H3K9ac and H4K8ac), and the dimethylation of lysine 9 and the trimethylation of lysine 4 and 79 on histone 3 (H3K9me2, H3K4me3 and H3K79me3). Immunoprecipitated DNA was analysed by real time PCR, focussing on the regions surrounding the cis-regulatory elements identified by DNAseI HSS assay in order to determine the pattern of histone modifications around these elements. The relative enrichment displayed in each plot of this section corresponds to the ratio Bound specific IgG/Bound non-specific IgG (purified normal IgG) obtained by subtracting the non-specific binding from the IgG/protein A-G agarose bound. Specific patterns of modifications were determined after normalisation to the basal level across the locus, which provides the internal control. No reference to external negative or positive controls is shown.

4.4.1 H3K4me3

The analysis of anti-H3K4me3 immunoprecipitated DNA from HPC7 cells, a mark generally associated with transcriptionally active chromatin, revealed the presence of this modification just upstream of the transcriptional start site, and most predominantly in the region encompassing the intronic HS5 element. A similar analysis performed on FMH9 cells highlighted the broader presence of this mark on the intronic domain compared to that seen in HPC7 and a distinct similar profile around the promoter consisting of modification in the region of HS3 and a shift of the major peak away from HS4 to a position downstream of exon 1 (Figure 4.7).

4.4.2 H4K8ac

The H4K8Ac modification, a histone mark normally associated with active chromatin, seemed to exhibit no significant enrichment over the *flt3* locus in HPC7 cells, whereas in FMH9 cells the mark appears to be quite predominant, and in particular at the upstream HSS, HS1 and HS2, downstream of exon 1 and at the intronic HS5 element (Figure 4.8).

4.4.3 H3K9ac

Acetylation at histone 3 lysine 9, a histone modification tipically associated with active chromatin, was very marked upstream of the promoter and at the intronic HS5 region in HPC7. In contrast, in FMH9 the peak of modification around the promoter was down stream of exon 1, although a similar degree of modification was apparent at HS5, with a large peak of acetylation immediately upstream this regulatory domain (Figure 4.9).

4.4.4 H3K9me2

The analysis of DNA prepared from chromatin immunoprecipitated with an antibody anti-H3K9me2, an histone mark associated with gene repression, exhibited no significant peaks of modification across the *flt3* promoter/intron 1 region in HPC7 cells. However, a similar analysis of chromatin from FMH9 cells revealed an abundance of this mark in the region encompassing HS2 (Figure 4.10).

4.4.5 H3K79me3

No evidence was obtained for a significant concentration of this mark around the promoter and intron 1 regions of the *flt3* locus in either HPC7 or FMH9 cells, although a small degree of enrichment was perhaps seen in HPC7 at the transcription initiation site (Figure 4.11).

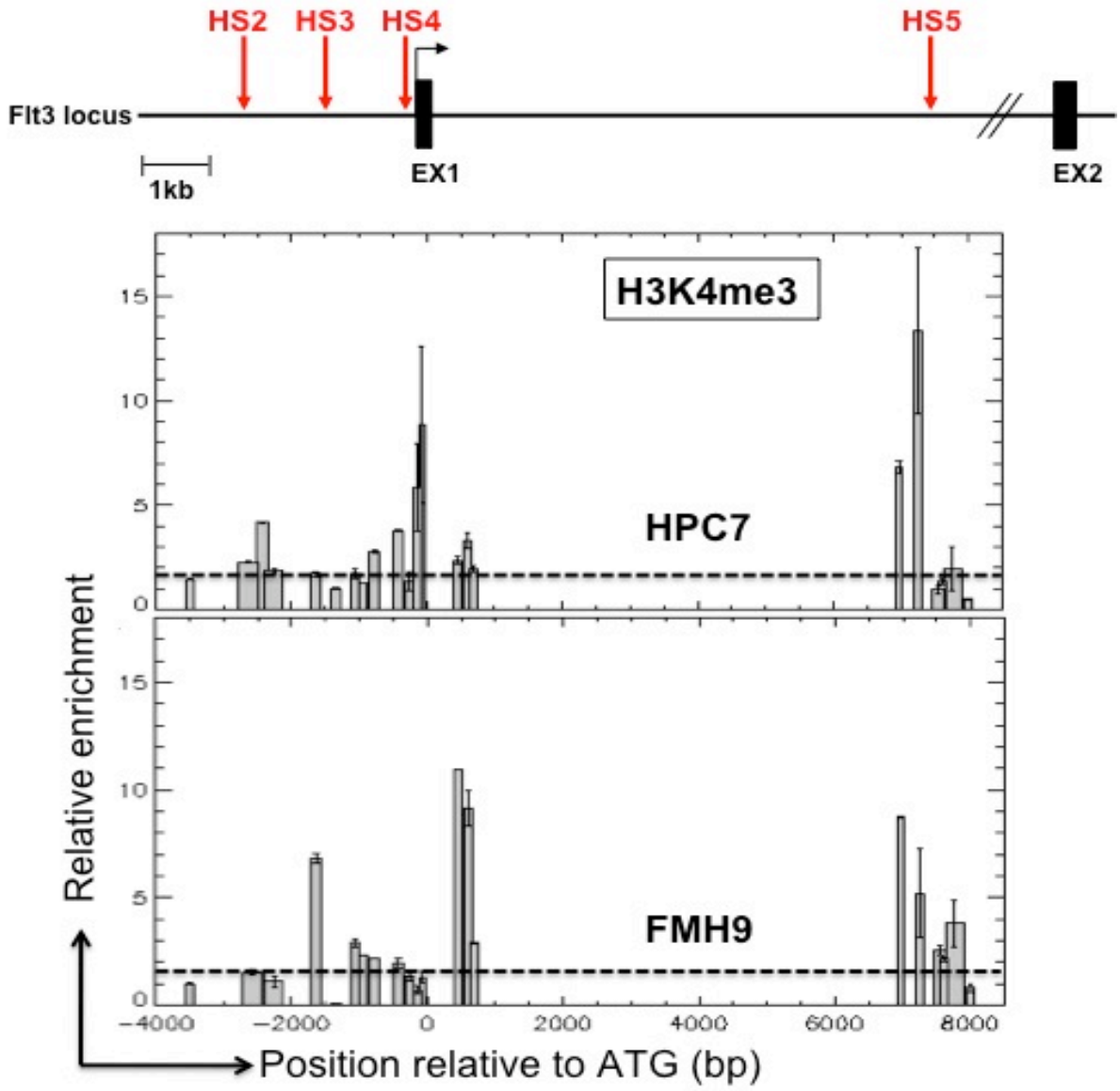

Figure 4.7 Analysis of the H3K4me3 histone modification at the *flt3* locus. X-ChIP experiments were performed on chromatin derived from both HPC7 and FMH9 cell lines using an antibody against the tri-methylation modification on lysine 4 of histone 3. Purified immunoprecipitated DNA was used as a template for Q-PCR amplifications to determine the relative enrichment compared to the control IgG ChIP material. The plots represent the relative enrichment on the Y-axis and the position relative to the transcriptional start site on the X-axis. The figure shows the alignment of the histograms with a schematic representation of the *flt3* promoter and first intron. DNAseI HSSs are indicated by red arrows. Dashed line represent the basal level across the locus. This figure represents the typical result obtained in three independent experiments in which each PCR was performed in triplicate. The width of the bars in the plot reflects the length of the amplicons. PCR amplicons overlap as indicated.

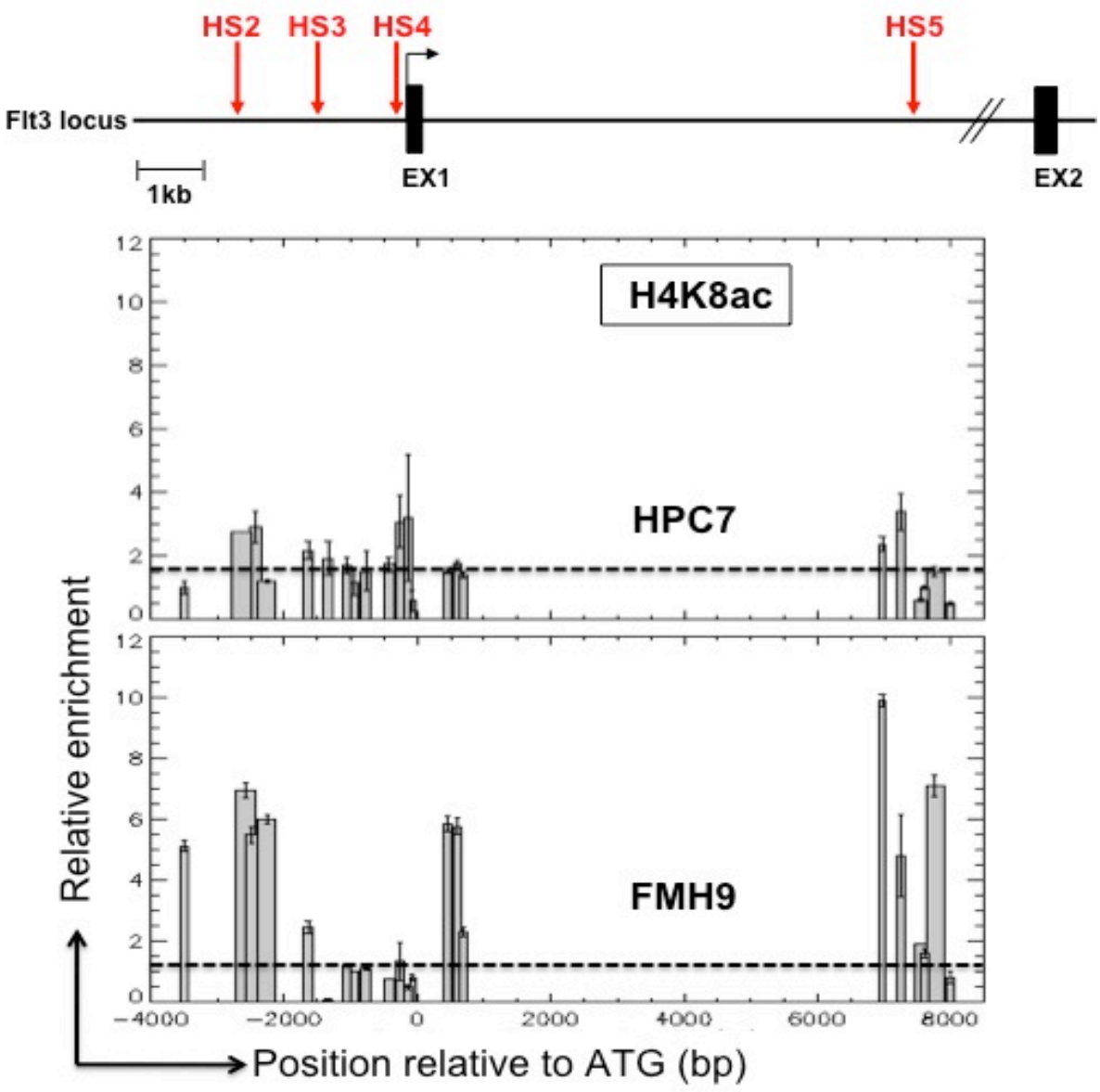

Figure 4.8 Analysis of the H4K8Ac histone modification at the *flt3* locus. X-ChIP experiments were performed on chromatin derived from both HPC7 and FMH9 cell lines using an antibody against the acetylation of lysine 8 on histone 4. Purified immunoprecipitated DNA was used as a template for Q-PCR amplifications to determine the relative enrichment compared to the control IgG ChIP material. The plots represent the relative enrichment on the Y-axis and the position relative to the transcriptional start site on the X-axis. The figure shows the alignment of the histograms with a schematic representation of the *flt3* promoter and first intron. DNAseI HSSs are indicated by red arrows. Dashed line represent the basal level across the locus. This figure represents the typical result obtained in four independent experiments in which each PCR was performed in triplicate. The width of the bars in the plot reflects the length of the amplicons. PCR amplicons overlap as indicated.

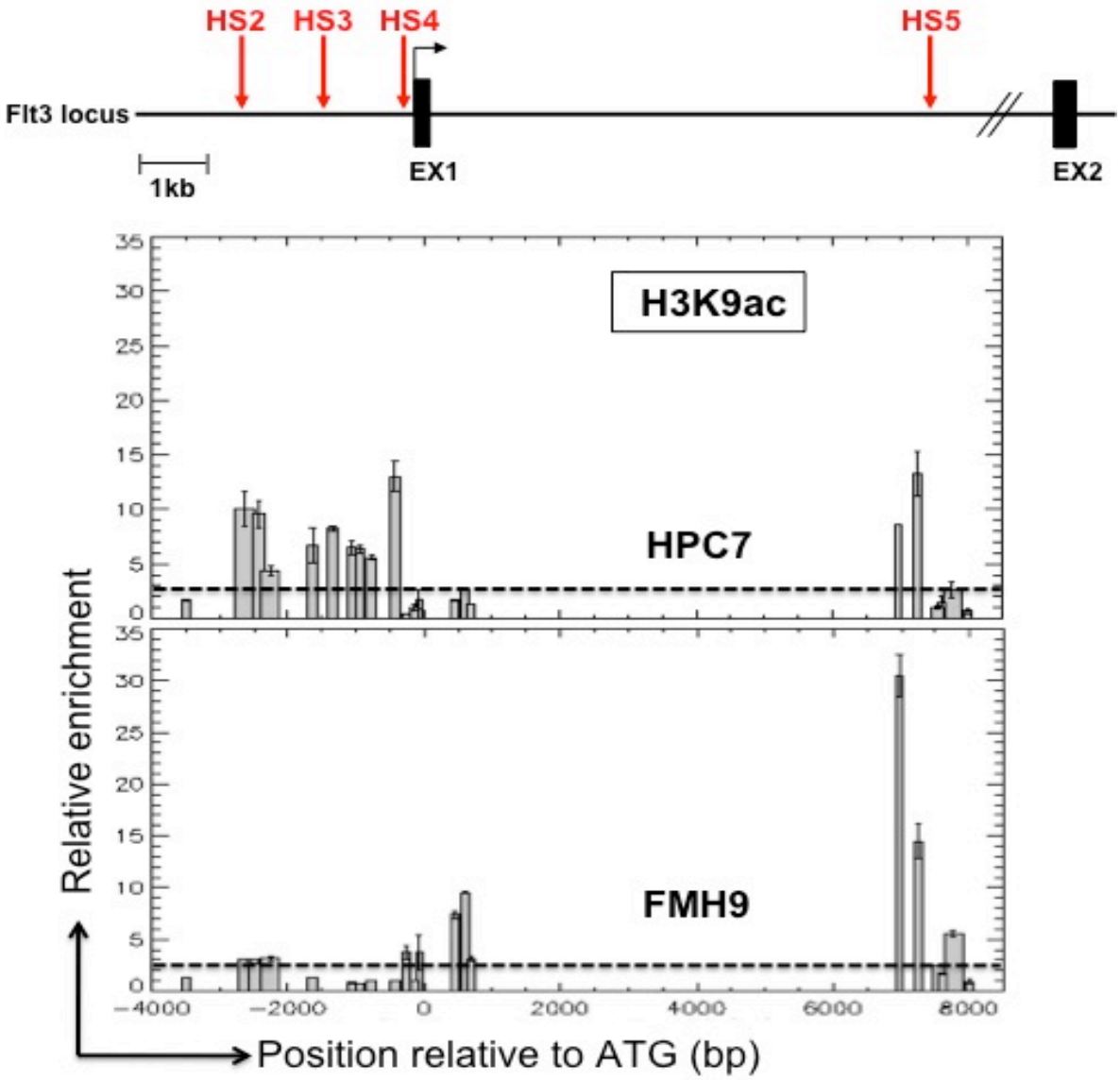

Figure 4.9 Analysis of the H3K9Ac histone modification at the *flt3* locus. X-ChIP experiments were performed on chromatin derived from both HPC7 and FMH9 cell lines using an antibody against the acetylation of lysine 9 on histone 3. Purified immunoprecipitated DNA was used as a template for Q-PCR amplifications to determine the relative enrichment compared to the control IgG ChIP material. The plots represent the relative enrichment on the Y-axis and the position relative to the transcriptional start site on the X-axis. The figure shows the alignment of the histograms with a schematic representation of the *flt3* promoter and first intron. DNAseI HSSs are indicated by red arrows. Dashed line represent the basal level across the locus. This figure represents the typical result obtained in four independent experiments in which each PCR was performed in triplicate. The width of the bars in the plot reflects the length of the amplicons. PCR amplicons overlap as indicated.

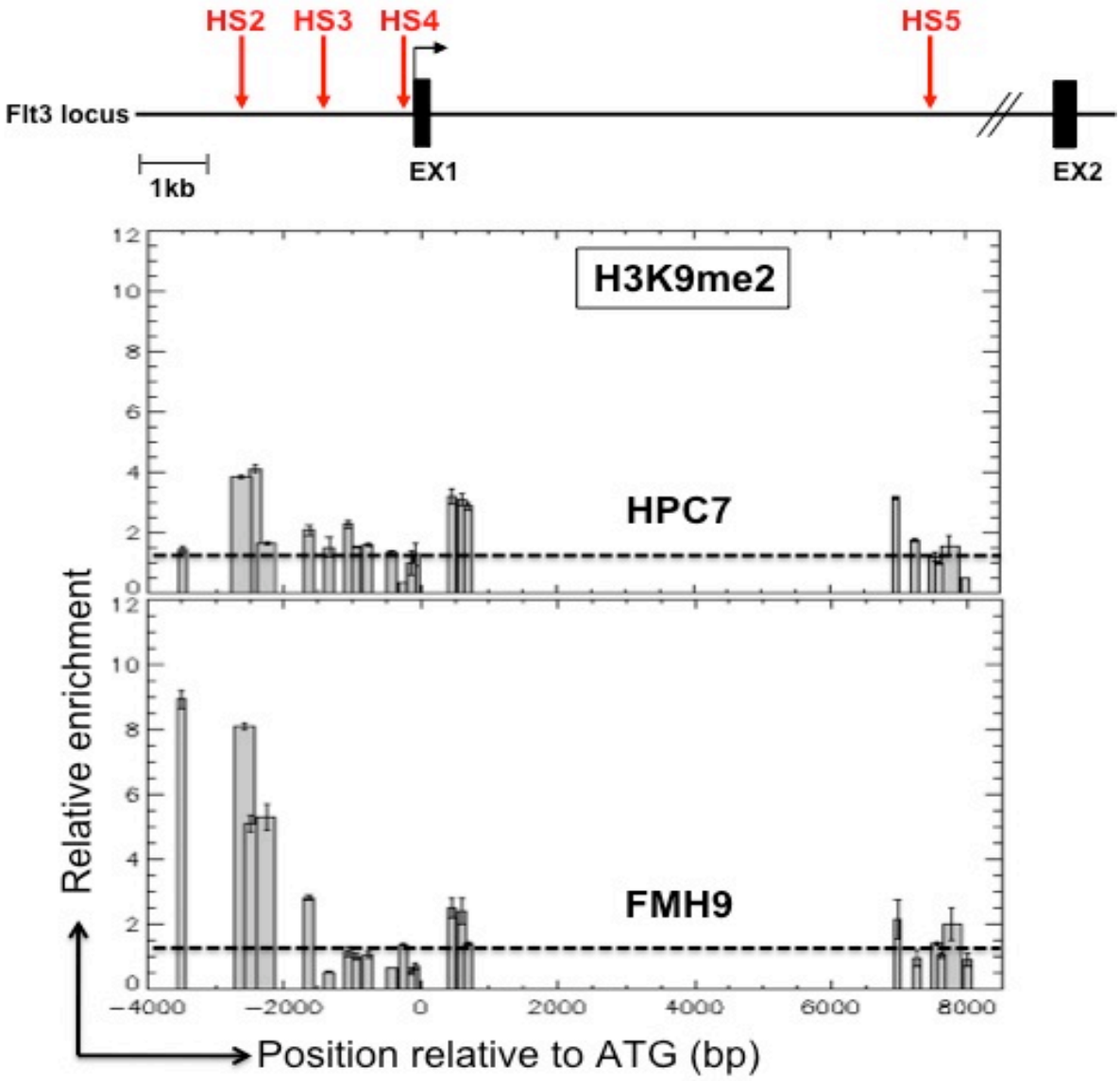

Figure 4.10 Analysis of the H3K9Me2 histone modification at the *flt3* locus. X-ChIP experiments were performed on chromatin derived from both HPC7 and FMH9 cell lines using an antibody against the dimethylation of lysine 9 on histone 3. Purified immunoprecipitated DNA was used as a template for Q-PCR amplifications to determine the relative enrichment compared to the control IgG ChIP material. The plots represent the relative enrichment on the Y-axis and the position relative to the transcriptional start site on the X-axis. The figure shows the alignment of the histograms with a schematic representation of the *flt3* promoter and first intron. DNAseI HSSs are indicated by red arrows. Dashed line represent the basal level across the locus. This figure represents the typical result obtained in three independent experiments in which each PCR was performed in triplicate. The width of the bars in the plot reflects the length of the amplicons. PCR amplicons overlap as indicated.

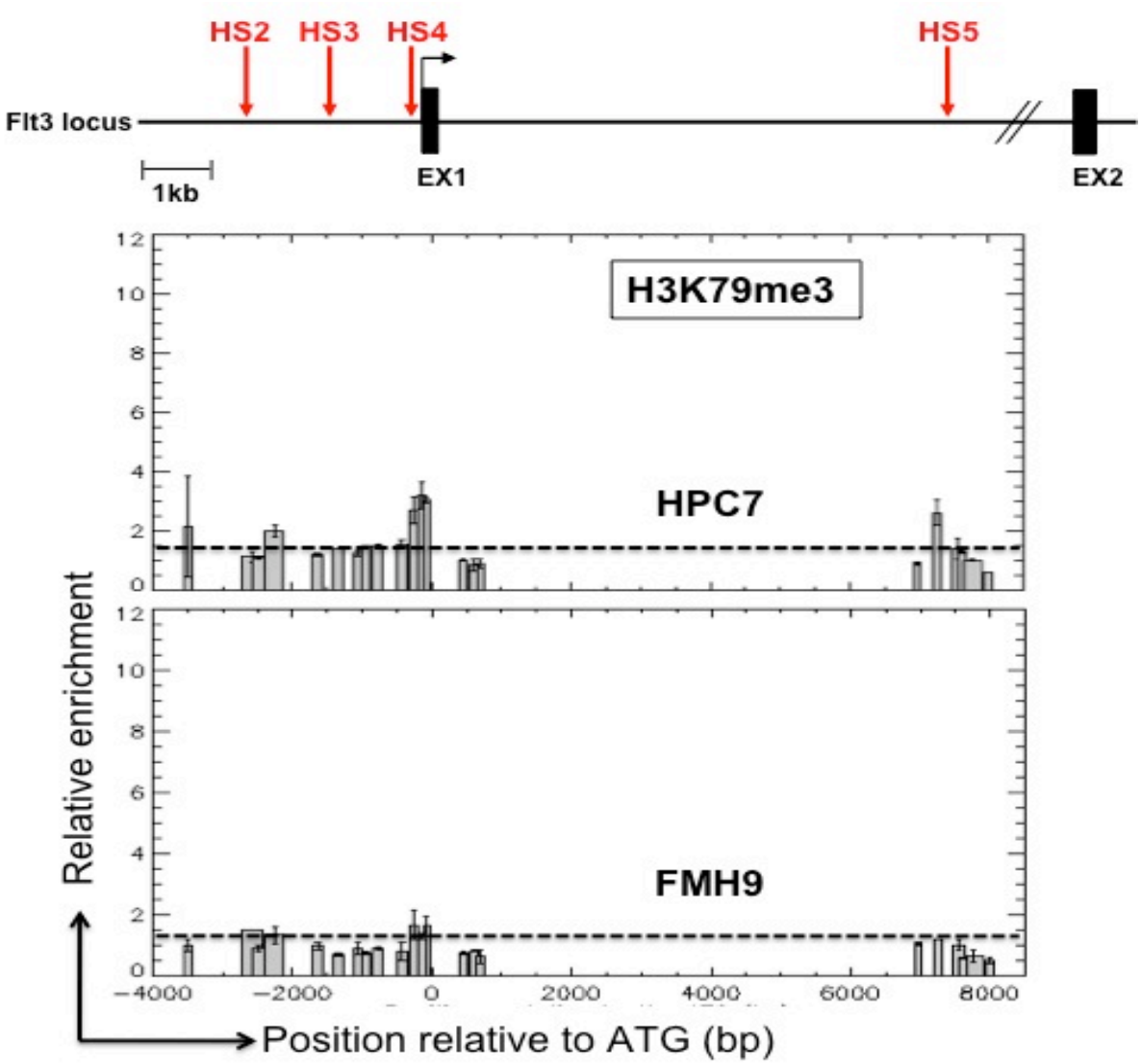

Figure 4.11 Analysis of the H3K79me3 histone modification at the *flt3* locus. X-ChIP experiments were performed on chromatin derived from both HPC7 and FMH9 cell lines using an antibody against the tri-methylation of lysine 79 of histone 3. Purified immunoprecipitated DNA was used as a template for Q-PCR amplifications to determine the relative enrichment compared to the control IgG ChIP material. The plots represent the relative enrichment on the Y-axis and the position relative to the transcriptional start site on the X-axis. The figure shows the alignment of the histograms with a schematic representation of the *flt3* promoter and first intron. DNAseI HSSs are indicated by red arrows. Dashed line represent the basal level across the locus. This figure represents the typical result obtained in two independent experiments in which each PCR was performed in triplicate. The width of the bars in the plot reflects the length of the amplicons. PCR amplicons overlap as indicated.

4.5 Transcriptional regulation of the *flt3* locus in normal versus leukaemia-like cells

4.5.1 Bioinformatic analysis of potential cis-regulatory regions

Different histone modifying enzymes, such as acetylases and deacetylases, can be recruited to a gene locus by specific transcription factors and at the same time their activity can be a pre-requisite to allow transcription factor binding to the DNA. In order to identify possible trans-regulators of *flt3* expression in HSCs and leukaemia cells, I performed an alignment of the genomic DNA sequences from human, mouse, rat and dog covering those regions of the flt3 promoter and first intron that had been shown to exhibit HSS and specific epigenetic modifications in HPC7 and FMH9 cells. The search for potential transcription factor binding sites was performed using MAT-Inspector and Transcription Element Search System (T.E.S.S) software.

In those regions (HS3, 4 and 5) for which the sequence information allowed alignment of all four of the mammalian genomes, and showed strong conservation (shown in black shading), a number of good matches to known transcription factor consensus binding sites were identified. Only mouse and rat sequences could be aligned across HS2 (shown in grey shading). Conserved concensus binding sites for c-Myb (blue), Ets (green), RUNX1 (red), PU.1 (orange), GATA (pale blue), C/EBPα (beige), Pax5 (purple), Pbx/Meis1 (maroon) and Sox2 (pink) were identified in one or more of the HSS as indicated in Figures 4.12-15. All the consensus

binding sites shown in these figures were selected on the basis of an arbitrary threshold of 90% of homology against the consensus matrix.

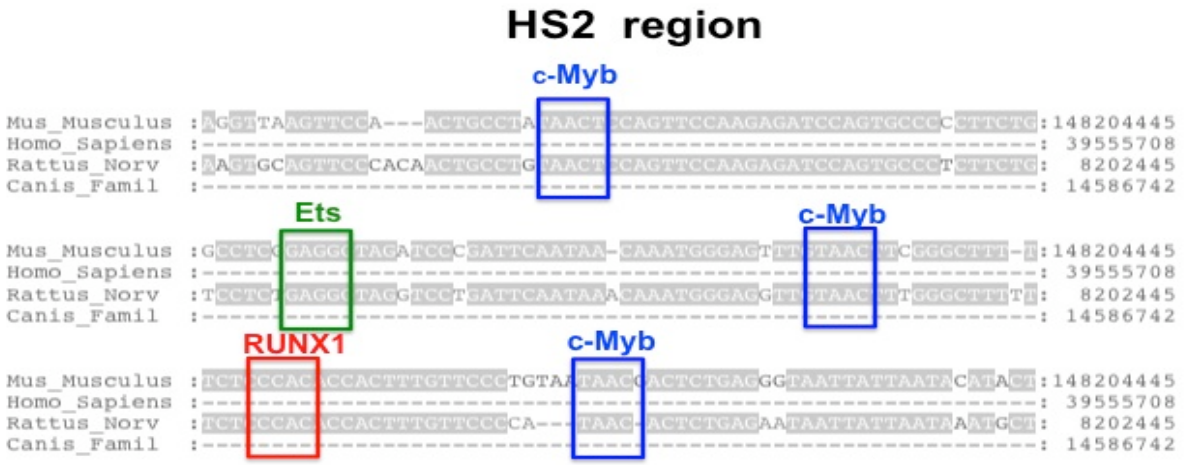

Figure 4.12. Putative transcription factor binding sites in the *flt3* HS2 regulatory element. Multi-species alignment of mammalian genome sequences highlighting the sequence conservation (in grey) in the region of HS2. The blue, green and red boxes highlight the potential c-Myb, Ets and AML1 binding sites, respectively.

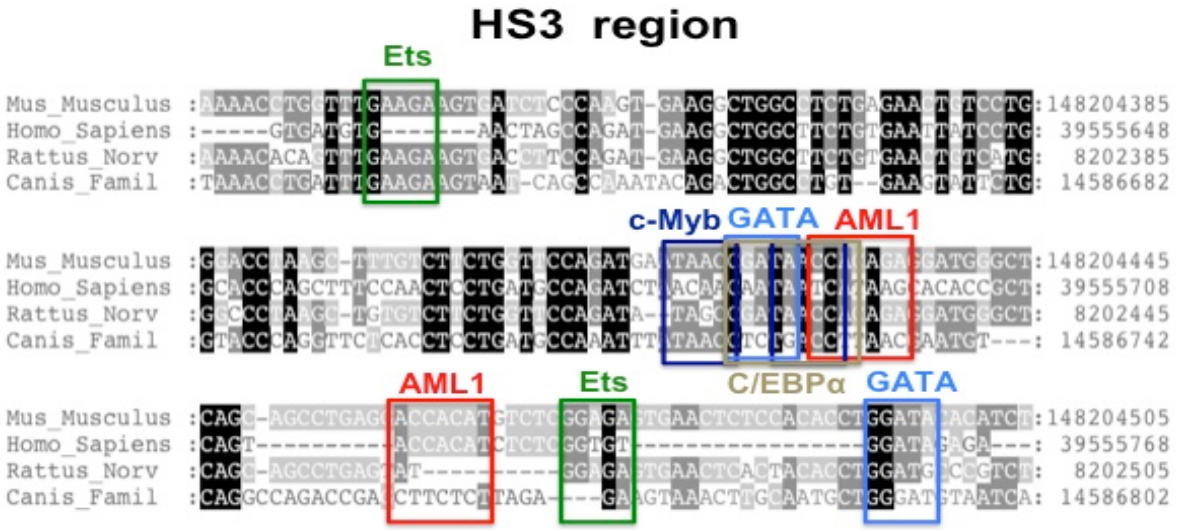

Figure 4.13 Putative transcription factor binding sites in the *flt3* HS3 regulatory element. Multi-species alignment of mammalian genome sequences highlighting the sequence conservation (in black and grey) in the region of HS3. The blue, green, red, beige and pale blue boxes highlight the potential c-Myb, Ets, AML1, c/EBP and GATA bin

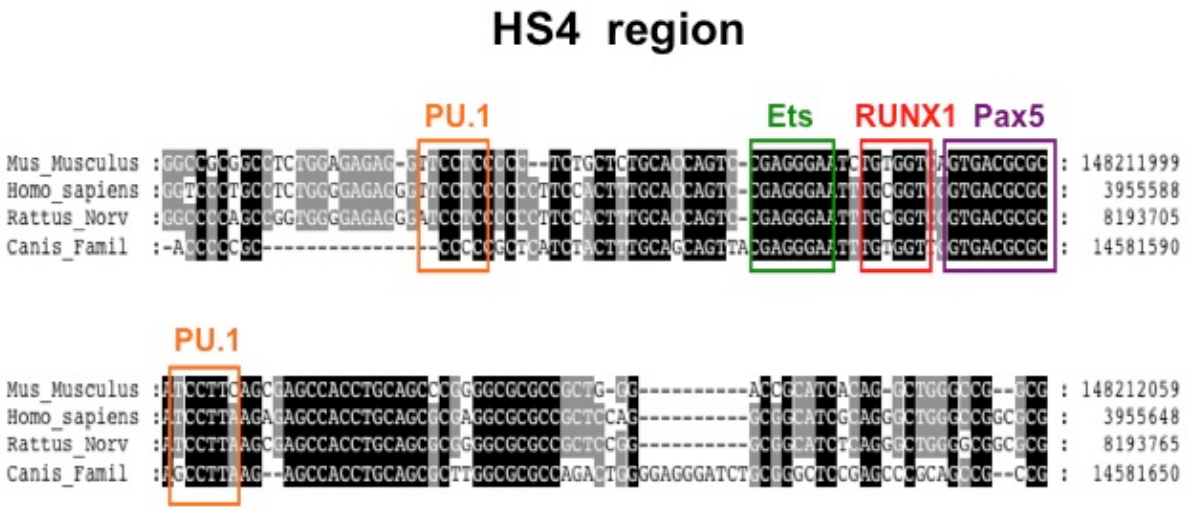

Figure 4.14 Putative transcription factor binding sites in the *flt3* HS4 regulatory element. Multi-species alignment of mammalian genome sequences highlighting the sequence conservation (in black and grey) in the region of HS4. The green, red, orange and purple boxes highlight the potential Ets, AML1, PU.1 and Pax5 binding sites, respectively.

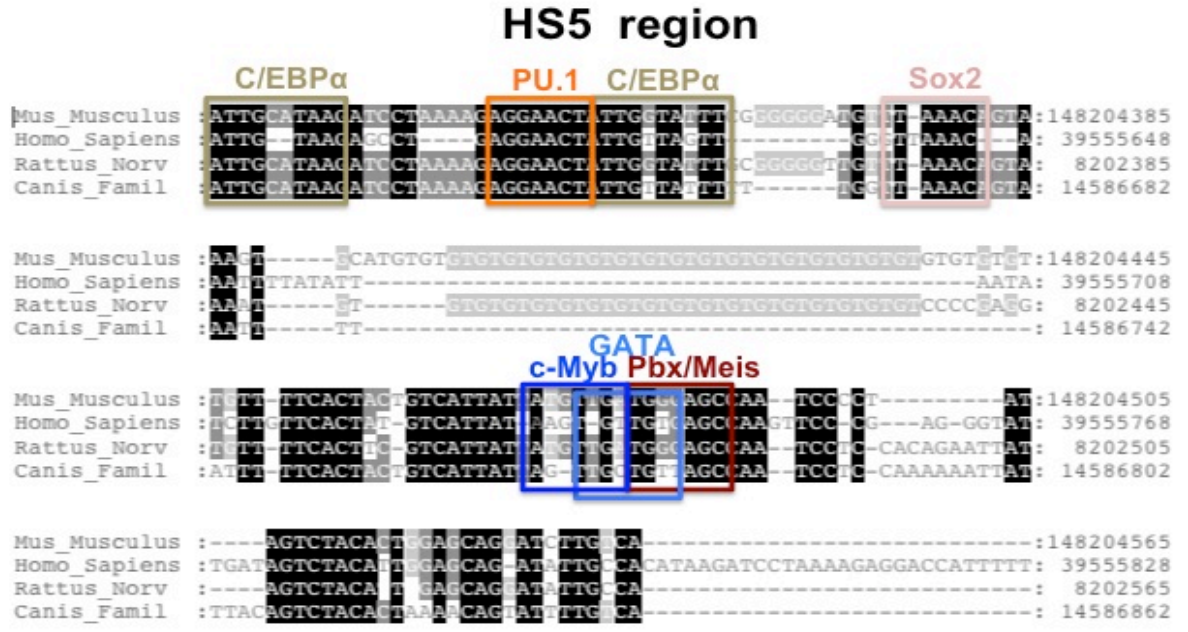

Figure 4.15 Putative transcription factor binding sites in the *flt3* intronic HS5 regulatory element. Multi-species alignment of mammalian genome sequences highlighting the sequence conservation (in black and grey) in the region of HS5. The blue, orange, beige, pale blue and maroon boxes highlight the potential c-Myb, PU.1, C/EBPα, GATA and Pbx/Meis1 binding sites, respectively.

4.5.2 In vivo transcription factor binding to the *flt3* promoter and intron 1 regulatory elements

As described in Section 4.6.1, the regions of nuclease hypersensitivity encompass several binding sites for Ets, GATA, c-Myb, C/EBPα and other stem cell- and leukaemia-associated transcription factors. Therefore, I next investigated by X-ChIP which of the proteins known to be expressed are actually bound in vivo to the *flt3* promoter and/or intron 1 in HPC7 and FMH9 cells. ChIP products were analysed by real time PCR and relative enrichments were determined by comparison with the matching IgG control.

4.5.2.1 HoxA9, Meis1, Pbx1/2

As mentioned above, Wang and colleagues reported the direct binding of HoxA9 and Meis1 to the *flt3* promoter in myeloid leukaemia cells (Wang et al.; 2006). As described in section 3.3 the cell model used was generated by retroviral co-transduction of bone marrow cells with HoxA9-HA and Meis1-FLAG. In order to assess the direct interaction of these two transcription factors, Wang and colleagues performed ChIP analysis using antibodies against the FLAG and HA tags on the transforming exogenous Meis1 and HoxA9 (Wang et al.; 2006). In order to confirm these findings I adopted the same approach in FMH9 cells. In agreement with previous observations, ChIP assays using α-FLAG and α-HA antibodies revealed the binding of both HoxA9 (Figure 4.16, lower panel) and Meis1 (Figure 4.17, lower panel) on the HS3 region. No enrichments were observed at HS2 or HS5. HS4 was not investigated due to the lack of sufficient purified DNA. ChIP analysis was also

performed with chromatin from both HPC7 and FMH9 cells, using antibodies against the N-terminus of HoxA9 and the C-terminus of Meis1. These latter studies indicated the recruitment of both HoxA9 and Meis1 at HS3, but not at other regions, in both HSC- and leukaemia-like cells (Figures 4.16 and 4.17, upper and middle panels).

Wang and coworkers also provided evidence for recruitment of Meis1/Pbx complexes on leukaemia-associated gene promoters. Therefore, I next investigated the in vivo binding of both Pbx1 and Pbx2 to the *flt3* locus. PCR analysis of Pbx1 ChIP DNA demonstrated binding at the HS3 region only, with a similar profile in HPC7 cells to that observed for HoxA9 and Meis1 (Figure 4.18). In contrast, the analysis of occupancy of the *flt3* promoter by Pbx1 only revealed a small enrichment at the HS3 region in FMH9 cells. No significant binding of Pbx2 could be shown, using chromatin from either in HPC7 or in FMH9 cells (Figure 4.19). No positive controls are shown for Pbx2 in this section, however the antibody used has been proved to ChIP efficiently (Dasse et al, unpublished data).

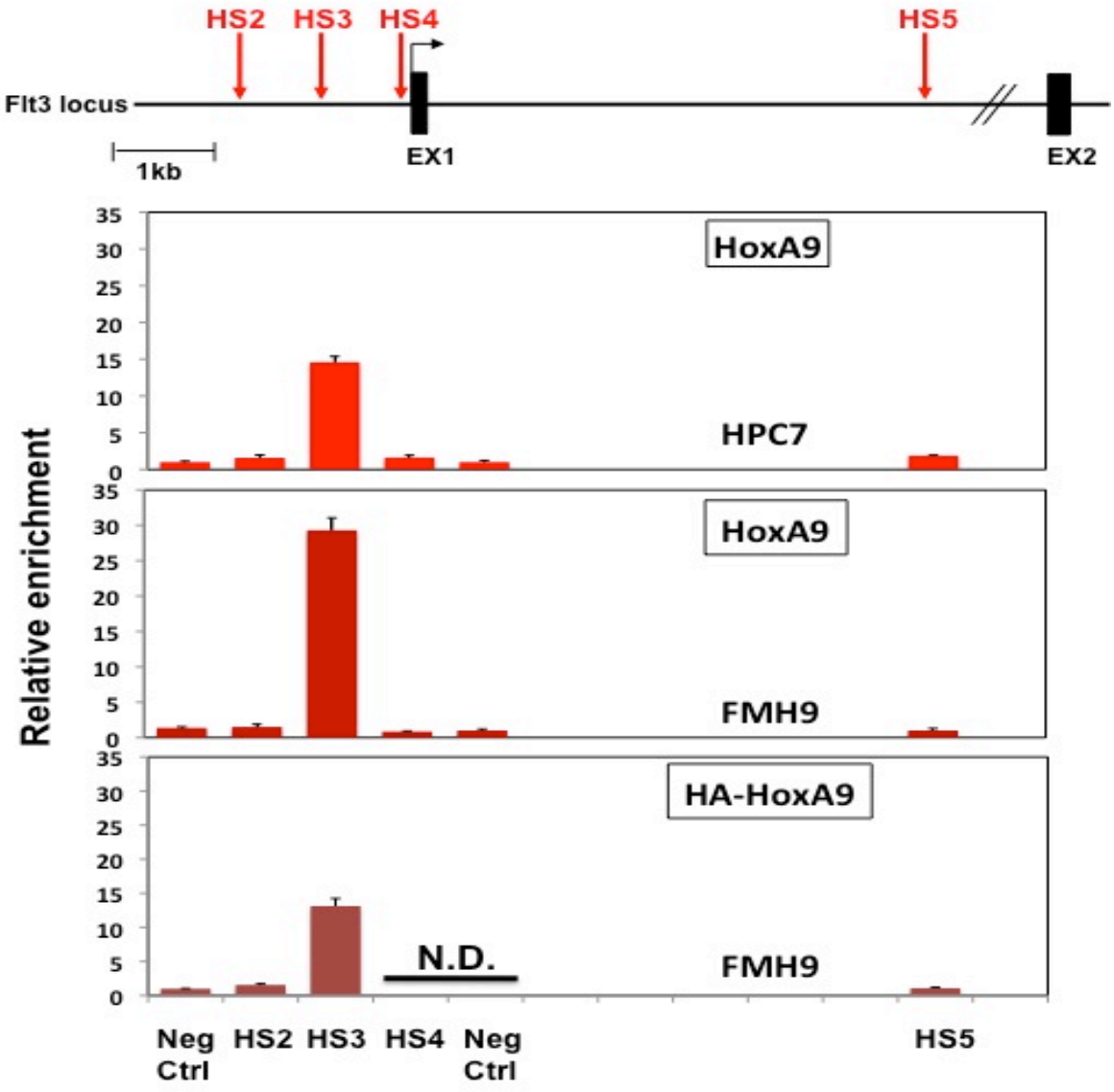

Figure 4.16 X-ChIP analysis of in vivo binding of HoxA9 on the *flt3* locus. X-ChIP analysis was performed on chromatin derived from HPC7 and FMH9 cells using antibodies directed against the N-terminus of HoxA9 in both cell lines (represented in the top and middle histograms) or the HA-tag of HA-HoxA9 in FMH9 cells (lower panel). Specific ChIP DNA fragments encompassing the four HSS (indicated by the red arrows in the top schematic) and two internal control regions were quantified by Q-PCR to determine their enrichment relative to the control IgG ChIP. The figure shows histograms depicting the extent of enrichment aligned with the structure of the *flt3* promoter and first intron. ND: not determined, due to the lack of sufficient ChIP DNA material. This figure represents the typical result obtained in three independent experiments in which each PCR was performed in triplicate from one ChIP experiment. Error bars represent the standard error of the mean.

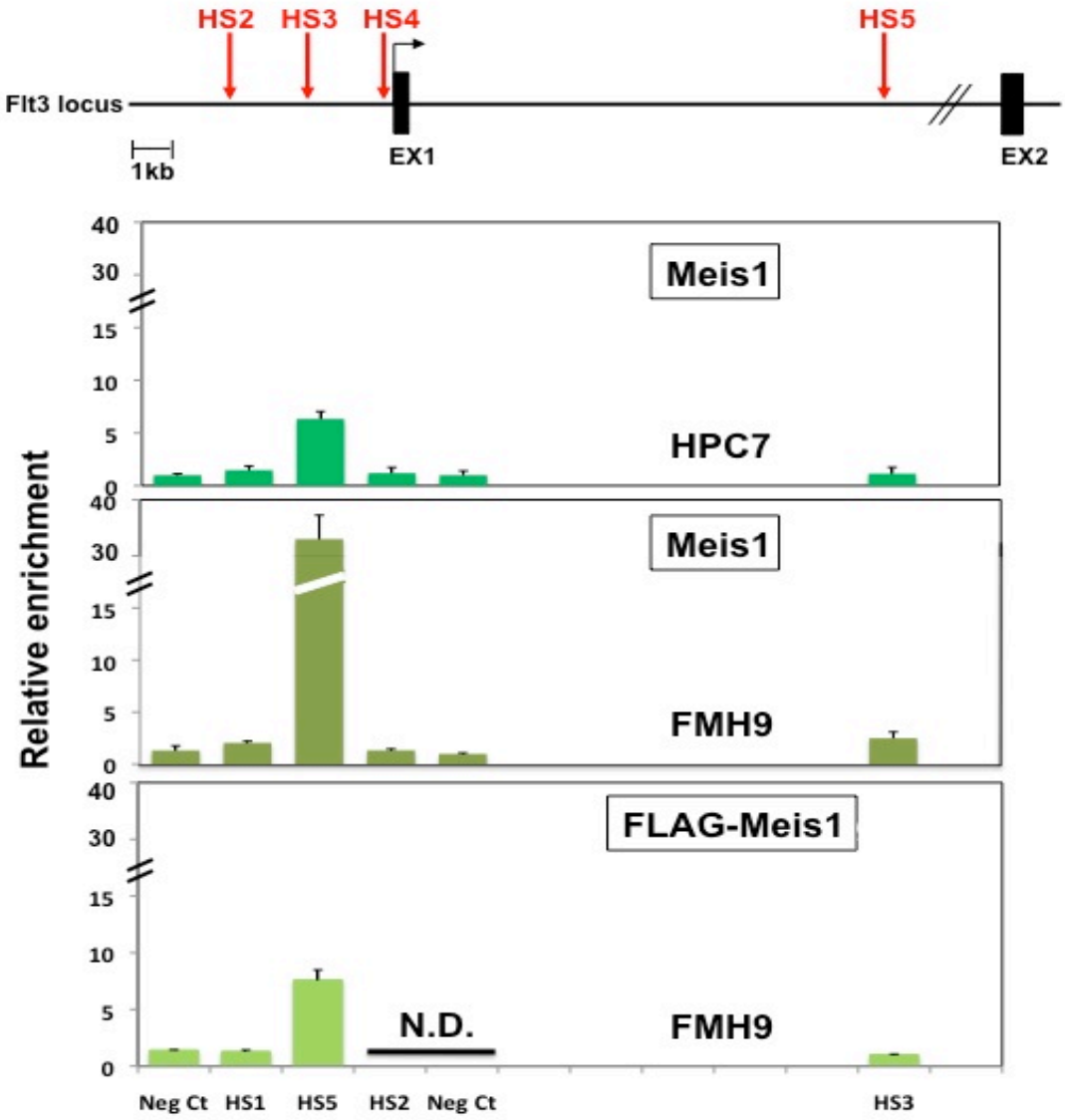

Figure 4.17 X-ChIP analysis of in vivo binding of Meis1 on the *flt3* locus. X-ChIP analysis was performed on chromatin derived from HPC7 and FMH9 cells using antibodies directed against the C-terminus of Meis1 in both cell lines (represented in the top and middle histograms) or the FLAG-tag of FLAG-Meis1 in FMH9 cells (lower panel). Specific ChIP DNA fragments encompassing the four HSS (indicated by the red arrows in the top schematic) and two internal control regions were quantified by Q-PCR to determine their enrichment relative to the control IgG ChIP. The figure shows histograms depicting the extent of enrichment aligned with the structure of the *flt3* promoter and first intron. ND: not determined, due to the lack of sufficient ChIP DNA material. This figure represents the typical result obtained in three independent experiments in which each PCR was performed in triplicate from one ChIP experiment. Error bars represent the standard error of the mean.

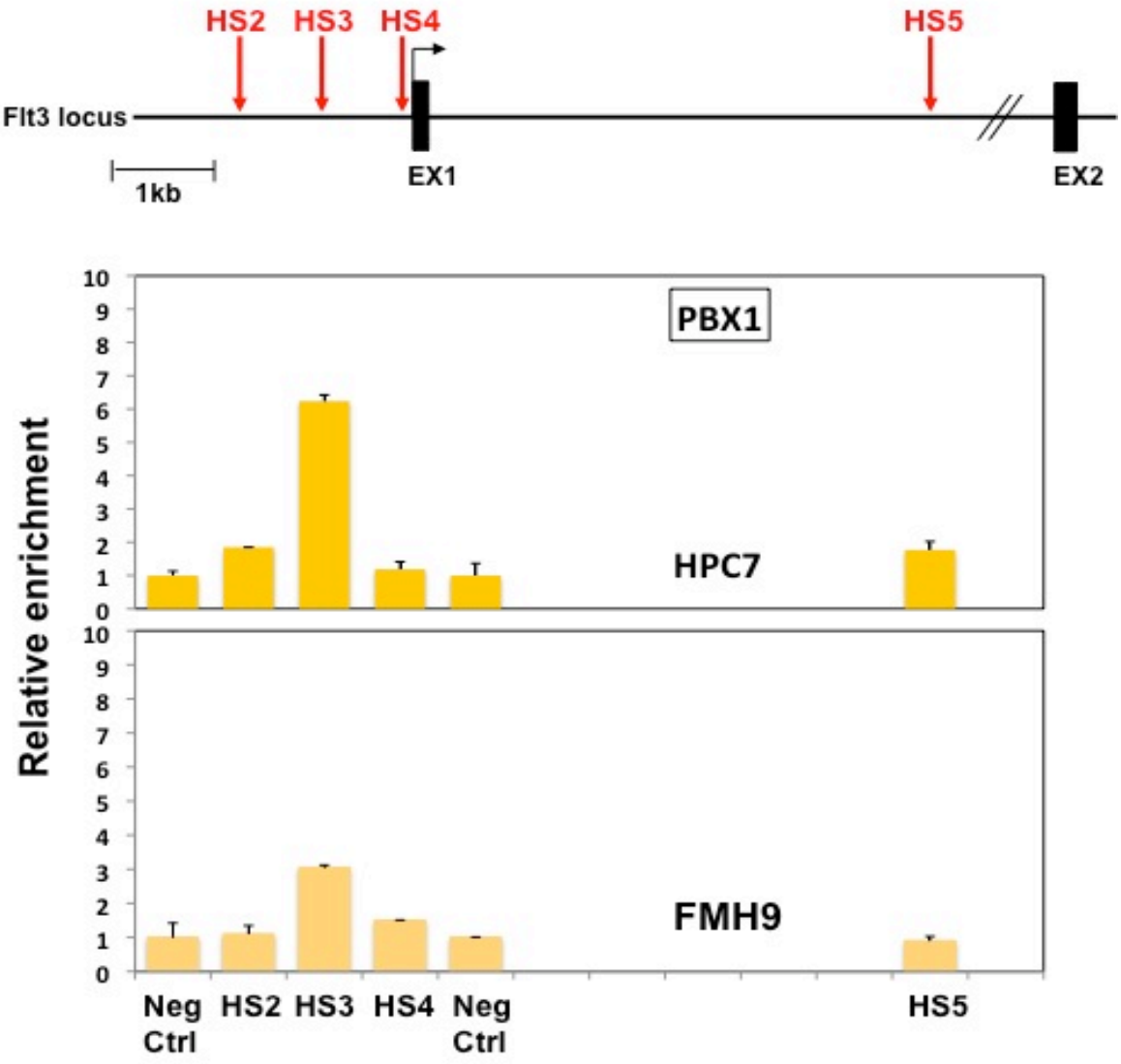

Figure 4.18 X-ChIP analysis of in vivo binding of Pbx1 on the *flt3* locus. X-ChIP analysis was performed on chromatin derived from HPC7 and FMH9 cells using using an antibody directed against the N-terminus of Pbx1. Specific ChIP DNA fragments encompassing the four HSS (indicated by the red arrows in the top schematic) and two internal control regions were quantified by Q-PCR to determine their enrichment relative to the control IgG ChIP. The figure shows histograms depicting the extent of enrichment aligned with the structure of the *flt3* promoter and first intron. This figure represents the typical result obtained in three independent experiments in which each PCR was performed in triplicate from one ChIP experiment. Error bars represent the standard error of the mean.

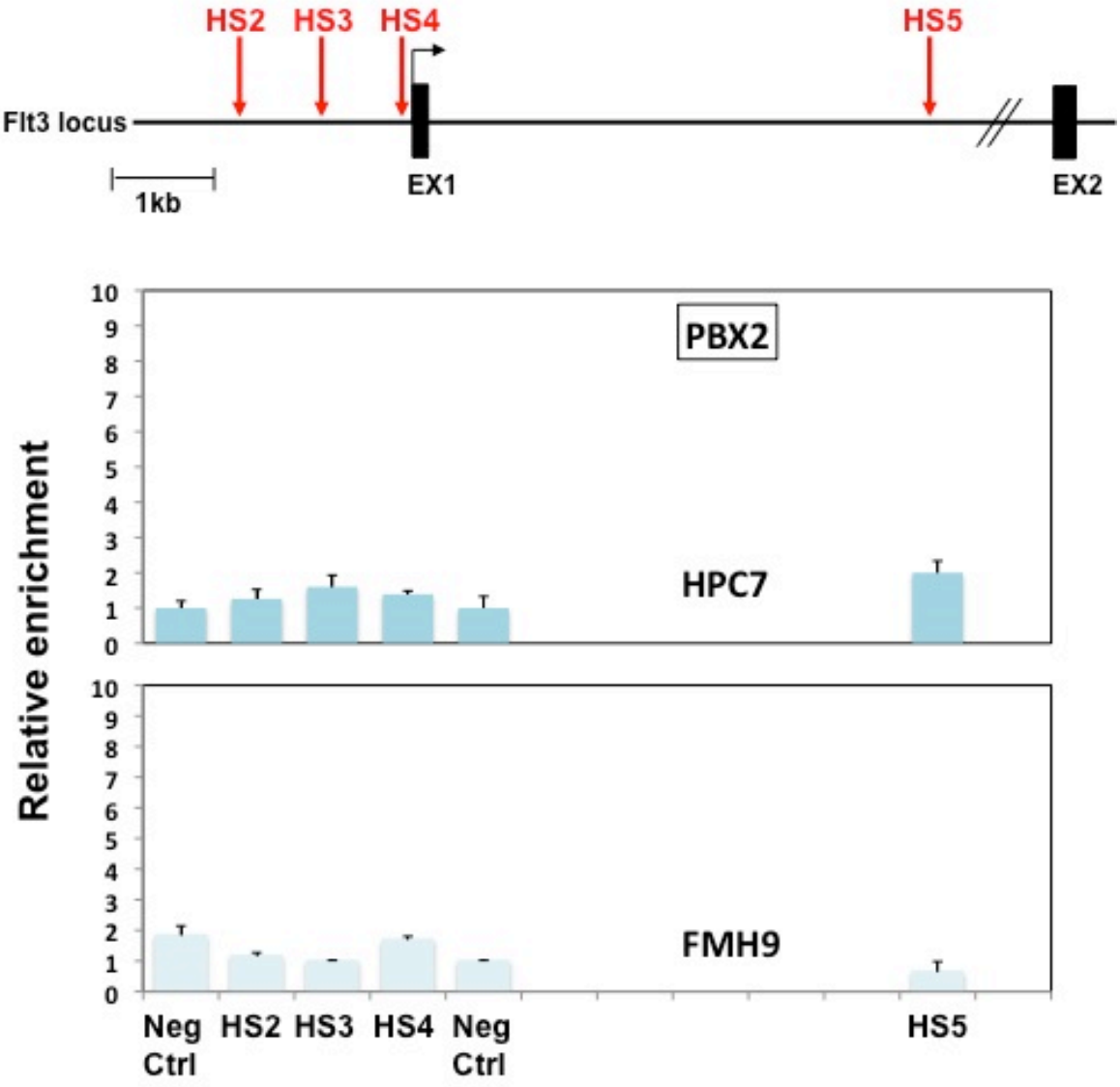

Figure 4.19 ChIP analysis of in vivo binding of Pbx2 on the *flt3* locus. X-ChIP analysis was performed on chromatin derived from HPC7 and FMH9 cells using using an antibody directed against the N-terminus of Pbx2. Specific ChIP DNA fragments encompassing the four HSS (indicated by the red arrows in the top schematic) and two internal control regions were quantified by Q-PCR to determine their enrichment relative to the control IgG ChIP. The figure shows histograms depicting the extent of enrichment aligned with the structure of the *flt3* promoter and first intron. This figure represents the typical result obtained in two independent experiments in which each PCR was performed in triplicate from one ChIP experiment. Error bars represent the standard error of the mean.

4.5.2.2 c-Myb

ChIP using an anti-c-Myb antibody on chromatin derived from both HPC7 and FMH9 cells resulted in a clear enrichment of sequences encompassing HS3. A lesser degree of enrichment was also observed over the intronic HS5 region, this being somewhat more pronounced in HPC7 cells compared to FMH9 (Figure 4.20).

4.5.2.3 Ets and GATAs

Since several putative Ets and GATA binding sites were identified in four of the *flt3* HSS, I examined the in vivo binding of PU.1, GATA-1 and GATA-2. The analysis of the GATA factors was restricted to HPC7s since their expression was not detected in FMH9 cells (see Figure 3.5, Section 3.3.3). GATA1 ChIP revealed in vivo binding of this factor on HS2, HS5 and most significantly on the HS3 region (Figure 4.21, upper panel). No binding of GATA1 was detected on the HS4 element. Similar analysis of GATA2 in vivo binding showed this to occur exclusively at HS3 (Figure 4.21, lower panel). Direct interaction of PU.1 with the *flt3* locus was detected on the HS3 element in HPC7, while no interaction with the promoter or intron was seen in FMH9 cells (Figure 4.22).

4.5.2.4 Sox2

Analysis of the in vivo binding of Sox2, another stem cell-associated transcription factor for which concensus binding sites were identified in the *flt3* HSS, was only performed using HPC7 chromatin as expression could be detected in these cells but not in FMH9. Interestingly, this revealed the interaction of Sox2 with the intronic HS5 region, but not significantly with the promoter HSS (Figure 4.23).

4.5.2.5 C/EBPα

Since recent publications have highlighted a direct link in some leukaemias between Flt3 activating mutations and altered C/EBPα expression, I investigated whether the concensus binding sites found in the *flt3* gene are reflected by in vivo binding of his leucine zipper transcription factor in either of the cell models. C/EBPα ChIP of HPC7 cells revealed the binding of the protein on both the promoter (HS3) and the intronic HS5 regions (Figure 4.24, upper panel), whereas in FMH9 binding was restricted to the intronic element (Figure 4.24, lower panel).

4.5.2.6 Runx1

Good matches to the concensus binding site for Runx1 were identified in three of the four HSS, and of these two, HS3 and HS5 were shown to be enriched in chromatin precipitated by Runx1 ChIP from HPC7 cells (Figure 4.25, upper panel). The bioinformatic analysis did not reveal the presence of Runx binding sites in the HS5 elements, hence suggesting that the in vivo interaction of this transcription factor could be mediated by other protein directly interacting with the *flt3* intronic regulatory element. In the same analysis performed in FMH9 cells none of the sites was convincingly shown to bind Runx1 (Figure 4.25, lower panel).

4.5.2.7 MLL

Many research groups have reported the importance of the MLL methyltransferase in both haematopoiesis and leukaemia and my data has demonstrated differences between HPC7 and FMH9 cells with respect to the methylation status of histone H3 across the *flt3* promoter/intron region (see Section 4.5.1). MLL ChIP revealed in

vivo binding of the protein to the *flt3* locus in HPC7 at HS2, HS3 and HS5 (Figure 4.26, upper panel), but little or no evidence for its presence at any position on chromatin obtained from FMH9 cells (Figure 4.26, lower panel).

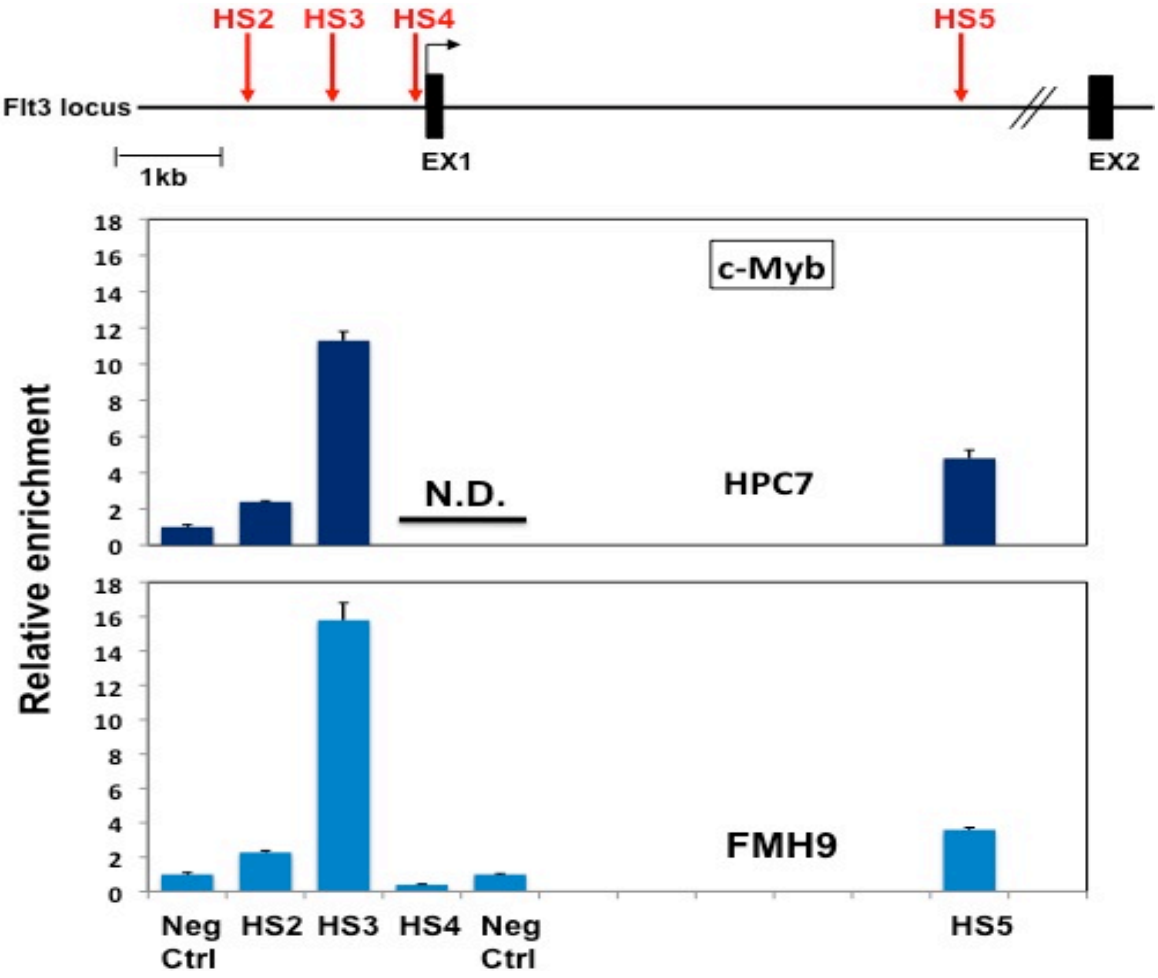

Figure 4.20 In vivo binding of c-Myb at the *flt3* locus. Formaldehyde cross-linked chromatin from both HPC7 and FMH9 cells was immunoprecipitated using an antibody against the C-terminus of c-Myb and the resulting purified DNA was analysed by Q-PCR using primers covering the four HSS (indicated in the top panel by the red arrows) and two internal controls. Relative enrichments were determined versus the control IgG ChIP. Each histogram represents the relative enrichment on the Y-axis and the position relative to the transcriptional start site on the X-axis, and is aligned with the structure of the *flt3* gene represented in the top panel. ND: not determined due to the lack of sufficient DNA material for Q-PCR amplification. This figure represents the typical result obtained in two independent experiments in which each PCR was performed in triplicate from one ChIP experiment. Error bars represent the standard error of the mean.

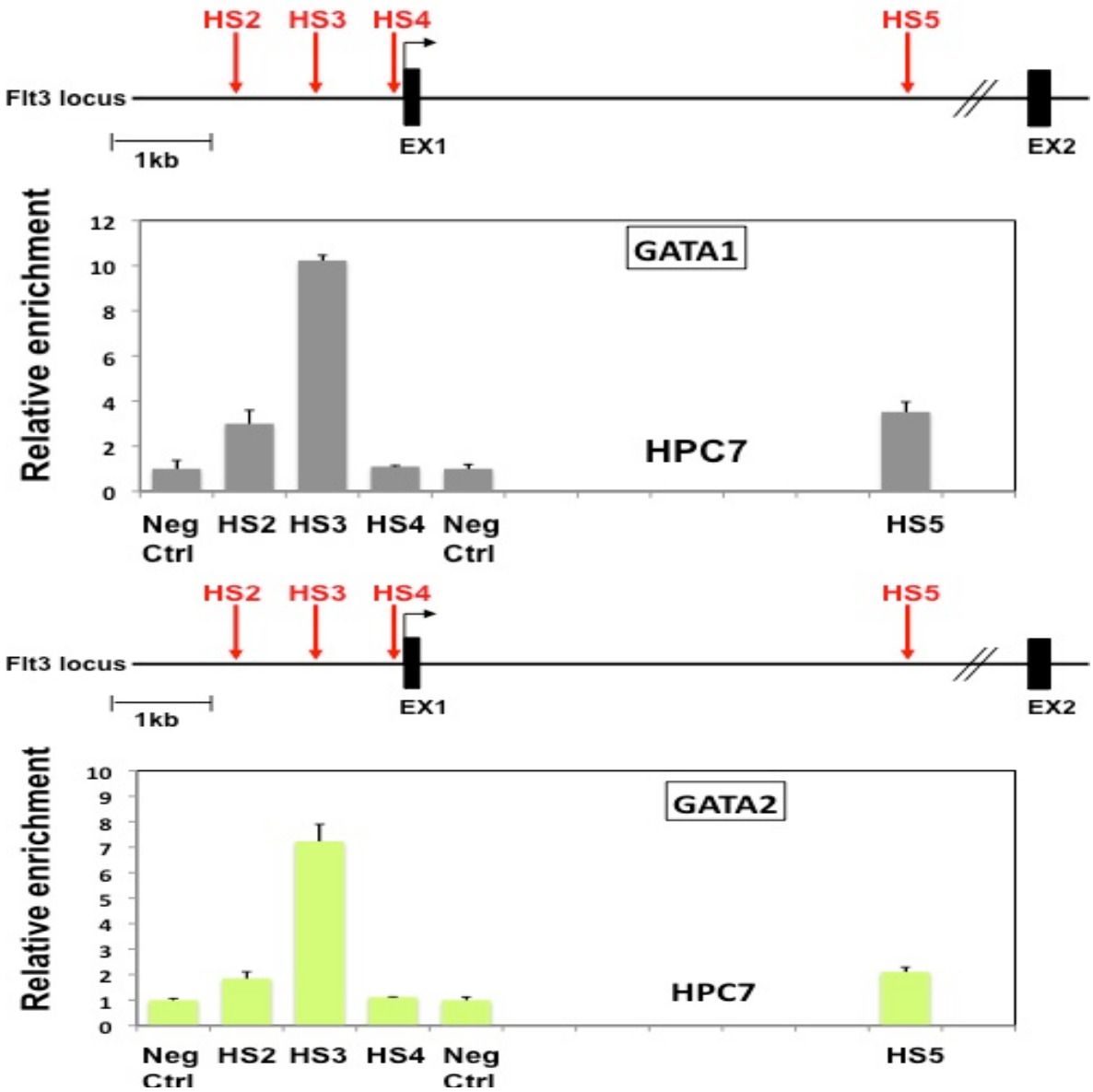

Figure 4.21 In vivo binding of GATA factors at the *flt3* locus. Formaldehyde cross-linked chromatin from HPC7 cells was immunoprecipitated using an antibody against the C-terminus of either GATA1 (top histogram) or GATA2 (bottom histogram) and the resulting purified DNA was analysed by Q-PCR using primers covering the four HSS (indicated in the top panel by the red arrows) and two internal controls. Relative enrichments were determined versus the control IgG ChIP. Each histogram represents the relative enrichment on the Y-axis and the position relative to the transcriptional start site on the X-axis, and is aligned with the structure of the *flt3* gene represented in the top panel. This figure represents the typical result obtained in two independent experiments in which each PCR was performed in triplicate from one ChIP experiment. Error bars represent the standard error of the mean.

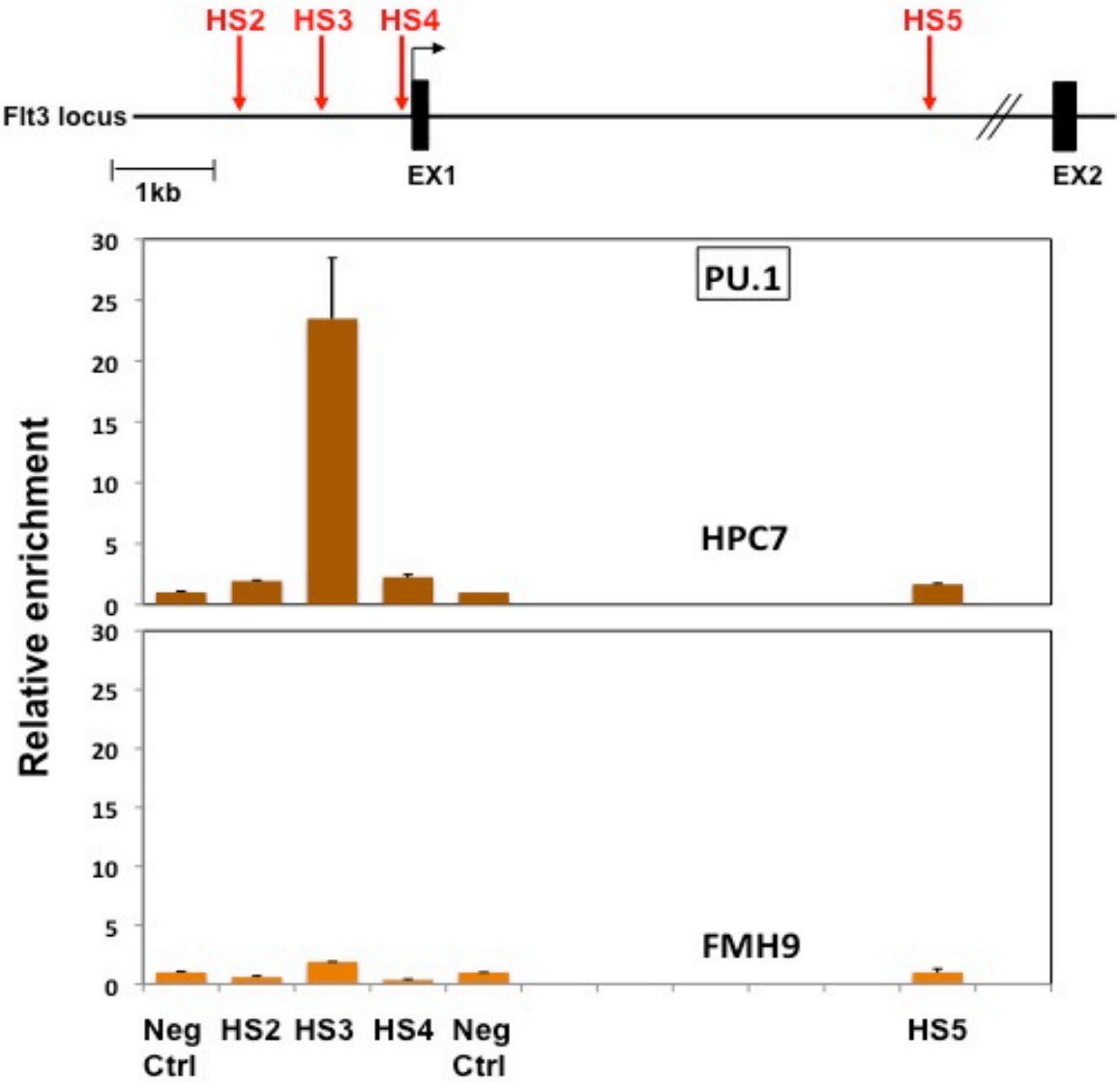

Figure 4.22 In vivo binding of PU.1 at the *flt3* locus. Formaldehyde cross-linked chromatin from both HPC7 and FMH9 cells was immunoprecipitated using an antibody against the C-terminus of PU.1 and the resulting purified DNA was analysed by Q-PCR using primers covering the four HSS (indicated in the top panel by the red arrows) and two internal controls. Relative enrichments were determined versus the control IgG ChIP. Each histogram represents the relative enrichment on the Y-axis and the position relative to the transcriptional start site on the X-axis, and is aligned with the structure of the *flt3* gene represented in the top panel. This figure represents the typical result obtained in four independent experiments in which each PCR was performed in triplicate from one ChIP experiment. Error bars represent the standard error of the mean.

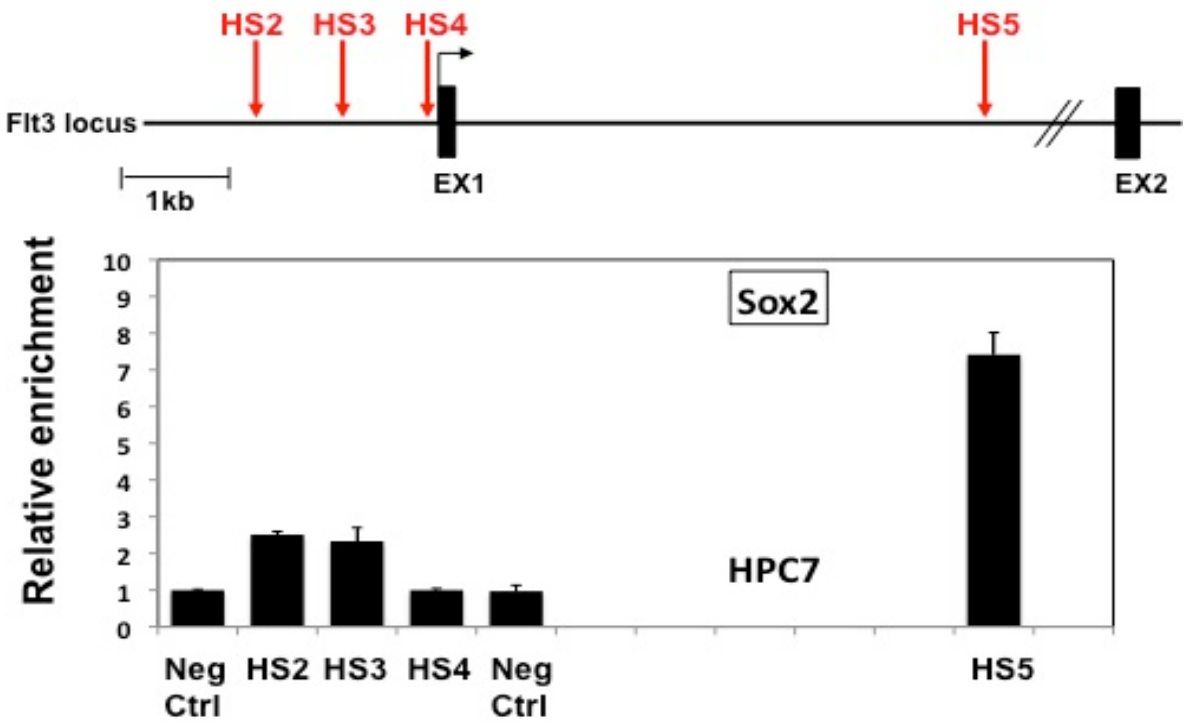

Figure 4.23 In vivo binding of Sox2 at the *flt3* locus. Formaldehyde cross-linked chromatin from HPC7 cells was immunoprecipitated using an antibody against the N-terminus of Sox2 and the resulting purified DNA was analysed by Q-PCR using primers covering the four HSS (indicated in the top panel by the red arrows) and two internal controls. Relative enrichments were determined versus the control IgG ChIP. Each histogram represents the relative enrichment on the Y-axis and the position relative to the transcriptional start site on the X-axis, and is aligned with the structure of the *flt3* gene represented in the top panel. This figure represents the typical result obtained in two independent experiments in which each PCR was performed in triplicate from one ChIP experiment. Error bars represent the standard error of the mean.

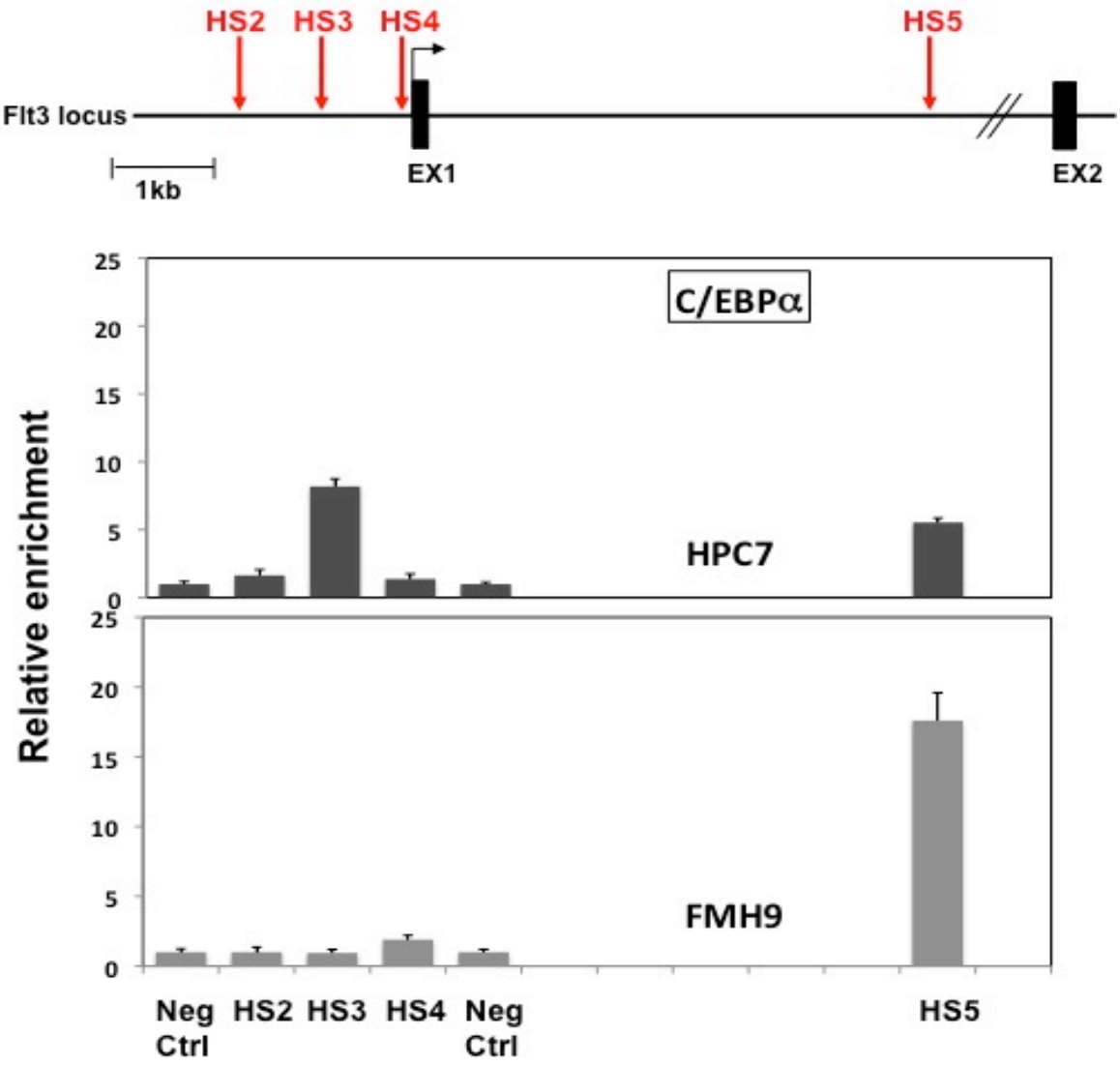

Figure 4.24 In vivo binding of C/EBPα at the *flt3* locus. Formaldehyde cross-linked chromatin from both HPC7 and FMH9 cells was immunoprecipitated using an antibody against C/EBPα and the resulting purified DNA was analysed by Q-PCR using primers covering the four HSS (indicated in the top panel by the red arrows) and two internal controls. Relative enrichments were determined versus the control IgG ChIP. Each histogram represents the relative enrichment on the Y-axis and the position relative to the transcriptional start site on the X-axis, and is aligned with the structure of the *flt3* gene represented in the top panel. This figure represents the typical result obtained in four independent experiments in which each PCR was performed in triplicate from one ChIP experiment. Error bars represent the standard error of the mean.

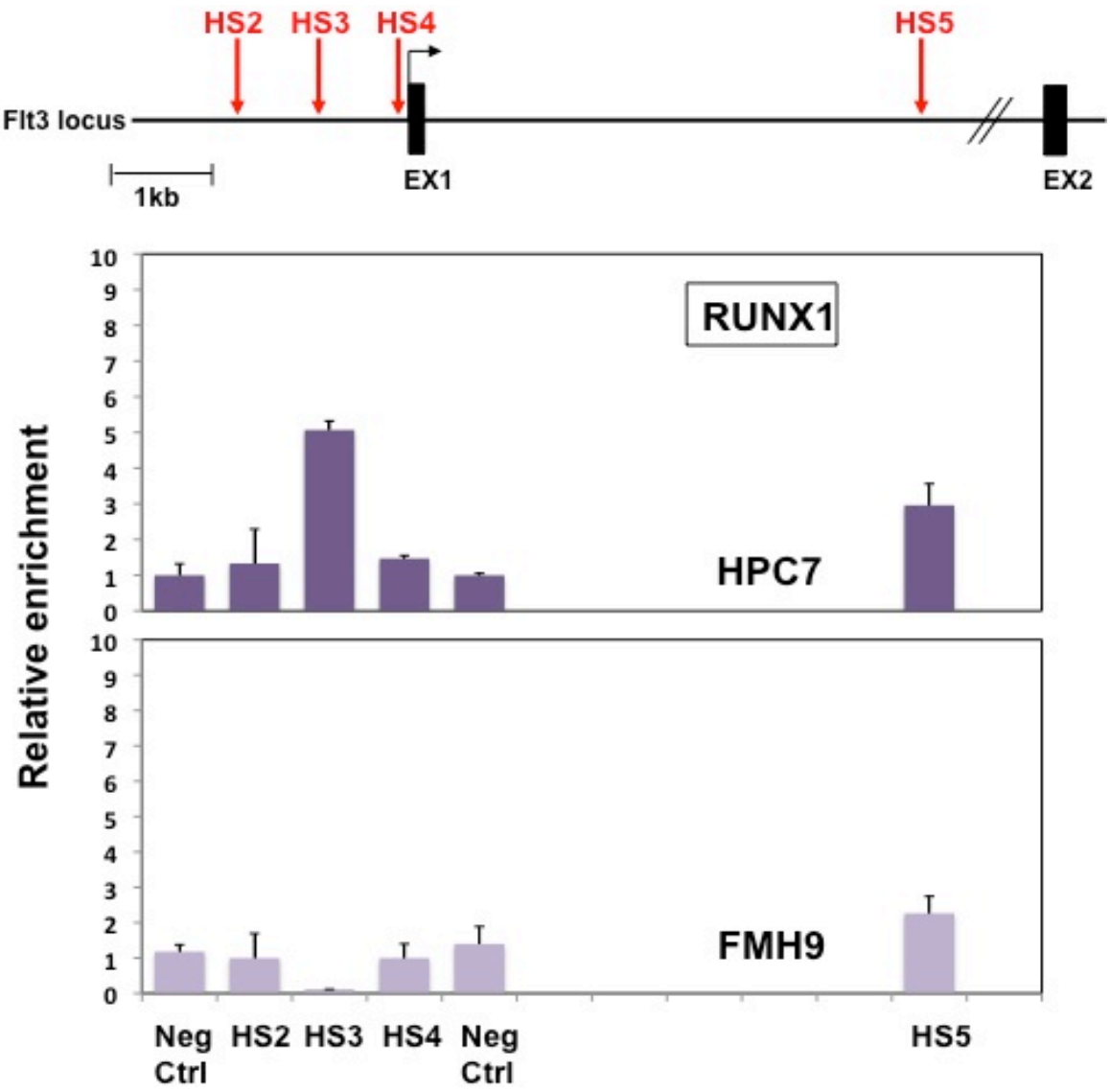

Figure 4.25 In vivo binding of Runx1 at the *flt3* locus. Formaldehyde cross-linked chromatin from both HPC7 and FMH9 cells was immunoprecipitated using an antibody against against the C-terminus of Runx1 and the resulting purified DNA was analysed by Q-PCR using primers covering the four HSS (indicated in the top panel by the red arrows) and two internal controls. Relative enrichments were determined versus the control IgG ChIP. Each histogram represents the relative enrichment on the Y-axis and the position relative to the transcriptional start site on the X-axis, and is aligned with the structure of the *flt3* gene represented in the top panel. This figure represents the typical result obtained in five independent experiments in which each PCR was performed in triplicate from one ChIP experiment. Error bars represent the standard error of the mean.

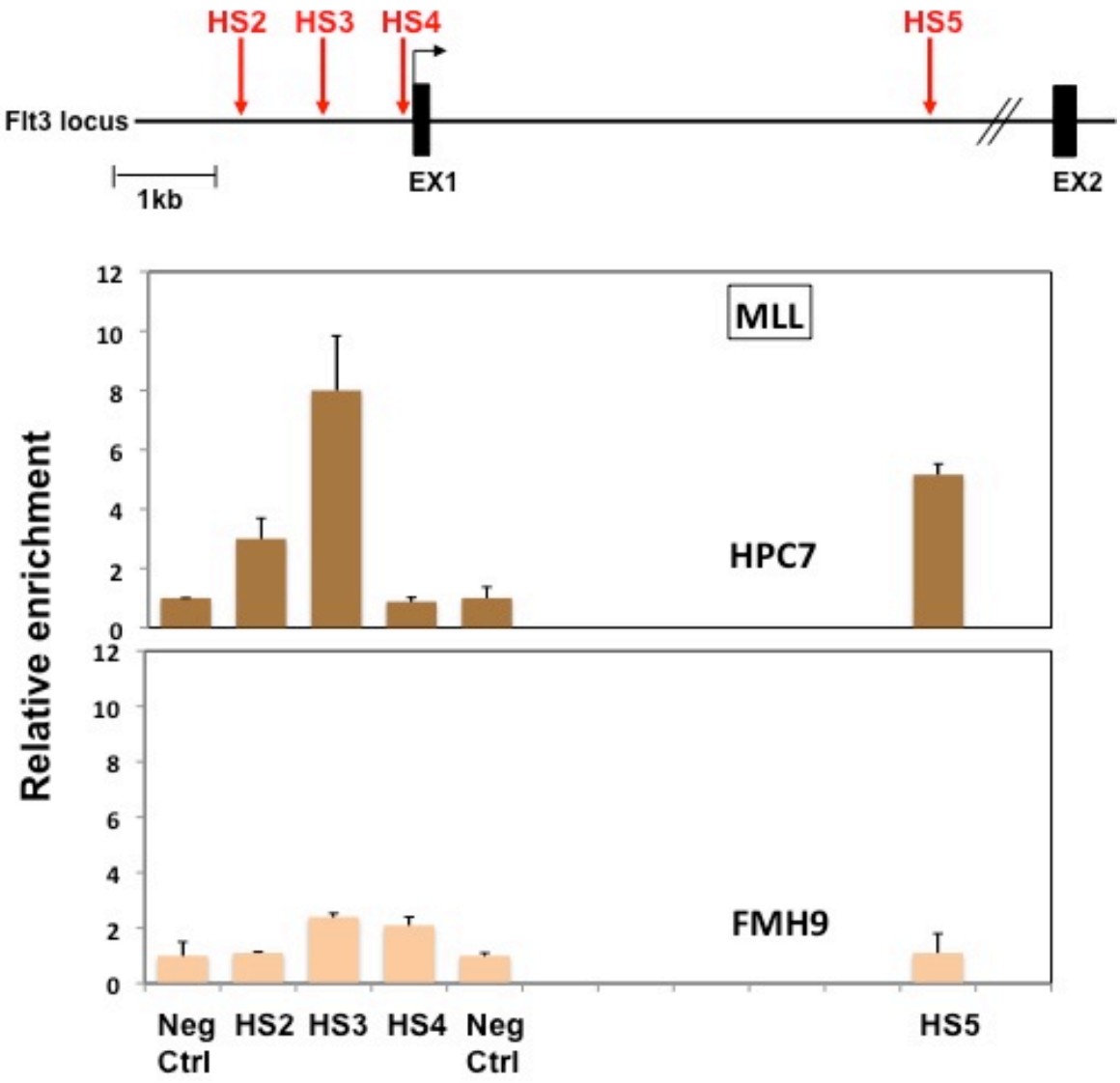

Figure 4.26 In vivo binding of MLL1 at the *flt3* locus. Formaldehyde cross-linked chromatin from both HPC7 and FMH9 cells was immunoprecipitated using an antibody against against the C-terminus of MLL1 and the resulting purified DNA was analysed by Q-PCR using primers covering the four HSS (indicated in the top panel by the red arrows) and two internal controls. Relative enrichments were determined versus the control IgG ChIP. Each histogram represents the relative enrichment on the Y-axis and the position relative to the transcriptional start site on the X-axis, and is aligned with the structure of the *flt3* gene represented in the top panel. This figure represents the typical result obtained in two independent experiments in which each PCR was performed in triplicate from one ChIP experiment. Error bars represent the standard error of the mean.

4.5.3 Evaluation of the relative importance of c-Myb and C/EBPα in the transcriptional regulation of *flt3*.

In section 4.6.2 I demonstrated the in vivo interaction of several transcription factors with the regulatory elements of the flt3 locus. This analysis, performed in HSC-like versus AML-like cell lines, revealed some striking differences regarding the in vivo binding of c-Myb (section 4.6.2.2) and C/EBPα (section 4.6.2.5), with binding of the latter in particular being restricted to the intronic region only in FMH9 cells. Therefore, in order to further elucidate the molecular pathways regulating *flt3* expression, I next performed a gene expression manipulation study in both HSC- and AML-like cells, by either silencing or over expressing c-Myb or C/EBPα.

For the knock down experiments several shRNA vectors have been used to validate our results. More over, a non-effective scrambled shRNA vector was used a negative control to ensure that the c-Myb and C/EBPα knock down effect were specific, therefore avoiding off target effects.

Furthermore, FMH9 cells cannot be efficiently transfected using standard nucleofector reagents (AMAXA), resulting in a cell death higher then 80% after 24 hours in culture. Because to the high cell death, the only analysis presented in the following sections was carried out by Q-PCR, with cells available after sorting not being in a sufficient number for protein analysis.

4.5.3.1 Downregulation studies

RNA interference mediated silencing of both transcription factors was achieved by transfecting both HPC7 and FMH9 cells with plasmids containing short hairpin RNAs

(shRNA) sequences or their corresponding empty control plasmids. Cells were co-transfected with GFP plasmid in order to enable sorting of transfected cells by flow cytometry. The transcript abundance after transfection was evaluated by Q-PCR.

c-Myb **-** HPC7 and FMH9 cells were transfected with either *c-myb* shRNA plasmid (shc-Myb) or its respective control plasmid (pSiren) together with the GFP plasmid. 24 hours later the transfection efficiency was assessed and GFP-positive cells were sorted. Total RNA was then extracted from GFP-positive cells and analysed by Q-PCR to investigate the expression levels of both *c-myb* and *flt3*. This analysis revealed a 40% downregulation of *c-myb* mRNA in HPC7, which consequently resulted in a 60% decrease of *flt3* transcript expression (Figure 4.27 panel A). Q-PCR analysis of c-myb silencing performed in FMH9 cells also highlighted a dramatic downregulation of both *c-myb* (90%) and *flt3* (75%) mRNA expression (Figure 4.27 panel B), pointing out, in conjunction with the X-ChIP data presented in figure 4.20, at the direct involvement of *c-myb* in the regulation of *flt3*.

C/EBPα - Q-PCR analysis of C/EBPα shRNA plasmid (shC/EBPα) transfection in HPC7 revealed a 63% decrease in *C/EBPα* expression compared to cells transfected with the negative control plasmid pGFP-V-R. Interestingly, no differences were observed in *flt3* mRNA expression (Figure 4.28 panel A). Notably, the down regulation of *C/EBPα* (40%) in FMH9 was followed by a marked reduction in *flt3* mRNA expression (50%) (Figure 4.28 panel B). This observation is consistent with the specific recruitment of C/EBPα to the HS5 intronic element of the flt3 gene (Figure 4.24), indicating a key role for C/EBPα in the regulation of *flt3* expression in leukaemia-like cells.

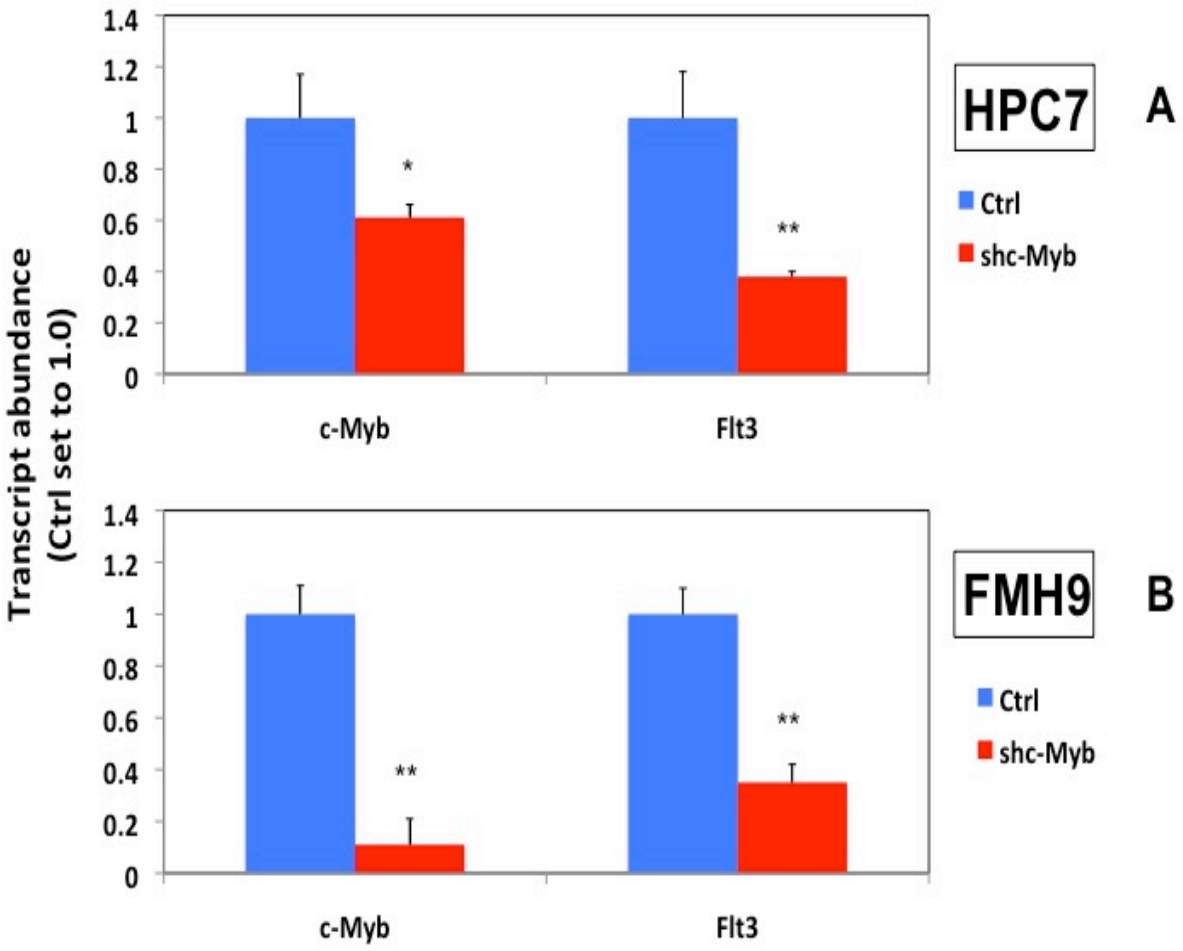

Figure 4.27 Downregulation of *c-myb* levels by shRNA. Q-PCR analysis of c-Myb and *flt3* mRNA expression in HPC7 versus FMH9 after transfection with c-Myb shRNA or its relative empty control vector. *Gapdh* was used as the housekeeping control gene and each PCR reaction was performed for 40 cycles. These data are representative of a single experiment, with each PCR performed in triplicate. The two-tailed p value was determined by paired t-test. Statistical significance: **<0.01, *<0.05. Error bars represent the standard error of the mean.

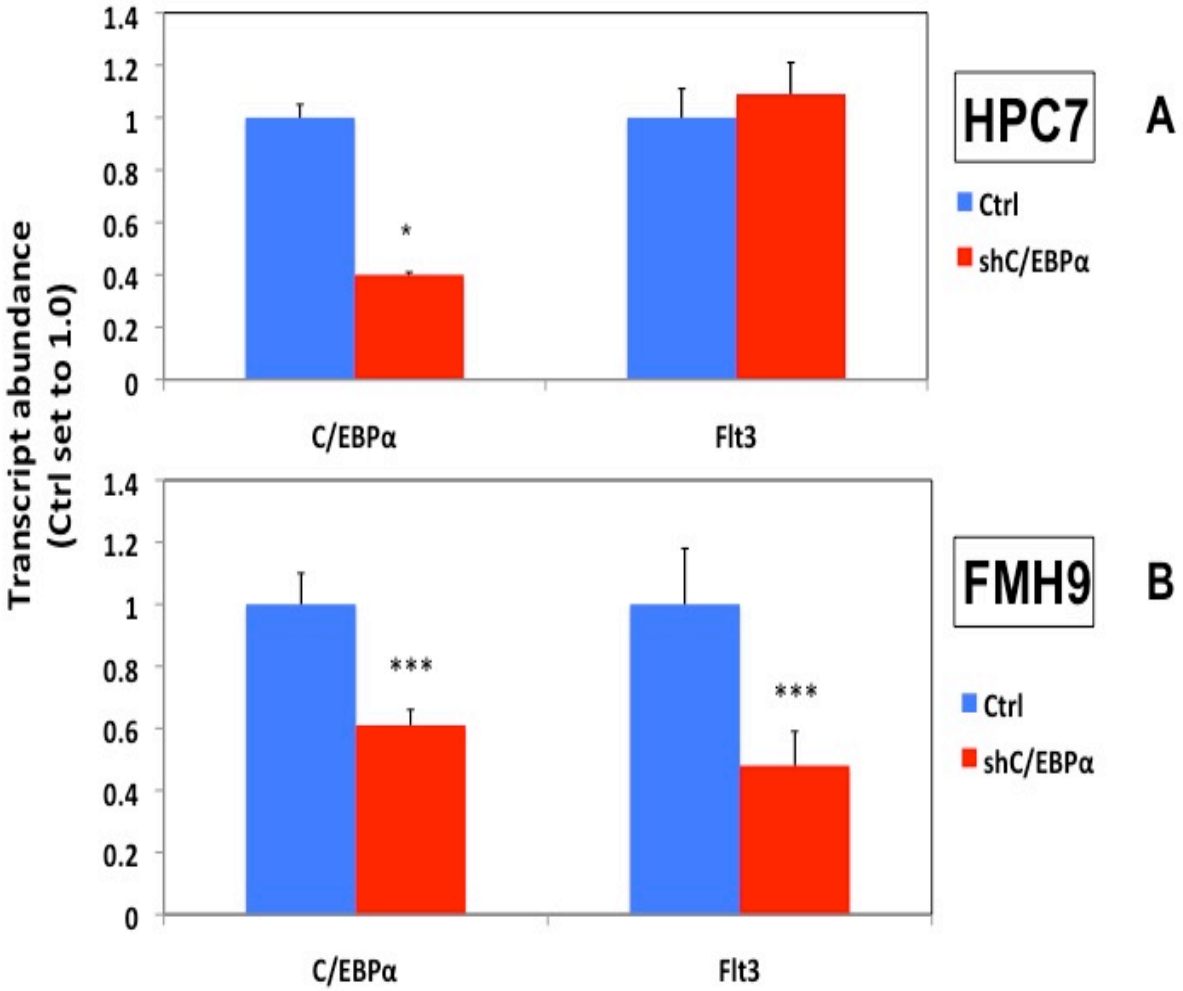

Figure 4.28 Downregulation of *C/EBPα* levels by shRNA. Q-PCR analysis of *C/EBPα* and flt3 mRNA expression in HPC7 versus FMH9 after transfection with C/EBPα shRNA (shC/EBPα) or its relative empty control vector. *Gapdh* was used as the housekeeping control gene and each PCR reaction was performed for 40 cycles. These data are representative of a single experiment, with each PCR performed in triplicate. Results were confirmed in 3 to 4 independent experiments. The two-tailed p value was determined by paired t-test. Statistical significance: ***<0.001, *<0.05. Error bars represent the standard error of the mean.

4.5.3.1 Overexpression studies

The overexpression of *c-myb* and *C/EBPα* was achieved by transfecting HPC7 and FMH9 cells with plasmids containing the full cDNA sequences compared to their corresponding empty control plasmids. Cells were co-transfected with GFP plasmid in order to enable sorting of transfected cells.

c-Myb - 24 hours after trasfection with either a c-Myb expression vector (pcDNA3Myb) or its relative control plasmid, HPC7 and FMH9 cells were sorted based on GFP expression and total RNA from GFP-positive cells was extracted. Q-PCR analysis was performed to assess the expression of both *c-myb* and *flt3*, and revealed the over-expression of *c-myb* in HPC7 (Figure 4.29 panel A), while the mRNA level of *flt3* was unaffected. Interestingly, the overexpression of *c-myb* in FMH9 (3.7 times) resulted in a significant up regulation of *flt3* RNA (Figure 4.29 panel B).

C/EBPα **-** Similar to what I had observed for c-Myb, Q-PCR analysis of *C/EBPα* overexpression in HPC7 cells did not produce significant changes in flt3 expression, although *C/EBPα* up regulation by 3.4 times was achieved (Figure 4.30 panel A); in a number of experiments the over expression of *C/EBPα* in FMH9 did not produce a great up regulation, while *flt3* expression was markedly down regulated (Figure 4.30 panel B). This may be explained by the fact that C/EBPα could induce leukaemic cells to differentiate, as previously published (Lidonnici et al, 2008), therefore losing the expression of *flt3*.

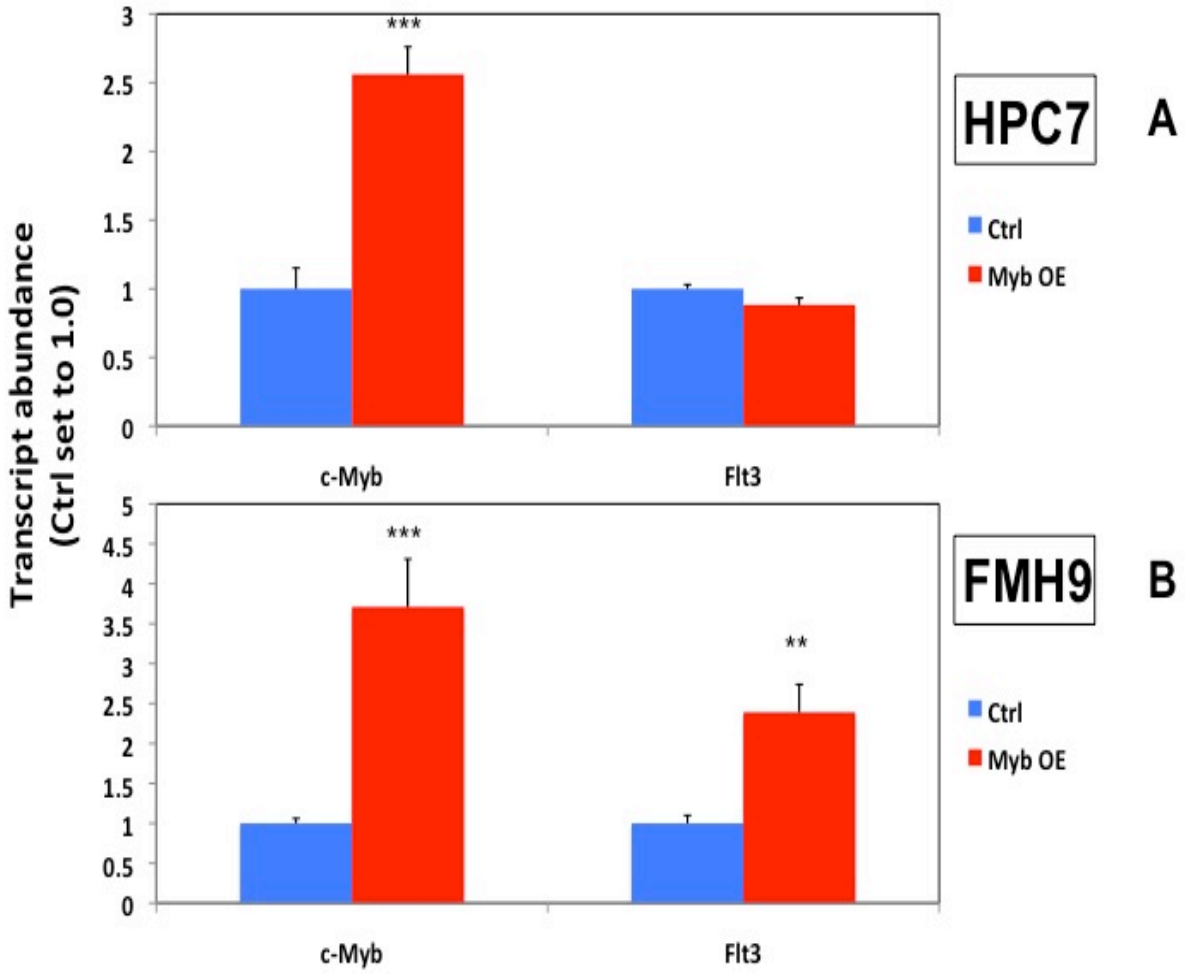

Figure 4.29 Overexpression of *c-myb*. Q-PCR analysis of *c-myb* and flt3 mRNA expression in HPC7 versus FMH9 after transfection with c-Myb expression vector or its relative empty control vector. *Gapdh* was used as the housekeeping control gene and each PCR reaction was performed for 40 cycles. These data are representative of a single experiment, with each PCR performed in triplicate. Results were confirmed in 3 to 4 independent experiments. The two-tailed p value was determined by paired t-test. Statistical significance: ***<0.001 and **<0.01. Error bars represent the standard error of the mean.

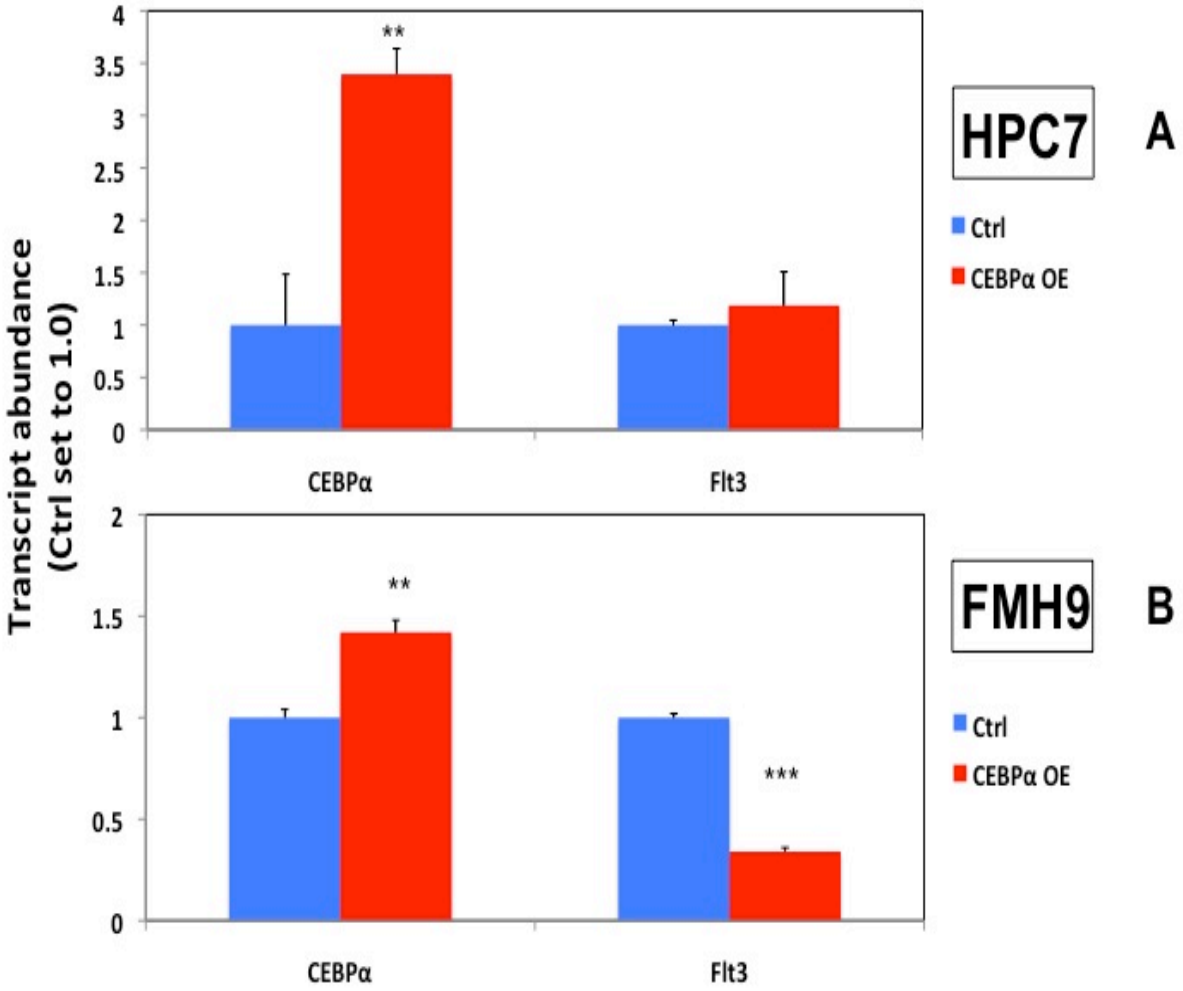

Figure 4.30 Overexpression of *C/EBPα*. Q-PCR analysis of *C/EBPα* and *flt3* mRNA expression in HPC7 versus FMH9 after transfection with c-Myb expression vector or its relative empty control vector. *Gapdh* was used as the housekeeping control gene and each PCR reaction was performed for 40 cycles. These data are representative of a single experiment, with each PCR performed in triplicate. Results were confirmed in 3 to 4 independent experiments. The two-tailed p value was determined by paired t-test. Statistical significance: ***<0.001 and **<0.01.Error bars represent the standard error of the mean.

4.6 Histone modifying enzyme recruitment to *flt3* regulatory regions.

The investigation of epigenetic modifications and transcription factor binding at the *flt3* locus revealed a strict correlation between the interaction of c-Myb and C/EBPα with *flt3* regulatory regions and the pattern of specific histone marks. This could be explained by the fact that either c-Myb or C/EBPα recruit different histone modifying enzymes, leading to the increased expression of *flt3* in AML-like cells. This idea is supported by previous observations by Dai and colleagues who demonstrated the involvement of the histone acetyltransferase CBP (CREB-binding protein) as a co-activator of c-Myb in the transcriptional regulation of several stem cell-related genes (Dai et al., 1996). Another histone acetyltransferase, TIP60, has been shown to synergize with C/EBPα in myeloid differentiation and to be an important player in leukaemia (Bararia et al., 2008). Hence, I next decided to investigate whether CBP and TIP60 were recruited at the *flt3* locus in line with the presence of specific acetylation marks and the direct binding of c-Myb and C/EBPα to *flt3* regulatory regions. For this purpose, X-ChIP analysis was performed using specific antibodies against CBP and TIP60. ChIP products were analyzed by real time PCR, focussing on the regions surrounding the cis-regulatory elements identified by DNAseI HSS assay, in order to determine the pattern for the recruitment of these histone-modifying enzymes around these elements. The relative enrichment displayed in each plot of this section correspond to the ratio Bound specific IgG/Bound non-

specific IgG (Pre-immune), obtained by subtracting the non-specific binding from the preimmune bound.

4.6.1 CBP

Analysis of anti-CBP immunoprecipitated DNA revealed no significant enrichment across the *flt3* promoter/intron 1 region in HPC7 cells (Figure 4.31 upper panel). A similar analysis performed on FMH9 cells highlighted a broader presence of this mark in the vicinity of the HS2 domain and downstream of the transcriptional start and most predominantly in the region immediately upstream the intronic HS5 element (Figure 4.31 lower panel). These findings reflect the difference in the acetylation status observed in FMH9 compared to the HPC7 cells, with the binding of CBP perfectly correlating with the peaks of H4K8ac (see section 4.4.2, Figure 4.8) around the regions of hypersensitivity of the *flt3* locus.

4.6.1 TIP60

The analysis of DNA prepared from anti-TIP60 immunoprecipitated chromatin did not provide any evidence for a significant interaction of TIP60 with the *flt3* locus in HPC7 cells, although a small degree of enrichment was seen at the transcription initiation site and in the vicinity of the intronic HS5 site (Figure 4.32 upper panel). However, a similar analysis of chromatin from FMH9 cells revealed an abundant binding of TIP60 around the regions encompassing the HS2, HS3 and HS4 domains and a large distribution around the HS5 element (Figure 4.32 lower panel), in agreement with the presence of the peak of H3K9 acetylation (Figure 4.9) and the predominance of H4K8 acetylation across the *flt3* locus (Figure 4.8).

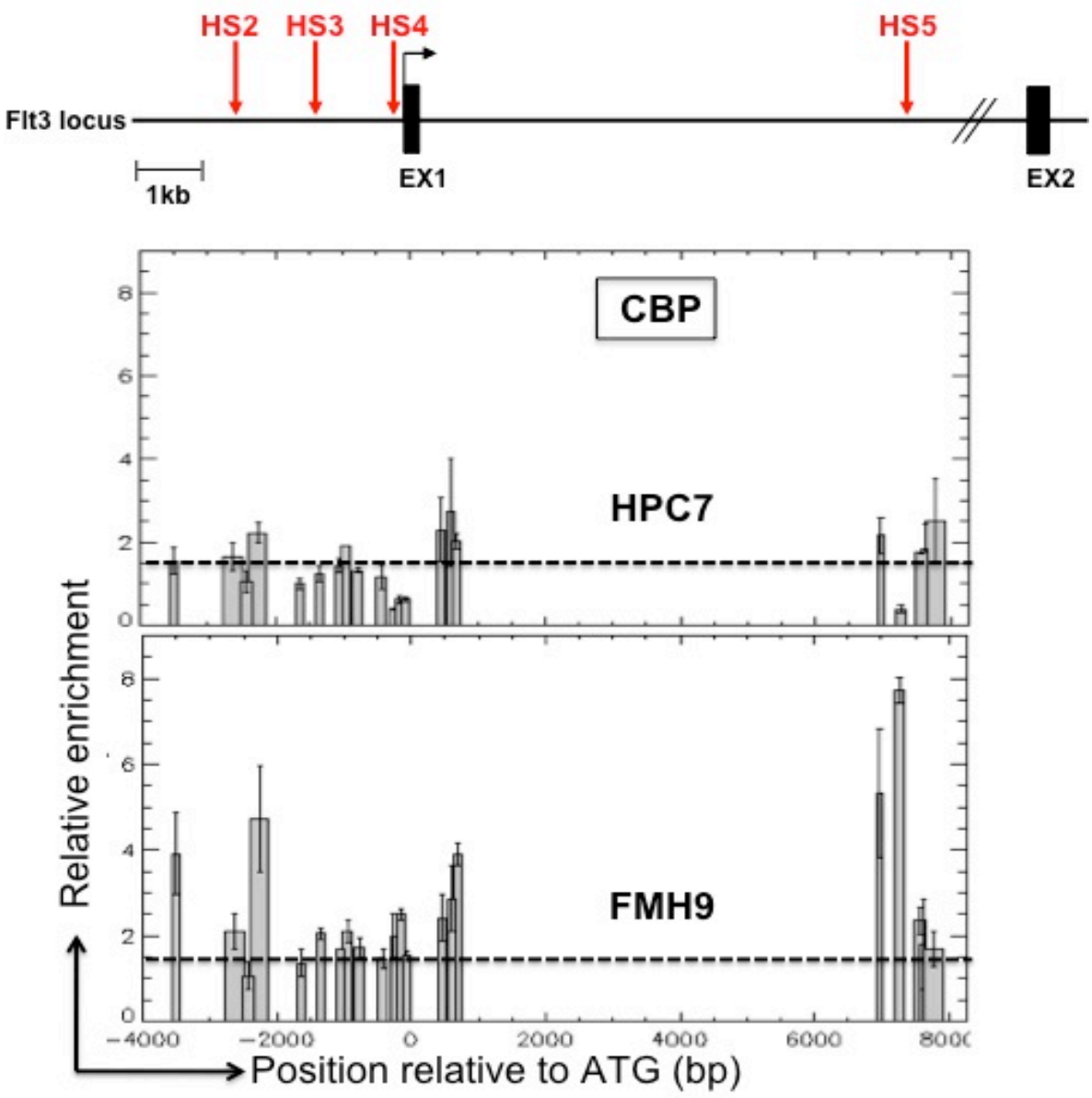

Figure 4.31 In vivo binding of CBP at the *flt3* locus. X-ChIP experiments were performed on chromatin derived from both HPC7 and FMH9 cell lines using an antibody anti-CBP. Purified immunoprecipitated DNA was used as a template for Q-PCR amplifications to determine the relative enrichment compared to the control IgG ChIP material. The plots represent the relative enrichment on the Y-axis and the position relative to the transcriptional start site on the X-axis. The figure shows the alignment of the histograms with a schematic representation of the *flt3* promoter and first intron. DNAseI HSSs are indicated by red arrows. Dashed line represent the basal level across the locus. The width of the bars in the plot reflects the length of the amplicons. PCR amplicons overlap as indicated. This figure represents the typical result obtained in two independent experiments in which each PCR was performed in triplicate from one ChIP experiment. Error bars represent the standard error of the mean.

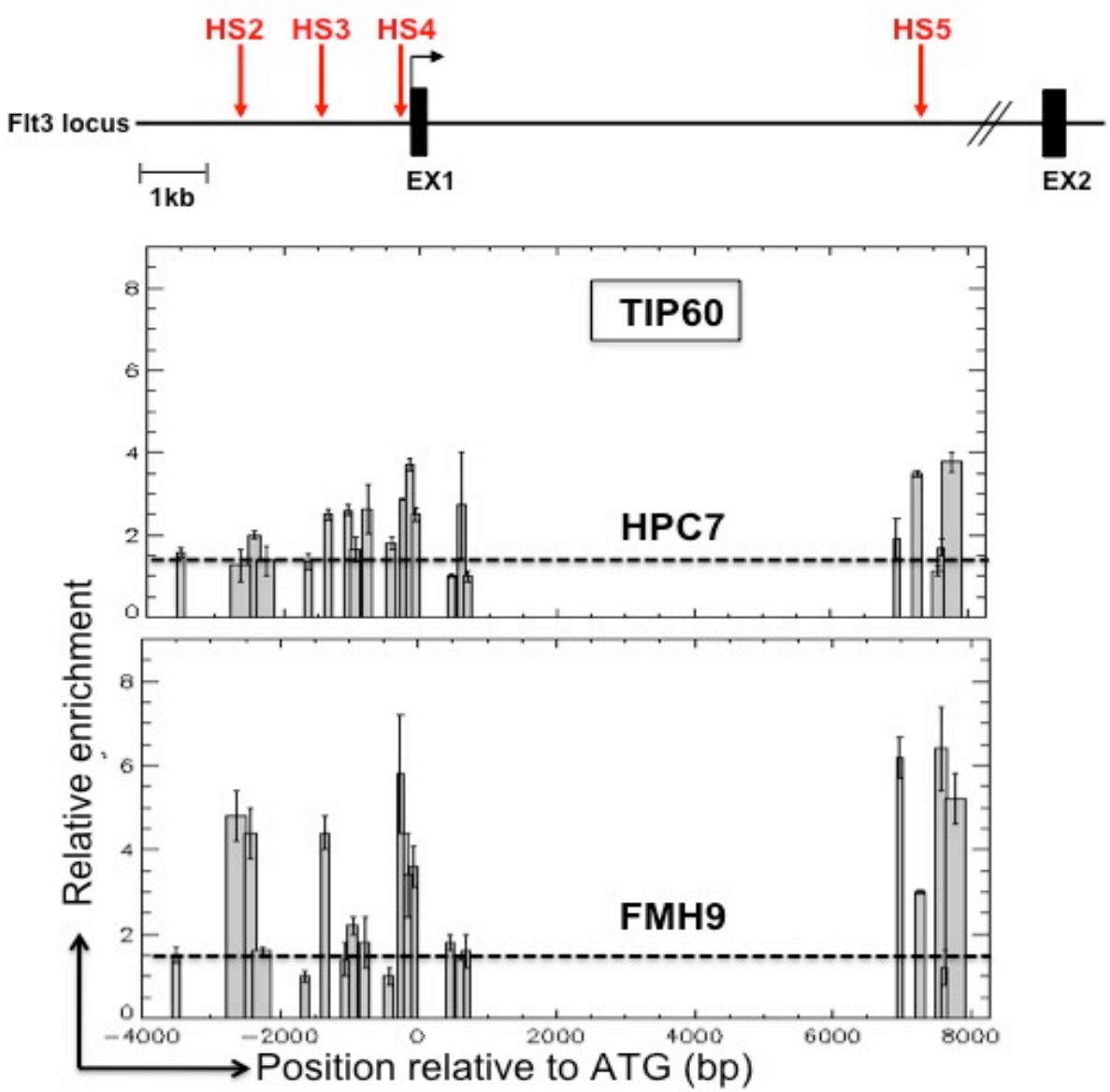

Figure 4.32 In vivo binding of TIP60 at the *flt3* locus. X-ChIP experiments were performed on chromatin derived from both HPC7 and FMH9 cell lines using an antibody anti-TIP60. Purified immunoprecipitated DNA was used as a template for Q-PCR amplifications to determine the relative enrichment compared to the control IgG ChIP material. The plots represent the relative enrichment on the Y-axis and the position relative to the transcriptional start site on the X-axis. The figure shows the alignment of the histograms with a schematic representation of the *flt3* promoter and first intron. DNAseI HSSs are indicated by red arrows. Dashed line represent the basal level across the locus. The width of the bars in the plot reflects the length of the amplicons. PCR amplicons overlap as indicated. This figure represents the typical result obtained in two independent experiments in which each PCR was performed in triplicate from one ChIP experiment. Error bars represent the standard error of the mean.

CHAPTER 5: DISCUSSION AND FUTURE WORK

5.1 Discussion

The last decade has seen a growing interest in the extent to which the receptor tyrosine kinase Flt3 is involved in both expansion and survival of HSCs, progenitors and leukaemic cells (Brasel et al 1995: Turner et al, 1996). Recently, Adolfsson and colleagues have demonstrated that the expression pattern of the Flt3 receptor can be used to distinguish the early stages of commitment of HSCs in the bone marrow compartment, since it is up regulated as the cells transit from LT-HSCs to ST-HSCs and MPPs, followed by rapid down regulation as MPP differentiation takes place (Adolfsson et al, 2001; Adolfsson et al, 2005). Furthermore, a flurry of publications has underlined the association of high-level expression of Flt3 with a broad spectrum of haematological malignancies (reviewed by Gilliland DG, 2002). At present, very little is known about the mechanisms associated with the transcriptional up regulation of *flt3* gene expression in HSCs or how the alteration of such mechanisms may trigger the persistent activation of the gene, either in its wild type or mutated form, in a wide range of leukaemias. To date, the mechanistic differences that might distinguish normal *flt3* expression in HSCs from that seen in leukaemic cells are still unclear and subject of debate.

Since the outset of the investigations described in this thesis, there were two questions to be addressed: 1. How is *flt3* gene transcription regulated in normal HSCs and 2. What mechanistic differences lead to the persistent expression of *flt3* in leukaemic cells? Data presented in this thesis have led to the identification of regions of the *flt3* gene that show features of regulatory activity in relation to its expression, and to a definition of the epigenetic environment and the composition of potential transcription factor complexes interacting with them in vivo in both stem cells and leukaemic cells.

Using two independent DNAseI hypersensitive site mapping approaches (Southern blot and a Q-PCR-based approach), I have identified five candidate cis-regulatory regions in the flt3 locus. Initially, the Southern blot approach was used in order to scan a large part of the gene that showed sequence conservation (see Figure 3.1). Although it is widely applied, the Southern blot approach is not quantitative and it has numerous technical limitations, such as being low-throughput and lacking of sequence specificity, as it is an indirect assay. Thus the Q-PCR approach, which is a quantitative, high-throughput, direct assay, was subsequently used to investigate more precisely the regions of hypersensitivity and to identify potential cis-regulatory domains. This latter analysis was also extended to sorted cells in order to confirm the presence of these regulatory regions in primary cells. Only two of the five domains, HS3 and HS5, appear to be significantly active in primary $Flt3^{-}$KSL (LT- and ST-HSC) and $Flt3^{+}$KSL (MPP) cells, with the intronic (HS5) regulatory element becoming active during the transition between the $Flt3^{-}$ and the $Flt3^{+}$ states. The importance of the HS3 and HS5 regions was emphasized by the characterization of

the epigenetic environment of the *flt3* locus. Hence, ChIP analysis of the acetylation (H3K9ac, H4K8ac) and methylation (H3K4me3, H3K9me2) status of the *flt3* promoter and intronic regions revealed considerable differences in the pattern of these epigenetic modifications (Figure 5.1). Interestingly, a large peak of H3K9 acetylation was detected in the vicinity of the HS5 intronic element (Figure 4.9). An apparent broad enrichment of H4K8 acetylation was seen only in the leukaemia-like cells, while H3K4me3 was differentially distributed in the vicinity of the hypersensitive sites. Importantly, this analysis revealed the predominance of several active histone marks around the intronic HS5 domain (Figure 5.1), which could point to a role of the intronic domain as an enhancer. The epigenetic features observed around the HS5 intronic region could also indicate the presence of an alternative promoter, although there is no evidence of any *flt3* transcript other than that originating at exon1. Whether the HS5 regulatory region is an enhancer or an alternative promoter is yet to be determined and this will be further investigated by performing Polymerase II ChIP and RACE PCR analysis.

In order to assess the link between the epigenetic modifications observed and the in vivo binding of specific transcription factors in stem cells versus leukaemic cells, I carried out a bioinformatic analysis to identify potential protein binding sequences encompassed by the DNAseI hypersensitive regions and then performed X-ChIP experiments for a selected set of transcription factors that could be potentially recruited there.

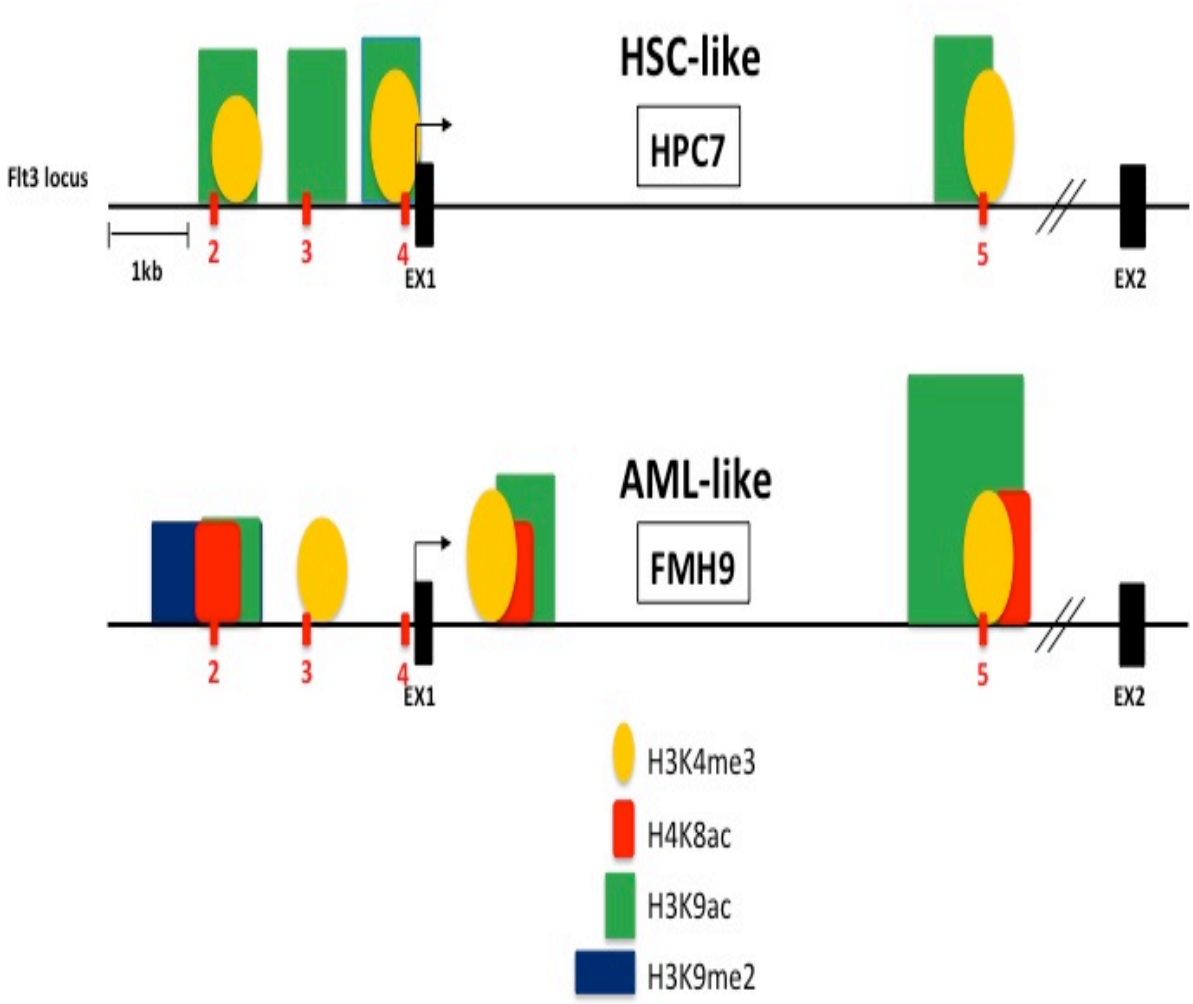

Figure 5.1 Epigenetic modification of the *flt3* gene in haematopoietic stem cells versus leukaemic cells. This figure shows the differential distribution of histone marks around the candidate cis-regulatory elements of the *flt3* gene. HSSs are indicated with red numbers and are aligned to the *flt3* schematic. The black boxes represent exon1 and 2, with the black arrow indicating the transcriptional start site. Histon modifications are represented with a colour code: H3K4me3 in yellow, H48ac in red, H3K9ac in green and H3K9me2 in blue. The size of each symbol is representative of the relative enrichment of each mark (see section 4.5)

This analysis, performed in the HSC-like HPC7 cell line, revealed the binding of multiple transcription factors on HS3 and HS5, including some of the crucial regulators of stem cell maintenance, proliferation and commitment, many of which

are also key players in leukaemogenesis. Following the identification of several conserved consensus binding sites for Ets and GATA factors, ChIP analysis demonstrated the direct interaction of PU.1 and GATA1/2 with the HS3 domain, with GATA1 also binding to HS2 and HS5. The analysis of GATA factors was only performed in HSC-like cells, since their expression was not detected in FMH9, while no interaction of PU.1 with *flt3* locus was observed in FMH9. Importantly, ChIP analysis revealed the binding of C/EBPα and c-Myb, both of them directly interacting with the *flt3* locus on HS3 and HS5 elements. Given the demonstration of an important role for HoxA9, Meis1 and Pbx1/2 in the regulation of *flt3* (Wang et al.; 2006), the direct association of these transcription factors with the *flt3* gene was investigated, and with the exception of Pbx2, each of them was observed to be bound to the HS3 domain in HSC-like cells.

Some of the transcription factors shown to interact with *flt3* regulatory regions appeared to be doing so even though their consensus binding sites are not present. This was the case for Runx1 (Figure 4.25) and MLL (Figure 4.26), suggesting that the in vivo binding of these two transcription factors may be mediated by one or more other protein that are directly recruited to the HS3 and HS5 regions.

Comparative ChIP analysis between HPC7 and FMH9 cells revealed striking differences in the transcription factor occupancy of the *flt3* gene in stem cells and leukaemic cells. Although Mesi1, HoxA9, Pbx1 and c-Myb ChIP revealed a similar profile in both cell types, the recruitment of C/EBPα was noticeably different, being present in HS3 and HS5 in HPC7 cells, but only on the intronic HS5 element in AML-like FMH9 cells. Furthermore, unlike the situation in HPC7 cells, no in vivo

binding of PU.1, Runx1 or MLL was detected in AML-like cells. The binding of MLL was of particular interest, as the in vivo interaction of this transcription factor in HPC7 correlates with the presence of the H3K4me3 histone mark. In fact, in HPC7 cells this mark was found enriched both upstream and downstream of the HS3 region and upstream the HS5 region, where MLL was shown to be recruited on the *flt3* locus (Figure 4.26). No such correlation was observed in FMH9, since MLL binding on the *flt3* gene was not detected in the leukaemic cells. However, it is worth noting that MLL ChIP analysis was performed using an antibody against the C-terminus of MLL and recently it has been observed that MLL^{C}, unlike MLL^{N}, could not be detected in leukaemic cells (personal communication). Therefore, further ChIP analysis using an N-terminal MLL antibody will be needed to follow up on the observations in FMH9 cells.

The ChIP data for transcription factor binding to the *flt3* locus collectively suggests a crucial role for Meis1, HoxA9, C/EBPα and c-Myb in the leukaemic context. Some of these latter transcription factors have been shown to synergize in the regulation of specific genes. For example, it was demonstrated that c-Myb, C/EBPα and PU.1 cooperate in the activation of the *neutrophil elastase* (NE) promoter in myeloid cells (Oelgeshlager et al., 1996) and on the promoter of the avian myeloid gene *mim-1* (Burk et al., 1993; Dudek et al., 1992; Ness et al., 1993). Some of these transcription factors can also exert antagonistic effects, as demonstrated by Soliera and co-workers who have recently established a connection between the transcriptional repression of c-Myb- and C/EBPα-mediated differentiation of leukaemia-like stem cells. The downregulation of *c-myb* mRNA levels was seen

upon C/EBPα activation with consequent differentiation of K562 cells, while c-Myb expression instead resulted in *C/EBPα* downregulation and differentiation arrest (Soliera et al, 2008). However, as the latter authors suggested, this effect seemed to be dependent on the cell context. In fact, in the AML cell model used here, the downregulation of *c-myb* did not produce an effect on *C/EBPα* activity, nor did the overexpression of *C/EBPα* result in significant down regulation of *c-myb* RNA levels (data not shown). However, this suggests that there is a tight balance between different transcription factors that must be maintained in normal stem cells, the alteration of which may result in leukaemogenesis.

The analysis of *in vivo* transcription factor binding also revealed that GATA1, GATA2 and PU.1 are recruited to the *flt3* promoter in HSCs, but appear to be dispensable for *flt3* regulation in leukaemic cells, clearly indicating the involvement of different transcription factor complexes in AML cells compared to normal HSCs (Figure 5.2). Whether this is a reflection of the leukaemic state or the stage myeloid lineage differentiation still needs to be elucidated, and this will be pursued through the analysis of transcription factors complexes recruited to the *flt3* promoter in normal myeloid progenitors.

The potential role of C/EBPα in *flt3* gene regulation is particularly interesting as it exhibits *in vivo* binding to HS3 and HS5 in HSCs, while in AML-like cells its interaction with the *flt3* locus was restricted to the intronic domain. C/EBPα function during commitment towards myeloid progenitors mainly involves the repression of gene expression (Zhang et al 1997; Radomska et al, 1998; Keeshan et al, 2003)

and the loss of C/EBPα expression or activity is an important requirement for leukaemogenesis (Tenen DG, 2003).

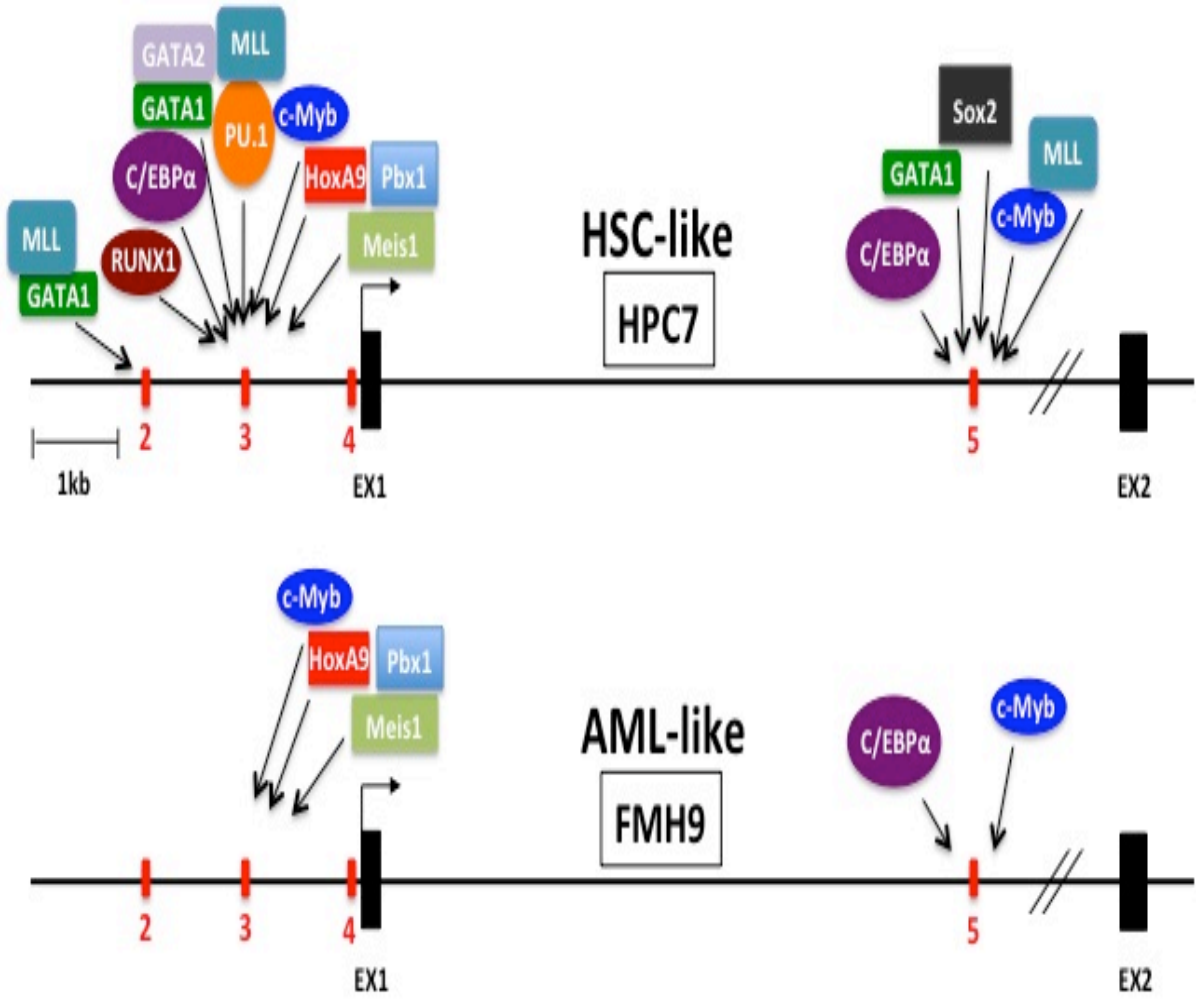

Figure 5.2. Transcription factor binding to the *flt3* gene in haematopoietic stem cells versus leukaemic cells. This figure shows the differential *in vivo* binding of specific transcription factors to the candidate cis-regulatory elements of the *flt3* gene in HSC-like and AML-like cells. HSSs are indicated with red numbers and are aligned to the *flt3* schematic. The black boxes represent exon1 and 2, with the black arrow indicating the transcriptional start site.

C/EBPα mutations have been identified in 10% of AML patient and several studies have demonstrated a higher overall survival in those cases. The most common

alteration to C/EBPα expression consists of the loss of the full-length 42kDa isoform (p42), which regulates the proliferation of myeloid progenitors, and the retention of the oncogenic 30kDa isoform (p30), which functions principally by sumoylating p42, thus decreasing its transactivation capacity (Kirstetter et al., 2008; Geletu et al., 2007). I investigated the presence of both isoforms in the FMH9 and HPC7 cell lines by performing a Western blot analysis (data not shown); this revealed that the p42 isoform is predominant in both cell types.

The relative importance of c-Myb and C/EBPα function in *flt3* regulation was further examined by a combination of shRNA-mediated knock down and overexpression. These studies revealed an important role for c-Myb as its down-regulation produced a significant decrease in *flt3* RNA in both cell lines, while C/EBPα seemed to exert an important function in AML-like cells only, *flt3* expression being unaffected by C/EBPα shRNA-mediated knock down in HPC7 (see Figure 4.30). The overexpression of c-Myb in HPC7 cells did not induce a change in *flt3* mRNA levels, whereas in FMH9 cells it resulted in a large induction of *flt3* expression. Similarly, C/EBPα activation did not induce a significant up-regulation of *flt3* expression in HPC7. Several attempts to over express C/EBPα in FMH9 cells only resulted in a small increase in the level of this transcription factor, but this seemed to be sufficient to achieve a consistent and large down-regulation of *flt3* mRNA. This latter observation could be explained by the propensity of C/EBPα to induce monocytic differentiation in leukaemic cells, as already observed in K562 and in leukaemic $CD34^+$ stem progenitor cells (Soliera et al, 2009; Schepers et al, 2007; Matsushita et al, 2008), or it may reflect a perturbation of the tight balance between the expression

of c-Myb and C/EBPα that is needed for the enhanced flt3 expression in FMH9 cells. As mentioned in section 4.5.3, data for shRNA knock down and overexpression experiments presented in this thesis have been analysed by Q-PCR only, due to the lack of sufficient cell numbers to allow protein analysis by western blot. Having defined a correlation on the *flt3* locus between the epigenetic environment and the *in vivo* binding of c-Myb and C/EBPα, as well as the relative importance of these two transcription factors in the regulation of the gene, I next tried to understand how c-Myb and C/EBPα contribute to the establishment of the epigenetic environment in leukaemia-like cells (see Figure 5.1). The hypothesis that c-Myb and C/EBPα both act to recruit specific chromatin modifying enzymes responsible for the deposition of acetyl marks over the flt3 locus in FMH9 cells is supported by the demonstration that the acetyltransferases CBP and TIP60 function as co-activators of c-Myb and C/EBPα, respectively (Figure 5.3). In fact, Pattabiraman and colleagues reported that mutations in the CBP c-Myb binding domains disturb the interaction of c-Myb with CBP/p300, abrogating its ability to transform myeloid cells (Pattabiraman et al, 2009). Similarly, Bararia and co-workers demonstrated a requirement for TIP60 in C/EBPα function in myeloid differentiation and leukaemia (Bararia et al, 2008). Therefore, the higher level of acetylation observed on the *flt3* locus in FMH9 cells compared to HPC7 cells could be brought about by CBP and TIP60, recruited by c-Myb and C/EBPα, respectively (Figure 5.3).

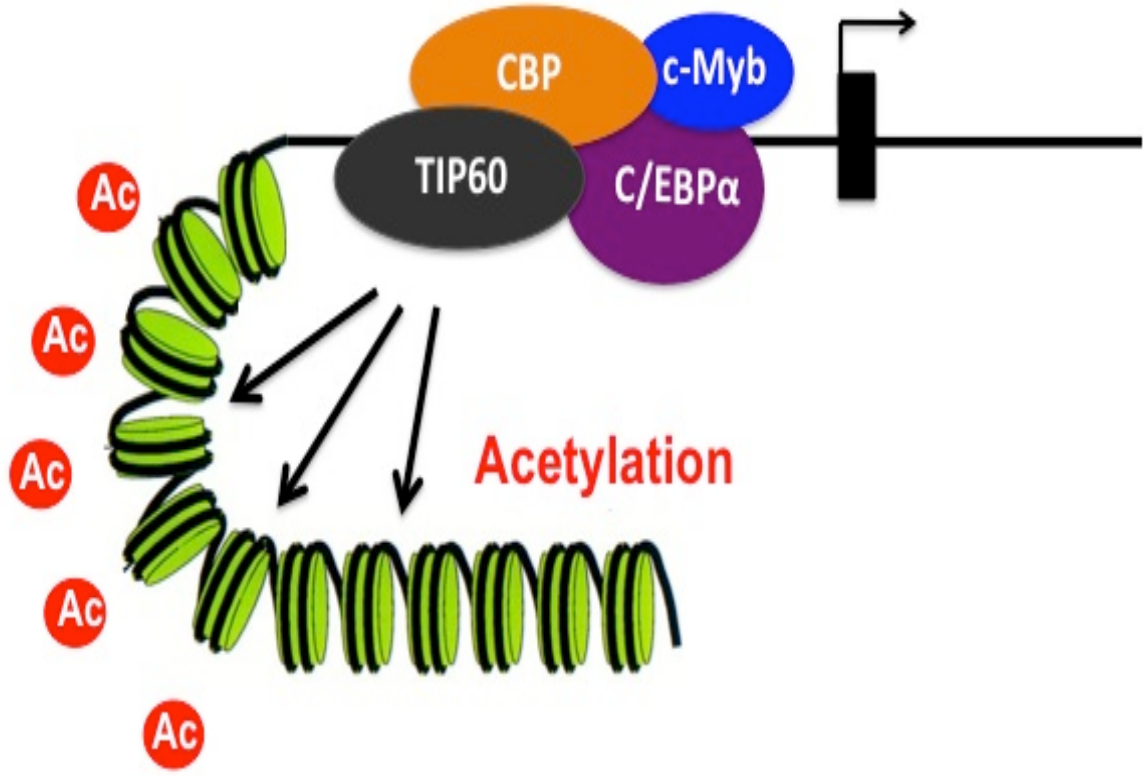

Figure 5.3. Model for recruitment of histone modifying enzymes to the promoter of target genes. This figure summarises the observation obtained by Bararia (Bararia et al., 2008) and Pattabiraman (Pattabiraman et al., 2009), who have demonstrated that c-Myb (blue) and C/EBPα (purple), recruit CBP (orange) and TIP60 (dark grey), respectively, to the promoter region of target genes. These co-factors are histone acetyltransferases, hence being responsible for the deposition of the acetyl marks (Ac, indicated in read).

Interestingly, ChIP analysis in FMH9 for CBP and TIP60 revealed a similar pattern for the recruitment of these two histone modifying enzymes to the *flt3* locus, while no interaction with the promoter or intronic region was observed in HPC7 cells. Notably, the binding observed for CBP mirrors precisely the pattern of H4K8 acetylation observed in FMH9 cells: analysis of both CBP and TIP60 revealed a large peak of binding in the vicinity of the intronic element, co-localizing with H3K9 acetylation. Furthermore, the recruitment of CBP and TIP60 also co-localises with the *in vivo*

binding of both c-Myb and C/EBPα (Figure 5.4): Whether this co-localization is a direct consequence of c-Myb and C/EBPα binding to the *flt3* locus still remains to be elucidated.

This analysis points to a potential role for CBP and TIP60 in the establishment or maintenance of the higher acetylation status observed in the leukaemic context. Whether these two acetyltransferases are the main effectors still needs to be clarified, and this will be assessed initially by performing shRNA analysis of CBP and TIP60 followed by ChIP analysis for both H3K9 and H4K8 acetylation.

Altogether, the data presented in this thesis show that defining the details of epigenetic and transcriptional regulation underlying *flt3* expression can help to elucidate the mechanisms that dictate not only the commitment and differentiation of normal haematopoietic stem cells, but may also shed light on the processes that lead to lineage-restricted cells assuming a leukaemic fate.

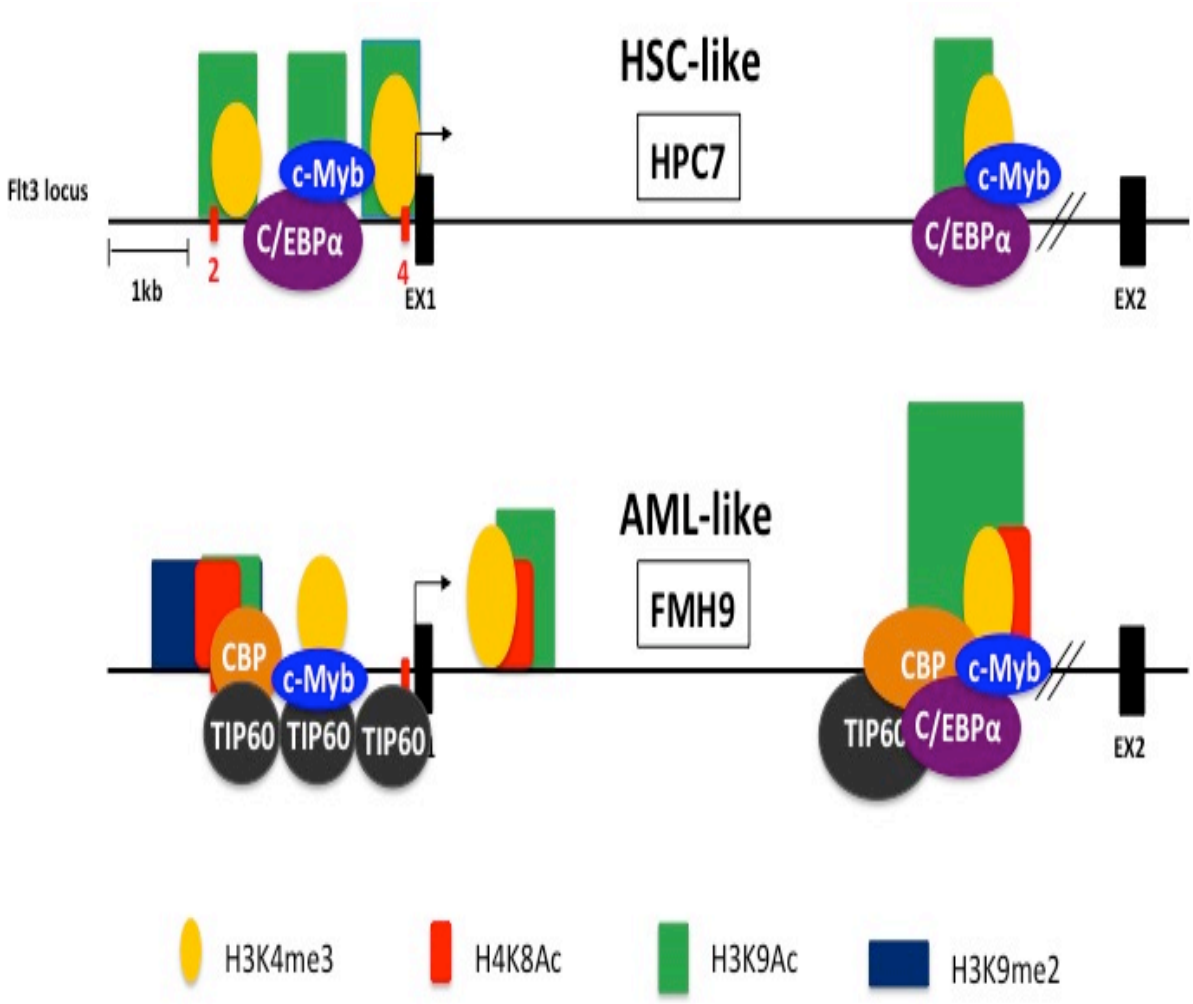

Figure 5.4. Epigenetic and transcriptional regulation of the *flt3* gene in haematopoietic stem cells versus leukaemic cells. This figure shows the differential distribution of histone marks around the candidate cis-regulatory elements of the *flt3* gene, together with the binding of transcription factors c-Myb (blue) and C/EBPα (purple). This figure also shows the differential recruitment of acetyl transferases CBP (orange) and TIP60 (black) in the leukaemic context. HSSs are indicated with red numbers and are aligned to the *flt3* schematic. The black boxes represent exon1 and 2, with the black arrow indicating the transcriptional start site. Histone modifications are represented with a colour code: H3K4me3 in yellow, H48ac in red, H3K9ac in green and H3K9me2 in blue. The size of each symbol is representative of the relative enrichment of each mark (see section 4.5)

5.2 Future directions

Having identified several regions of hypersensitivity that correlate with the presence of epigenetic marks indicative of active transcription as well as the *in vivo* binding of stem cell-related transcription factors, it would be of interest to investigate the relative contribution of each of the candidate regulatory elements identified to the regulation of the *flt3* gene. For this purpose it will be necessary to perform transient transfection assays using promoter-reporter constructs. These constructs will be engineered by linking the promoter either alone or in combination with the intronic element respectively upstream and downstream of the luciferase reporter gene. The importance of each regions of hypersensitivity in the promoter and intronic region will be established by generating specific deletions and point mutations in each of them.

My observations on the differential distribution of active histone epigenetic marks around the intronic HS5 element has led to the hypothesis that this region could either be an enhancer of *flt3* transcription or an alternative promoter. In order to resolve these possibilities, ChIP analysis for H3K4me1 and p300 will need to be performed to assess if the intronic region acts as an enhancer, while ChIP for Polymerase II, in parallel with the RACE PCR, will help to determine the existence of any alternative transcription start site.

It would be interesting also to assess the relative importance of CBP and TIP60. ChIP-ReChIP analysis will be performed in order to determine the direct association of c-Myb with CBP and of C/EBPα with TIP60 on the *flt3* regulatory regions. To

investigate whether CBP and TIP60 are responsible for the higher acetylation status observed in FMH9 cells, shRNA knock down experiments of CBP and TIP60 will be performed, followed by ChIP analysis of H4K8 and H3K9 acetylation.

REFERENCES

Adolfsson, J., O. J. Borge, et al. (2001). "Upregulation of Flt3 expression within the bone marrow Lin(-)Sca1(+)c-kit(+) stem cell compartment is accompanied by loss of self-renewal capacity." Immunity **15**(4): 659-69.

Adolfsson, J., R. Mansson, et al. (2005). "Identification of Flt3+ lympho-myeloid stem cells lacking erythro-megakaryocytic potential a revised road map for adult blood lineage commitment." Cell **121**(2): 295-306.

Agnes, F., B. Shamoon, et al. (1994). "Genomic structure of the downstream part of the human FLT3 gene: exon/intron structure conservation among genes encoding receptor tyrosine kinases (RTK) of subclass III." Gene **145**(2): 283-8.

Akashi, K., D. Traver, et al. (2000). "A clonogenic common myeloid progenitor that gives rise to all myeloid lineages." Nature **404**(6774): 193-7.

Argiropoulos, B. and R. K. Humphries (2007). "Hox genes in hematopoiesis and leukemogenesis." Oncogene **26**(47): 6766-76.

Ayton, P. M. and M. L. Cleary (2001). "Molecular mechanisms of leukemogenesis mediated by MLL fusion proteins." Oncogene **20**(40): 5695-707.

Bararia, D., A. K. Trivedi, et al. (2008). "Proteomic identification of the MYST domain histone acetyltransferase TIP60 (HTATIP) as a co-activator of the myeloid transcription factor C/EBPalpha." Leukemia **22**(4): 800-7.

Begley, C. G. and A. R. Green (1999). "The SCL gene: from case report to critical hematopoietic regulator." Blood **93**(9): 2760-70.

Bellantuono, I. (2004). "Haemopoietic stem cells." Int J Biochem Cell Biol **36**(4): 607-20.

Bird, A. P. and A. P. Wolffe (1999). "Methylation-induced repression--belts, braces, and chromatin." Cell **99**(5): 451-4.

Bonnet, D. (2005a). "Cancer stem cells: lessons from leukaemia." Cell Prolif **38**(6): 357-61.

Bonnet, D. (2005b). "Normal and leukaemic stem cells." Br J Haematol **130**(4): 469-79.

Bonnet, D. and J. E. Dick (1997). "Human acute myeloid leukemia is organized as a hierarchy that originates from a primitive hematopoietic cell." Nat Med **3**(7): 730-7.

Bradbury, C. A., F. L. Khanim, et al. (2005). "Histone deacetylases in acute myeloid leukaemia show a distinctive pattern of expression that changes selectively in response to deacetylase inhibitors." Leukemia **19**(10): 1751-9.

Bradley, T. R. and D. Metcalf (1966). "The growth of mouse bone marrow cells in vitro." Aust J Exp Biol Med Sci **44**(3): 287-99.

Bruce, W. R. and H. Van Der Gaag (1963). "A Quantitative Assay for the Number of Murine Lymphoma Cells Capable of Proliferation in Vivo." Nature **199**: 79-80.

Cao, R., L. Wang, et al. (2002). "Role of histone H3 lysine 27 methylation in Polycomb-group silencing." Science **298**(5595): 1039-43.

Carow, C. E., E. Kim, et al. (1995). "Localization of the human stem cell tyrosine kinase-1 gene (FLT3) to 13q12-->q13." Cytogenet Cell Genet **70**(3-4): 255-7.

Carow, C. E., M. Levenstein, et al. (1996). "Expression of the hematopoietic growth factor receptor FLT3 (STK-1/Flk2) in human leukemias." Blood **87**(3): 1089-96.

Ceredig, R., A. G. Rolink, et al. (2009). "Models of haematopoiesis: seeing the wood for the trees." Nat Rev Immunol **9**(4): 293-300.

Cheshier, S. H., S. J. Morrison, et al. (1999). "In vivo proliferation and cell cycle kinetics of long-term self-renewing hematopoietic stem cells." Proc Natl Acad Sci U S A **96**(6): 3120-5.

Clappier, E., W. Cuccuini, et al. (2007). "The C-MYB locus is involved in chromosomal translocation and genomic duplications in human T-cell acute leukemia (T-ALL), the translocation defining a new T-ALL subtype in very young children." Blood **110**(4): 1251-61.

Constantinidou, C., J. L. Hobman, et al. (2006). "A reassessment of the FNR regulon and transcriptomic analysis of the effects of nitrate, nitrite, NarXL, and NarQP as Escherichia coli K12 adapts from aerobic to anaerobic growth." J Biol Chem **281**(8): 4802-15.

Cumano, A., F. Dieterlen-Lievre, et al. (1996). "Lymphoid potential, probed before circulation in mouse, is restricted to caudal intraembryonic splanchnopleura." Cell **86**(6): 907-16.

Dai, P., H. Akimaru, et al. (1996). "CBP as a transcriptional coactivator of c-Myb." Genes Dev **10**(5): 528-40.

Dakic, A., L. Wu, et al. (2007). "Is PU.1 a dosage-sensitive regulator of haemopoietic lineage commitment and leukaemogenesis?" Trends Immunol **28**(3): 108-14.

Deuring, R., L. Fanti, et al. (2000). "The ISWI chromatin-remodeling protein is required for gene expression and the maintenance of higher order chromatin structure in vivo." Mol Cell **5**(2): 355-65.

Di Croce, L., V. A. Raker, et al. (2002). "Methyltransferase recruitment and DNA hypermethylation of target promoters by an oncogenic transcription factor." Science **295**(5557): 1079-82.

Dick, J. E. (2003). "Stem cells: Self-renewal writ in blood." Nature **423**(6937): 231-3.

Dieterlen-Lievre, F. (1975). "On the origin of haemopoietic stem cells in the avian embryo: an experimental approach." J Embryol Exp Morphol **33**(3): 607-19.

Domen, J. (2001). "The role of apoptosis in regulating hematopoietic stem cell numbers." Apoptosis **6**(4): 239-52.

Domen, J. and I. L. Weissman (1999). "Self-renewal, differentiation or death: regulation and manipulation of hematopoietic stem cell fate." Mol Med Today **5**(5): 201-8.

Dosil, M., S. Wang, et al. (1993). "Mitogenic signalling and substrate specificity of the Flk2/Flt3 receptor tyrosine kinase in fibroblasts and interleukin 3-dependent hematopoietic cells." Mol Cell Biol **13**(10): 6572-85.

Downing, J. R. (2001). "AML1/CBFbeta transcription complex: its role in normal hematopoiesis and leukemia." Leukemia **15**(4): 664-5.

Drexler, H. G. (1996). "Expression of FLT3 receptor and response to FLT3 ligand by leukemic cells." Leukemia **10**(4): 588-99.

Ebihara, Y., K. Tsuji, et al. (1997). "Synergistic action of Flt3 and gp130 signalings in human hematopoiesis." Blood **90**(11): 4363-8.

Erickson, P., J. Gao, et al. (1992). "Identification of breakpoints in t(8;21) acute myelogenous leukemia and isolation of a fusion transcript, AML1/ETO, with similarity to Drosophila segmentation gene, runt." Blood **80**(7): 1825-31.

Frampton, J., T. Ramqvist, et al. (1996). "v-Myb of E26 leukemia virus up-regulates bcl-2 and suppresses apoptosis in myeloid cells." Genes Dev **10**(21): 2720-31.

Georgopoulos, K., M. Bigby, et al. (1994). "The Ikaros gene is required for the development of all lymphoid lineages." Cell **79**(1): 143-56.

Gilliland, D. G., C. T. Jordan, et al. (2004). "The molecular basis of leukemia." Hematology Am Soc Hematol Educ Program: 80-97.

Godin, I., F. Dieterlen-Lievre, et al. (1995). "Emergence of multipotent hemopoietic cells in the yolk sac and paraaortic splanchnopleura in mouse embryos, beginning at 8.5 days postcoitus." Proc Natl Acad Sci U S A **92**(3): 773-7.

Greenberger, J. S., R. J. Eckner, et al. (1983). "Interleukin 3-dependent hematopoietic progenitor cell lines." Fed Proc **42**(10): 2762-71.

Greenberger, J. S., M. A. Sakakeeny, et al. (1983). "Demonstration of permanent factor-dependent multipotential (erythroid/neutrophil/basophil) hematopoietic progenitor cell lines." Proc Natl Acad Sci U S A **80**(10): 2931-5.

Gu, Y., T. Nakamura, et al. (1992). "The t(4;11) chromosome translocation of human acute leukemias fuses the ALL-1 gene, related to Drosophila trithorax, to the AF-4 gene." Cell **71**(4): 701-8.

Hannum, C., J. Culpepper, et al. (1994). "Ligand for FLT3/FLK2 receptor tyrosine kinase regulates growth of haematopoietic stem cells and is encoded by variant RNAs." Nature **368**(6472): 643-8.

Harada, H., Y. Harada, et al. (2004). "High incidence of somatic mutations in the AML1/RUNX1 gene in myelodysplastic syndrome and low blast percentage myeloid leukemia with myelodysplasia." Blood **103**(6): 2316-24.

Harada, H., Y. Harada, et al. (2003). "Implications of somatic mutations in the AML1 gene in radiation-associated and therapy-related myelodysplastic syndrome/acute myeloid leukemia." Blood **101**(2): 673-80.

Hawley, T. S., A. Z. Fong, et al. (1998). "Leukemic predisposition of mice transplanted with gene-modified hematopoietic precursors expressing flt3 ligand." Blood **92**(6): 2003-11.

Herman, J. G. and S. B. Baylin (2003). "Gene silencing in cancer in association with promoter hypermethylation." N Engl J Med **349**(21): 2042-54.

Hess, J. L., C. B. Bittner, et al. (2006). "c-Myb is an essential downstream target for homeobox-mediated transformation of hematopoietic cells." Blood **108**(1): 297-304.

Hisa, T., S. E. Spence, et al. (2004). "Hematopoietic, angiogenic and eye defects in Meis1 mutant animals." EMBO J **23**(2): 450-9.

Ho, A. D. (2005). "Kinetics and symmetry of divisions of hematopoietic stem cells." Exp Hematol **33**(1): 1-8.

Holmes, M. L., S. Carotta, et al. (2006). "Repression of Flt3 by Pax5 is crucial for B-cell lineage commitment." Genes Dev **20**(8): 933-8.

Horvitz, H. R. and I. Herskowitz (1992). "Mechanisms of asymmetric cell division: two Bs or not two Bs, that is the question." Cell **68**(2): 237-55.

Hsieh, J. J., E. H. Cheng, et al. (2003). "Taspase1: a threonine aspartase required for cleavage of MLL and proper HOX gene expression." Cell **115**(3): 293-303.

Hu, Y. L., S. Fong, et al. (2009). "HOXA9 modulates its oncogenic partner Meis1 to influence normal hematopoiesis." Mol Cell Biol **29**(18): 5181-92.

Ichikawa, M., T. Asai, et al. (2004). "AML-1 is required for megakaryocytic maturation and lymphocytic differentiation, but not for maintenance of hematopoietic stem cells in adult hematopoiesis." Nat Med **10**(3): 299-304.

Ichikawa, Y. (1969). "Differentiation of a cell line of myeloid leukemia." J Cell Physiol **74**(3): 223-34.

Ikuta, K. and I. L. Weissman (1992). "Evidence that hematopoietic stem cells express mouse c-kit but do not depend on steel factor for their generation." Proc Natl Acad Sci U S A **89**(4): 1502-6.

Iwasaki, H., C. Somoza, et al. (2005). "Distinctive and indispensable roles of PU.1 in maintenance of hematopoietic stem cells and their differentiation." Blood **106**(5): 1590-600.

Kastner, P. and S. Chan (2008). "PU.1: a crucial and versatile player in hematopoiesis and leukemia." Int J Biochem Cell Biol **40**(1): 22-7.

Kawashima, T., K. Murata, et al. (2001). "STAT5 induces macrophage differentiation of M1 leukemia cells through activation of IL-6 production mediated by NF-kappaB p65." J Immunol **167**(7): 3652-60.

Kitabayashi, I., A. Yokoyama, et al. (1998). "Interaction and functional cooperation of the leukemia-associated factors AML1 and p300 in myeloid cell differentiation." EMBO J **17**(11): 2994-3004.

Klemsz, M. J., S. R. McKercher, et al. (1990). "The macrophage and B cell-specific transcription factor PU.1 is related to the ets oncogene." Cell **61**(1): 113-24.

Koeffler, H. P. and D. W. Golde (1980). "Human myeloid leukemia cell lines: a review." Blood **56**(3): 344-50.

Kondo, M., I. L. Weissman, et al. (1997). "Identification of clonogenic common lymphoid progenitors in mouse bone marrow." Cell **91**(5): 661-72.

Kornberg, R. D. (1974). "Chromatin structure: a repeating unit of histones and DNA." Science **184**(139): 868-71.

Kornberg, R. D. and J. O. Thomas (1974). "Chromatin structure; oligomers of the histones." Science **184**(139): 865-8.

Kottaridis, P. D., R. E. Gale, et al. (2001). "The presence of a FLT3 internal tandem duplication in patients with acute myeloid leukemia (AML) adds important prognostic information to cytogenetic risk group and response to the first cycle of chemotherapy: analysis of 854 patients from the United Kingdom Medical Research Council AML 10 and 12 trials." Blood **98**(6): 1752-9.

Kouzarides, T. (2003). "Wellcome Trust Award Lecture. Chromatin-modifying enzymes in transcription and cancer." Biochem Soc Trans **31**(Pt 4): 741-3.

Krivtsov, A. V. and S. A. Armstrong (2007). "MLL translocations, histone modifications and leukaemia stem-cell development." Nat Rev Cancer **7**(11): 823-33.

Krysinska, H., M. Hoogenkamp, et al. (2007). "A Two-Step, PU.1-Dependent Mechanism for Developmentally Regulated Chromatin Remodeling and Transcription of the c-*fms* Gene"

Kroon, E., J. Krosl, et al. (1998). "Hoxa9 transforms primary bone marrow cells through specific collaboration with Meis1a but not Pbx1b." EMBO J **17**(13): 3714-25.

Kuzmichev, A., T. Jenuwein, et al. (2004). "Different EZH2-containing complexes target methylation of histone H1 or nucleosomal histone H3." Mol Cell **14**(2): 183-93.

Lachner, M., D. O'Carroll, et al. (2001). "Methylation of histone H3 lysine 9 creates a binding site for HP1 proteins." Nature **410**(6824): 116-20.

Lapidot, T., C. Sirard, et al. (1994). "A cell initiating human acute myeloid leukaemia after transplantation into SCID mice." Nature **367**(6464): 645-8.

Lawrence, H. J., J. Christensen, et al. (2005). "Loss of expression of the Hoxa-9 homeobox gene impairs the proliferation and repopulating ability of hematopoietic stem cells." Blood **106**(12): 3988-94.

Lawrence, H. J., C. D. Helgason, et al. (1997). "Mice bearing a targeted interruption of the homeobox gene HOXA9 have defects in myeloid, erythroid, and lymphoid hematopoiesis." Blood **89**(6): 1922-30.

Li, L. and T. Xie (2005). "Stem cell niche: structure and function." Annu Rev Cell Dev Biol **21**: 605-31.

Lidonnici, M. R., F. Corradini, et al. (2008). "Requirement of c-Myb for p210(BCR/ABL)-dependent transformation of hematopoietic progenitors and leukemogenesis." Blood **111**(9): 4771-9.

Lionberger, J. M. and D. L. Stirewalt (2009). "Gene expression changes in normal haematopoietic cells." Best Pract Res Clin Haematol **22**(2): 249-69.

Lochner, K., G. Siegler, et al. (1996). "A specific deletion in the breakpoint cluster region of the ALL-1 gene is associated with acute lymphoblastic T-cell leukemias." Cancer Res **56**(9): 2171-7.

Lowenberg, B., J. R. Downing, et al. (1999). "Acute myeloid leukemia." N Engl J Med **341**(14): 1051-62.

Luger, K., A. W. Mader, et al. (1997). "Crystal structure of the nucleosome core particle at 2.8 A resolution." Nature **389**(6648): 251-60.

Lund, A. H. and M. van Lohuizen (2004). "Epigenetics and cancer." Genes Dev **18**(19): 2315-35.

Lyman, S. D. (1995). "Biology of flt3 ligand and receptor." Int J Hematol **62**(2): 63-73.

Lyman, S. D., K. Brasel, et al. (1994). "The flt3 ligand: a hematopoietic stem cell factor whose activities are distinct from steel factor." Stem Cells **12 Suppl 1**: 99-107; discussion 108-10.

Lyman, S. D., L. James, et al. (1993). "Molecular cloning of a ligand for the flt3/flk-2 tyrosine kinase receptor: a proliferative factor for primitive hematopoietic cells." Cell **75**(6): 1157-67.

Mackarehtschian, K., J. D. Hardin, et al. (1995). "Targeted disruption of the flk2/flt3 gene leads to deficiencies in primitive hematopoietic progenitors." Immunity **3**(1): 147-61.

Maraskovsky, E., K. Brasel, et al. (1996). "Dramatic increase in the numbers of functionally mature dendritic cells in Flt3 ligand-treated mice: multiple dendritic cell subpopulations identified." J Exp Med **184**(5): 1953-62.

Maraskovsky, E., E. Daro, et al. (2000). "In vivo generation of human dendritic cell subsets by Flt3 ligand." Blood **96**(3): 878-84.

Margueron, R., P. Trojer, et al. (2005). "The key to development: interpreting the histone code?" Curr Opin Genet Dev **15**(2): 163-76.

Mathews, L. S. and W. W. Vale (1991). "Expression cloning of an activin receptor, a predicted transmembrane serine kinase." Cell **65**(6): 973-82.

Matthews, W., C. T. Jordan, et al. (1991). "A receptor tyrosine kinase cDNA isolated from a population of enriched primitive hematopoietic cells and exhibiting close genetic linkage to c-kit." Proc Natl Acad Sci U S A **88**(20): 9026-30.

Mayani, H., W. Dragowska, et al. (1993). "Lineage commitment in human hemopoiesis involves asymmetric cell division of multipotent progenitors and does not appear to be influenced by cytokines." J Cell Physiol **157**(3): 579-86.

Mayotte, N., D. C. Roy, et al. (2002). "Oncogenic interaction between BCR-ABL and NUP98-HOXA9 demonstrated by the use of an in vitro purging culture system." Blood **100**(12): 4177-84.

McKenna, H. J., K. L. Stocking, et al. (2000). "Mice lacking flt3 ligand have deficient hematopoiesis affecting hematopoietic progenitor cells, dendritic cells, and natural killer cells." Blood **95**(11): 3489-97.

McKercher, S. R., B. E. Torbett, et al. (1996). "Targeted disruption of the PU.1 gene results in multiple hematopoietic abnormalities." Embo J **15**(20): 5647-58.

Medvinsky, A. and E. Dzierzak (1996). "Definitive hematopoiesis is autonomously initiated by the AGM region." Cell **86**(6): 897-906.

Mikkola, H. K. and S. H. Orkin (2006). "The journey of developing hematopoietic stem cells." Development **133**(19): 3733-44.

Miller, J., A. Horner, et al. (2002). "The core-binding factor beta subunit is required for bone formation and hematopoietic maturation." Nat Genet **32**(4): 645-9.

Miyoshi, H., K. Shimizu, et al. (1991). "t(8;21) breakpoints on chromosome 21 in acute myeloid leukemia are clustered within a limited region of a single gene, AML1." Proc Natl Acad Sci U S A **88**(23): 10431-4.

Moore, M. A. and D. Metcalf (1970). "Ontogeny of the haemopoietic system: yolk sac origin of in vivo and in vitro colony forming cells in the developing mouse embryo." Br J Haematol **18**(3): 279-96.

Moreno, I., G. Martin, et al. (2003). "Incidence and prognostic value of FLT3 internal tandem duplication and D835 mutations in acute myeloid leukemia." Haematologica **88**(1): 19-24.

Morrison, S. J. and J. Kimble (2006). "Asymmetric and symmetric stem-cell divisions in development and cancer." Nature **441**(7097): 1068-74.

Morrison, S. J. and I. L. Weissman (1994). "The long-term repopulating subset of hematopoietic stem cells is deterministic and isolatable by phenotype." Immunity **1**(8): 661-73.

Mucenski, M. L., K. McLain, et al. (1991). "A functional c-myb gene is required for normal murine fetal hepatic hematopoiesis." Cell **65**(4): 677-89.

Muller, A. M., A. Medvinsky, et al. (1994). "Development of hematopoietic stem cell activity in the mouse embryo." Immunity **1**(4): 291-301.

Nakamura, T., T. Mori, et al. (2002). "ALL-1 is a histone methyltransferase that assembles a supercomplex of proteins involved in transcriptional regulation." Mol Cell **10**(5): 1119-28.

Nakao, M., S. Yokota, et al. (1996). "Internal tandem duplication of the flt3 gene found in acute myeloid leukemia." Leukemia **10**(12): 1911-8.

Namikawa, R., M. O. Muench, et al. (1999). "Administration of Flk2/Flt3 ligand induces expansion of human high-proliferative potential colony-forming cells in the SCID-hu mouse." Exp Hematol **27**(6): 1029-37.

Nichogiannopoulou, A., M. Trevisan, et al. (1999). "Defects in hemopoietic stem cell activity in Ikaros mutant mice." J Exp Med **190**(9): 1201-14.

Nightingale, K. P., L. P. O'Neill, et al. (2006). "Histone modifications: signalling receptors and potential elements of a heritable epigenetic code." Curr Opin Genet Dev **16**(2): 125-36.

Niki, M., H. Okada, et al. (1997). "Hematopoiesis in the fetal liver is impaired by targeted mutagenesis of a gene encoding a non-DNA binding subunit of the transcription factor, polyomavirus enhancer binding protein 2/core binding factor." Proc Natl Acad Sci U S A **94**(11): 5697-702.

Novotny, E., S. Compton, et al. (2009). "In vitro hematopoietic differentiation of mouse embryonic stem cells requires the tumor suppressor menin and is mediated by Hoxa9." Mech Dev **126**(7): 517-22.

Nutt, S. L., B. Heavey, et al. (1999). "Commitment to the B-lymphoid lineage depends on the transcription factor Pax5." Nature **401**(6753): 556-62.

O'Carroll, D., S. Erhardt, et al. (2001). "The polycomb-group gene Ezh2 is required for early mouse development." Mol Cell Biol **21**(13): 4330-6.

Okuda, T., J. van Deursen, et al. (1996). "AML1, the target of multiple chromosomal translocations in human leukemia, is essential for normal fetal liver hematopoiesis." Cell **84**(2): 321-30.

Orkin, S. H. (1995). "Transcription factors and hematopoietic development." J Biol Chem **270**(10): 4955-8.

Osato, M. (2004). "Point mutations in the RUNX1/AML1 gene: another actor in RUNX leukemia." Oncogene **23**(24): 4284-96.

Osato, M., N. Asou, et al. (1999). "Biallelic and heterozygous point mutations in the runt domain of the AML1/PEBP2alphaB gene associated with myeloblastic leukemias." Blood **93**(6): 1817-24.

Osawa, M., K. Hanada, et al. (1996). "Long-term lymphohematopoietic reconstitution by a single CD34-low/negative hematopoietic stem cell." Science **273**(5272): 242-5.

Passegue, E., C. H. Jamieson, et al. (2003). "Normal and leukemic hematopoiesis: are leukemias a stem cell disorder or a reacquisition of stem cell characteristics?" Proc Natl Acad Sci U S A **100 Suppl 1**: 11842-9.

Pina, C. and T. Enver (2007). "Differential contributions of haematopoietic stem cells to foetal and adult haematopoiesis: insights from functional analysis of transcriptional regulators." Oncogene **26**(47): 6750-65.

Pinto do, O. P., K. Richter, et al. (2002). "Hematopoietic progenitor/stem cells immortalized by Lhx2 generate functional hematopoietic cells in vivo." Blood **99**(11): 3939-46.

Porcher, C., W. Swat, et al. (1996). "The T cell leukemia oncoprotein SCL/tal-1 is essential for development of all hematopoietic lineages." Cell **86**(1): 47-57.

Preudhomme, C., D. Warot-Loze, et al. (2000). "High incidence of biallelic point mutations in the Runt domain of the AML1/PEBP2 alpha B gene in Mo acute myeloid leukemia and in myeloid malignancies with acquired trisomy 21." Blood **96**(8): 2862-9.

Rabbitts, T. H. (1998). "LMO T-cell translocation oncogenes typify genes activated by chromosomal translocations that alter transcription and developmental processes." Genes Dev **12**(17): 2651-7.

Ralph, P., H. E. Broxmeyer, et al. (1977). "Immunostimulators induce granulocyte/macrophage colony-stimulating activity and block proliferation in a monocyte tumor cell line." J Exp Med **146**(2): 611-6.

Ralph, P. and I. Nakoinz (1977). "Antibody-dependent killing of erythrocyte and tumor targets by macrophage-related cell lines: enhancement by PPD and LPS." J Immunol **119**(3): 950-54.

Ray, R. J., C. J. Paige, et al. (1996). "Flt3 ligand supports the differentiation of early B cell progenitors in the presence of interleukin-11 and interleukin-7." Eur J Immunol **26**(7): 1504-10.

Rodrigues, N. P., V. Janzen, et al. (2005). "Haploinsufficiency of GATA-2 perturbs adult hematopoietic stem-cell homeostasis." Blood **106**(2): 477-84.

Rosnet, O., H. J. Buhring, et al. (1996a). "Expression and signal transduction of the FLT3 tyrosine kinase receptor." Acta Haematol **95**(3-4): 218-23.

Rosnet, O., H. J. Buhring, et al. (1996b). "Human FLT3/FLK2 receptor tyrosine kinase is expressed at the surface of normal and malignant hematopoietic cells." Leukemia **10**(2): 238-48.

Rosnet, O., S. Marchetto, et al. (1991). "Murine Flt3, a gene encoding a novel tyrosine kinase receptor of the PDGFR/CSF1R family." Oncogene **6**(9): 1641-50.

Rosnet, O., M. G. Mattei, et al. (1991). "Isolation and chromosomal localization of a novel FMS-like tyrosine kinase gene." Genomics **9**(2): 380-5.

Rottapel, R., C. W. Turck, et al. (1994). "Substrate specificities and identification of a putative binding site for PI3K in the carboxy tail of the murine Flt3 receptor tyrosine kinase." Oncogene **9**(6): 1755-65.

Rusten, L. S., S. D. Lyman, et al. (1996). "The FLT3 ligand is a direct and potent stimulator of the growth of primitive and committed human CD34+ bone marrow progenitor cells in vitro." Blood **87**(4): 1317-25.

Savvides, S. N., T. Boone, et al. (2000). "Flt3 ligand structure and unexpected commonalities of helical bundles and cystine knots." Nat Struct Biol **7**(6): 486-91.

Sawyers, C. L., C. T. Denny, et al. (1991). "Leukemia and the disruption of normal hematopoiesis." Cell **64**(2): 337-50.

Scheijen, B., H. T. Ngo, et al. (2004). "FLT3 receptors with internal tandem duplications promote cell viability and proliferation by signaling through Foxo proteins." Oncogene **23**(19): 3338-49.

Schichman, S. A., M. A. Caligiuri, et al. (1994). "ALL-1 partial duplication in acute leukemia." Proc Natl Acad Sci U S A **91**(13): 6236-9.

Scott, E. W., M. C. Simon, et al. (1994). "Requirement of transcription factor PU.1 in the development of multiple hematopoietic lineages." Science **265**(5178): 1573-7.

Shen, W. F., J. C. Montgomery, et al. (1997). "AbdB-like Hox proteins stabilize DNA binding by the Meis1 homeodomain proteins." Mol Cell Biol **17**(11): 6448-58.

Shen, W. F., S. Rozenfeld, et al. (1999). "HOXA9 forms triple complexes with PBX2 and MEIS1 in myeloid cells." Mol Cell Biol **19**(4): 3051-61.

Shilatifard, A., W. S. Lane, et al. (1996). "An RNA polymerase II elongation factor encoded by the human ELL gene." Science **271**(5257): 1873-6.

Shivdasani, R. A., E. L. Mayer, et al. (1995). "Absence of blood formation in mice lacking the T-cell leukaemia oncoprotein tal-1/SCL." Nature **373**(6513): 432-4.

Siminovitch, L., E. A. McCulloch, et al. (1963). "The Distribution of Colony-Forming Cells among Spleen Colonies." J Cell Physiol **62**: 327-36.

Slany, R. K. (2005). "Chromatin control of gene expression: mixed-lineage leukemia methyltransferase SETs the stage for transcription." Proc Natl Acad Sci U S A **102**(41): 14481-2.

Snaddon, J., M. L. Smith, et al. (2003). "Mutations of CEBPA in acute myeloid leukemia FAB types M1 and M2." Genes Chromosomes Cancer **37**(1): 72-8.

Spooncer, E., D. Boettiger, et al. (1984). "Continuous in vitro generation of multipotential stem cell clones from src-infected cultures." Nature **310**(5974): 228-30.

Spooncer, E. and T. M. Dexter (1984). "Long-term bone marrow cultures." Bibl Haematol(48): 366-83.

Spradling, A., D. Drummond-Barbosa, et al. (2001). "Stem cells find their niche." Nature **414**(6859): 98-104.

Stirewalt, D. L. and J. P. Radich (2003). "The role of FLT3 in haematopoietic malignancies." Nat Rev Cancer **3**(9): 650-65.

Strahl, B. D. and C. D. Allis (2000). "The language of covalent histone modifications." Nature **403**(6765): 41-5.

Sumner, R., A. Crawford, et al. (2000). "Initiation of adult myelopoiesis can occur in the absence of c-Myb whereas subsequent development is strictly dependent on the transcription factor." Oncogene **19**(30): 3335-42.

Sun, L., A. Liu, et al. (1996). "Zinc finger-mediated protein interactions modulate Ikaros activity, a molecular control of lymphocyte development." Embo J **15**(19): 5358-69.

Szilvassy, S. J. (2003). "The biology of hematopoietic stem cells." Arch Med Res **34**(6): 446-60.

Szilvassy, S. J., P. L. Ragland, et al. (2003). "The marrow homing efficiency of murine hematopoietic stem cells remains constant during ontogeny." Exp Hematol **31**(4): 331-8.

Thorsteinsdottir, U., A. Mamo, et al. (2002). "Overexpression of the myeloid leukemia-associated Hoxa9 gene in bone marrow cells induces stem cell expansion." Blood **99**(1): 121-9.

Till, J. E. and C. E. Mc (1961). "A direct measurement of the radiation sensitivity of normal mouse bone marrow cells." Radiat Res **14**: 213-22.

Tkachuk, D. C., S. Kohler, et al. (1992). "Involvement of a homolog of Drosophila trithorax by 11q23 chromosomal translocations in acute leukemias." Cell **71**(4): 691-700.

Tkachuk, D. C., C. A. Westbrook, et al. (1990). "Detection of bcr-abl fusion in chronic myelogeneous leukemia by in situ hybridization." Science **250**(4980): 559-62.

Tsai, F. Y., G. Keller, et al. (1994). "An early haematopoietic defect in mice lacking the transcription factor GATA-2." Nature **371**(6494): 221-6.

Tsai, S., S. Bartelmez, et al. (1994). "Lymphohematopoietic progenitors immortalized by a retroviral vector harboring a dominant-negative retinoic acid receptor can recapitulate lymphoid, myeloid, and erythroid development." Genes Dev **8**(23): 2831-41.

Turner, B. M. (2003). "Memorable transcription." Nat Cell Biol **5**(5): 390-3.

Turner, B. M. (2005). "Reading signals on the nucleosome with a new nomenclature for modified histones." Nat Struct Mol Biol **12**(2): 110-2.

Turner, B. M., A. J. Birley, et al. (1992). "Histone H4 isoforms acetylated at specific lysine residues define individual chromosomes and chromatin domains in Drosophila polytene nuclei." Cell **69**(2): 375-84.

van der Vlag, J. and A. P. Otte (1999). "Transcriptional repression mediated by the human polycomb-group protein EED involves histone deacetylation." Nat Genet **23**(4): 474-8.

Vangala, R. K., M. S. Heiss-Neumann, et al. (2003). "The myeloid master regulator transcription factor PU.1 is inactivated by AML1-ETO in t(8;21) myeloid leukemia." Blood **101**(1): 270-7.

Varnum-Finney, B., L. Xu, et al. (2000). "Pluripotent, cytokine-dependent, hematopoietic stem cells are immortalized by constitutive Notch1 signaling." Nat Med **6**(11): 1278-81.

Veiby, O. P., F. W. Jacobsen, et al. (1996). "The flt3 ligand promotes the survival of primitive hemopoietic progenitor cells with myeloid as well as B lymphoid

potential. Suppression of apoptosis and counteraction by TNF-alpha and TGF-beta." J Immunol **157**(7): 2953-60.

Wang, G. G., M. P. Pasillas, et al. (2005). "Meis1 programs transcription of FLT3 and cancer stem cell character, using a mechanism that requires interaction with Pbx and a novel function of the Meis1 C-terminus." Blood **106**(1): 254-64.

Wang, G. G., M. P. Pasillas, et al. (2006). "Persistent transactivation by meis1 replaces hox function in myeloid leukemogenesis models: evidence for co-occupancy of meis1-pbx and hox-pbx complexes on promoters of leukemia-associated genes." Mol Cell Biol **26**(10): 3902-16.

Warren, A. J., W. H. Colledge, et al. (1994). "The oncogenic cysteine-rich LIM domain protein rbtn2 is essential for erythroid development." Cell **78**(1): 45-57.

Winandy, S., L. Wu, et al. (1999). "Pre-T cell receptor (TCR) and TCR-controlled checkpoints in T cell differentiation are set by Ikaros." J Exp Med **190**(8): 1039-48.

Wodnar-Filipowicz, A. (2003). "Flt3 ligand: role in control of hematopoietic and immune functions of the bone marrow." News Physiol Sci **18**: 247-51.

Yamanaka, R., C. Barlow, et al. (1997). "Impaired granulopoiesis, myelodysplasia, and early lethality in CCAAT/enhancer binding protein epsilon-deficient mice." Proc Natl Acad Sci U S A **94**(24): 13187-92.

Yamanaka, R., G. D. Kim, et al. (1997). "CCAAT/enhancer binding protein epsilon is preferentially up-regulated during granulocytic differentiation and its functional

versatility is determined by alternative use of promoters and differential splicing." Proc Natl Acad Sci U S A **94**(12): 6462-7.

Yang, X. J. and E. Seto (2007). "HATs and HDACs: from structure, function and regulation to novel strategies for therapy and prevention." Oncogene **26**(37): 5310-8.

Yang, X. J. and M. Ullah (2007). "MOZ and MORF, two large MYSTic HATs in normal and cancer stem cells." Oncogene **26**(37): 5408-19.

Yin, B., K. Morgan, et al. (2006). "Nfl gene inactivation in acute myeloid leukemia cells confers cytarabine resistance through MAPK and mTOR pathways." Leukemia **20**(1): 151-4.

Yu, B. D., J. L. Hess, et al. (1995). "Altered Hox expression and segmental identity in Mll-mutant mice." Nature **378**(6556): 505-8.

Zeisig, B. B., T. Milne, et al. (2004). "Hoxa9 and Meis1 are key targets for MLL-ENL-mediated cellular immortalization." Mol Cell Biol **24**(2): 617-28.

Zhang, S. (2008). "The role of aberrant transcription factor in the progression of chronic myeloid leukemia." Leuk Lymphoma **49**(8): 1463-9.

Zhang, S., S. Fukuda, et al. (2000). "Essential role of signal transducer and activator of transcription (Stat)5a but not Stat5b for Flt3-dependent signaling." J Exp Med **192**(5): 719-28.